

Ali Nasekhian

**Application of Non-probabilistic and Probabilistic  
Concepts in Finite Element Analysis of  
Tunnelling**

**Dissertation**

Eingereicht an der Fakultät für Bauingenieurwissenschaften  
der Technische Universität Graz

Begutachter

Ao.Univ.-Prof. Dipl.-Ing. Dr.techn. Helmut F. Schweiger  
*Institute for Soil Mechanics and Foundation Engineering*  
Graz University of Technology, Austria

Univ.-Prof. Dr. Michael Oberguggenberger  
*Institute of Basic Sciences in Civil Engineering*  
*Unit of Engineering Mathematics*  
University of Innsbruck, Austria

Graz, March 2011

# Acknowledgements

First and foremost, I would like to express my deep gratitude to my advisor, Ao.Univ.-Prof. Dipl.-Ing. Dr.techn. Helmut F. Schweiger, head of the Computational Geotechnics Group at the Institute for Soil Mechanics and Foundation Engineering in Graz University of Technology for the many hours of excellent guidance, for providing me with research facilities, and for ensuring financial support throughout my Ph.D. studies. I am grateful to him for his contributions, not only in this thesis, but also in training me to be a better researcher.

Gratitude is also due to O.Univ.-Prof.Dipl.-Ing. Dr.techn. Stephan Semprich, head of the Institute for Soil Mechanics and Foundation Engineering for making the research facilities of the Institute available to me. I would also like to thank Univ.-Prof. Dr. Michael Oberguggenberger from the University of Innsbruck, for reviewing my thesis. Moreover, I wish to sincerely thank the Austrian Society for Geomechanics (ÖGG) and its president, O.Univ.-Prof.Dipl.-Ing. Dr.techn. Wulf Schubert (and head of the Institute of Rock Mechanics and Tunnelling) for financing this research.

I am truly grateful to the late Dr.techn. Rudolf Pöttler, Managing Director of ILF Austria, who supported my research in Graz. I especially am thankful to Dr.techn. Thomas Marcher from ILF Innsbruck for his steady attentiveness, providing me a valuable opportunity to gain professional experience and supplying me with case study data.

I would like to express my gratitude to dear Dr.techn. Robert Thurner, for his thoughtfulness and precious comments. I'll never forget when he brought me an entire van full of his personal books and papers, which was a bomb of encouragement! Thank you Robert!

I appreciate the contribution of many of my dear friends especially Franz Tschuchnigg, Bert Schädlich, Dr. Vahid Galavi, Dr. Hartmut Schuller, Dr. Václav Račanský, Dr. Gerd Peschl, Dr. Gerhard Steger, Christian Lackner, Ikhyia, Indra Hamdhan, and Martin Gäb. I enjoyed joining you in such a warm research atmosphere.

Last but certainly not least, I wish to thank my parents for their prayers throughout my life. I am indebted to Reihaneh for her inspiration, love and devotion. I would like to dedicate my work to her. Thank you Reihaneh!

# Kurzfassung

In dieser Arbeit wird zuerst der heutige Kenntnisstand zur Analyse von Unsicherheiten/Unschärfe dargestellt. Im Bereich der Geotechnik sind aus Sicht der praktischen Ingenieursarbeit vor allem die non-probabilistischen oder unpräzisen Methoden interessant, deren Theorie in den letzten zwei Jahrzehnten eine rasante Entwicklung erfahren hat. Jeweils eine ausgewählte non-probabilistische und probabilistische Methode - die beide ohne Modifikation des Rechenkerns mit numerischen Methoden kombiniert werden können - wird erläutert, um zu zeigen, welche Informationen für ingenieurgemäße Beurteilungen und Entscheidungsfindungen im Tunnelbau aus diesen Verfahren gewonnen werden können. Unter den non-probabilistischen Methoden erbrachte besonders die Random Set Finite Elemente Methode (RS-FEM) sehr gute Ergebnisse für praktische ingenieurmäßige Problemstellungen.

Kapitel 3 und 4 widmen sich der weiteren Untersuchung der Vorzüge und Beschränkungen der RS-FEM in Hinblick auf Aufgabenstellungen des Tunnelbaus. Ein Vergleich zwischen Berechnung und Messungen demonstriert im weiteren die Effizienz der Methode in einer realen Fallstudie. In Kapitel 5 wird die Leistungsfähigkeit des Verfahrens untersucht, die Unsicherheiten bei der Auswahl des Stoffgesetzes und seiner Parameter zu berücksichtigen. Dazu wurden zwei RS-FEM Berechnungen durchgeführt, in denen Materialmodelle mit dem Mohr-Coulomb und dem Hoek-Brown Versagenskriterium verwendet wurden. Die Unterschiede in den Berechnungsergebnissen werden erörtert und mit den Messergebnissen verglichen. Zum Abschluss werden die Ergebnisse verschiedener RS-FEM Berechnungen unter Verwendung der „Evidence Aggregation Method“ zusammengeführt. Im letzten Kapitel wird am Beispiel der gleichen Fallstudie die Punktabeschätzmethode (Point Estimate Method, PEM) als eine der probabilistischen Methoden mit der RS-FEM verglichen. Es wird gezeigt, dass unter bestimmten Annahmen mit PEM und RS-FEM ähnliche Schlussfolgerungen in Bezug auf die Bandbreite des wahrscheinlichen Systemverhalten eines Tunnels gezogen werden können.

# Abstract

In the current study, first state-of-the-art uncertainty analysis methods are briefly reviewed. To deal with uncertainties involved in geotechnical problems, non-probabilistic or imprecise probability methods whose theories have been rapidly developing in the last two decades are appealing in engineering practice. Two selected non-probabilistic and probabilistic methods with the potential of being combined with numerical methods –without requiring any modification to the core of the numerical code– are investigated to demonstrate what useful information can be provided for more rational engineering judgments and decision making in tunnelling. Among non-probabilistic methods, Random Set Finite Element Method (RS-FEM) has demonstrated its attractive results in practical geotechnical problems.

Chapters 3 and 4 are devoted to the further investigation of merits and limitations of the method, focusing on tunnel engineering problems. Moreover, a comparison between calculation and field measurements highlights the efficiency of the RS-FEM in a real case study. In Chapter 5, an attempt is made to demonstrate the capability of the framework in considering the uncertainty involved in the selection of material constitutive model. For this purpose, two random set analyses were accomplished in which the Hoek-Brown and Mohr-Coulomb criteria have been used as the constitutive model. Discrepancies between the results are discussed and compared to the measurements. Finally, the results obtained from different random set analyses are combined using evidence aggregation methods. In the last chapter, a comparison has been made between the Point Estimate Method categorised as one of the probabilistic approaches and RS-FEM, using the same case study. It is shown that under certain assumptions, a similar conclusion regarding the range of most probable behaviour of a tunnel problem obtained from both PEM and RS-FEM approaches can be drawn.

# Table of contents

## List of symbols

<b>1</b>	<b>Introduction</b>	<b>1</b>
1.1	Motivation	1
<b>2</b>	<b>On approaches dealing with uncertainty</b>	<b>3</b>
2.1	Uncertainty	3
2.2	Uncertainty model	3
2.3	Approaches of uncertainty analysis	5
2.3.1	Probabilistic methods	6
2.3.1.1	Bayesian approach	7
2.3.1.2	Response surface method	7
2.3.1.3	Stochastic finite element method	8
2.3.1.4	Random field finite element method	8
2.3.2	Non-probabilistic methods	9
2.3.2.1	Interval Analysis	9
2.3.2.2	Fuzzy Method	13
2.3.2.3	Imprecise probability method based on p-box representation	15
2.4	Adopted approach in this study	17

<b>3</b>	<b>Random Set Finite Element Method in Tunnelling</b>	<b>19</b>
3.1	Concept of random set theory	20
3.1.1	Bounds on the system response	20
3.1.2	Types of random set and visualisation	22
3.2	Procedure of the RS-FEM	26
3.3	Principles of NATM and the historical background	29
3.4	Application of RS-FEM to tunnel excavation case study	31
3.4.1	Procedure for determining basic variable sets in a random set model	34
3.4.1.1	Determination of basic variables	34
3.4.1.2	Variance reduction technique	38
3.4.1.3	Sensitivity analysis	39
3.4.2	Calculation results and system response	43
3.4.2.1	Construction sequences	43
3.4.2.2	Probability share of each deterministic FE realisation	46
3.4.3	Validity of the model	47
3.4.4	Determination of performance function	52
3.4.5	Evaluating the serviceability limit state of the shotcrete lining	55
3.5	Summary and conclusion	60
<b>4</b>	<b>Possible limitations in RS-FEM</b>	<b>63</b>
4.1	Tunnel example in faulted zone	64

4.1.1	Random set finite element results	65
4.1.2	Scenarios concerning the unsuccessful random set results	69
4.2	Scenario 1: Revision of input random set according to Hoek-Brown parameters	70
4.2.1	Rock mass strength parameters	70
4.2.1.1	Hoek-Brown criterion	71
4.2.1.2	Equivalent Mohr-Coulomb parameters	72
4.2.2	Revised deformability modulus of the rock mass	74
4.2.3	Basic variables for the random set model	77
4.2.4	Validity of the RSFEM results	78
4.2.5	Evaluation of the lining performance function	84
4.3	Scenario 2: Change of construction sequence and reconsidering the tunnel design	85
4.3.1	Calculation results	88
4.4	Summary and conclusion	91
<b>5</b>	<b>On the effects of constitutive model change</b>	<b>93</b>
5.1	Problem statement	93
5.2	A tunnel example in rock with 25m overburden	93
5.2.1	Random set input parameters	94
5.2.2	Calculation results	98
5.2.3	Serviceability limit state	103

5.3 Merging of RS-FEM results obtained from different constitutive models	104
5.3.1 Intersection	105
5.3.2 Envelope	106
5.3.3 Mixing	106
5.3.4 Convolute averaging	107
5.4 Calculation and results	108
5.5 Conclusion and summary	112
<b>6 Comparison of RS-FEM and Point Estimate Method</b>	<b>113</b>
6.1 Point estimation method	114
6.2 Approach proposed by Zhou & Nowak (1988)	115
6.3 Accuracy of the PEM	118
6.4 Limitations and advantages	124
6.5 Evaluating PEM against RS-FEM for tunnel example	126
6.5.1 Providing distribution functions equivalent to random sets	126
6.5.2 Calculation results	131
6.6 Summary and conclusion	140
<b>7 Conclusions and further research</b>	<b>142</b>
7.1 Summary and achievements	142
7.2 Further research	143





# List of symbols and abbreviations

This section lists the definition of used symbols in alphabetical order. They are additionally explained in the text when they first appear. Units are not included in this list, they will be defined in the text when they are first used.

## Small letters

$a$	Hoek Brown model parameter
$c$	effective cohesion
$e$	eccentricity
$e_a$	imperfections
$f$	function
$f_c$	uniaxial compressive strength of concrete
$f_X$	joint probability density function
$g$	limit state function
$i$	index number
$j$	index number
$k$	index number
$l$	lower value of a closed interval
$m$	basic probability assignment
$m_i$	Hoek Brown model parameter for intact rock
$m_b$	Hoek Brown model parameter for rock mass
$n$	number of information sources
$n_c$	number of calculations
$p$	probability
$p_f$	probability of failure
$s$	Hoek Brown model parameter
$u$	upper value of a closed interval
$u_i$	a standard uniform random number
$x$	basic variable
$\mathbf{x}$	vector of basic variables
$x, y, z$	Cartesian coordinates

## Capital letters

$A_i$	focal element
$Bel$	belief function
$D$	Disturbance factor in Hoek Brown model

$E$	generic subset
$E_i$	Elastic modulus of intact rock
$E_{rm}$	elasticity modulus of the rock mass
$E_{sh}$	Young's modulus of young shotcrete
$E_s$	stiffness/deformation modulus
$F_*$	lower cumulative probability distribution function / upper cumulative probability distribution function
$F_s$	factor of safety
$H$	Tunnel depth below surface
$K_o$	coefficient of earth pressure at rest
$L$	length of potential failure surface
$M$	bending moment
$N$	axial force/ number of basic variables
$N_{lim}$	admissible normal force in shotcrete lining
$Pl$	plausibility function
$R$	random relation
$R_*$	lower bound on element of $R$ / upper bound on element of $R$
$R_f$	Relaxation factor
$S$	hull of a solution set
$X$	non-empty set
$\mathbf{X}$	vector of basic variables
$\mathfrak{S}$	support of random set
$\mathfrak{R}$	support of image of random set $\mathfrak{S}$

### Small Greek letters

$\alpha$	$\alpha$ -cut membership / relative sensitivity
$\beta$	Reliability index
$\gamma$	total unit weight of soil / statistical skewness
$\eta_{SR}$	sensitivity ratio
$\eta_{SS}$	sensitivity score
$\mu$	mean value
$\nu$	vertices/ Poisson's ratio/ statistical mode
$\rho$	basic probability assignment of image of $m$
$\sigma$	standard deviation
$\sigma_1$	Minor principal effective stress
$\sigma_3$	Major principal effective stress

$\sigma_{ci}$	Unconfined compressive strength of intact rock
$\sigma'_{cm}$	Global rock mass strength
$\varphi$	effective friction angle
$\psi$	dilation angle

#### Capital Greek letters

$\Gamma$	variance reduction factor
$\Theta$	spatial correlation length
$\Theta_y$	Spatial correlation length in y direction
$\Theta_x$	Spatial correlation length in x direction
$\Phi$	Standard normal cumulative distribution function

#### Abbreviation:

BEM	Boundary Element Method
CDF	Cumulative Distribution Function
COV	Coefficient Of Variation
FE	Finite Element
FEA	Finite Element Analysis
FEM	Finite Element Method
FOS	Factor Of Safety
FOSM	First Order Second Moment approximation
FORM	First Order Reliability Method
GSI	Geological Strength Index
HB	Hoek Brown criterion
IFEA	Interval Finite Element Analysis
LSF	Limit State Function
MC	Mohr Coulomb criterion / Monte Carlo simulation
NATM	New Austrian Tunnelling Method
p-box	A pair of CDFs which represents the imprecise probability distribution of a RV
PDF	Probability Distribution Function
QM	Quality of Model
RFEM	Random Finite Element Method
RMR	Rock Mass Rating
RQD	Rock Quality Designation
RS	Random Set
RS-FEM	Random Set Finite Element Method
RST	Random Set Theory

RV	Random Variable
SORM	Second Order Reliability Method
UCS	Unconfined Compressive Strength
ZN-II	Zhou and Nowak point estimate method – II
ZN-III	Zhou and Nowak point estimate method – III

# 1 Introduction

## 1.1 Motivation

In association with engineering judgement, Lacasse et al. (2004) state: “Engineering depends on judgment, the exercise of which depends on knowledge derived from theoretical concepts, experiment, measurements, observations, and past experience. These building blocks have to be recognized, assembled, and evaluated collectively before judgment can be rendered”. Specifically, in the tunnelling industry Wannick (2007) mentions: “Since the early 1990s, no other area of the construction industry has been as adversely affected by major losses as tunnelling. Besides property losses often in the two-digit million range, third-party liability losses have also been high, and numerous people have lost their lives. The international insurance industry has made payments exceeding US\$ 600m for large losses”. Certainly a variety of causes may be included for the losses such as flood, earthquake or fire. However, causes originating from uncertainties, lack of knowledge or insufficient data prior to tunnel construction cannot be overlooked. Therefore, modern concepts dealing with uncertainties (e.g. reliability analysis, risk management and sensitivity analysis) have to be introduced into common engineering practice, especially in large underground structures. This requires an efficient user-friendly framework to deal with uncertainties. It seems that there is a demand to utilise simple mathematical concepts regarding uncertainties in tunnel engineering and to introduce simple and user-friendly frameworks for analysing and designing underground structures.

The usage of numerical methods such as the Finite Element Analysis is becoming more widespread, as more designers recognise the advantages of using such techniques in analysing complex geotechnical problems.

Traditionally, there are two approaches that reflect uncertainty in the design, namely probabilistic and deterministic approaches. Quantities achieved by probabilistic and deterministic approaches, such as failure probabilities and safety factors respectively, play an important role in qualitative studies and standard codes of practice; however, they do not indicate a firm proposition about what takes place in reality. In addition, contrary to classical probability theory, the probability of failure computed in engineering practice cannot be interpreted as a frequency of failure (Oberuggenberger and Fellin, 2002). On the other hand, several authors have addressed the shortcomings of probabilistic methods in reliability analysis e.g. tail problems in which the failure of probability may vary by orders of magnitude when fitting different distributions to the same input data obtained from laboratory tests (Oberuggenberger and

Fellin, 2002). Moreover, Elishakoff (2000) has collected comments of a number of experts about possible shortcomings of probabilistic methods in engineering, in which interested readers could look into the opinions of current researchers about the application of probabilistic methods in practice.

In the present effort, two selected non-probabilistic and probabilistic methods with the potential of being combined with numerical methods –without requiring any modification to the core of the numerical code– are investigated to demonstrate what useful information can be provided for more rational engineering judgments and decision making in tunnelling.

The work presented herein is a follow-up to foregoing research on non-deterministic approaches in numerical analysis of geotechnical problems carried out in the Computational Geotechnics Group at the Institute of Soil Mechanics and Foundation Engineering of the Graz University of Technology. First, Thurner (2000) made an attempt to apply probabilistic methods such as Point Estimate Method, Monte Carlo simulation, and FOSM using the Taylor Series expansion method, as well as reliability analysis using FORM/SORM methods to illustrate the pros and cons of these probabilistic methods by applying them on different types of geotechnical boundary value problems. Peschl (2004) accomplished a research namely “Reliability Analyses in Geotechnics with Random Set Finite Element Method”. A successful effort was made to integrate the finite element method as a powerful computational tool with an adopted non-probabilistic method, namely the Random Set Approach to provide a procedure by which a reliability analysis of highly complex nonlinear geotechnical problems may be carried out where only scarce and incomplete data are available.

Therefore, in the present dissertation the objective is to investigate the merits and shortcomings of the Random Set Method and the Point Estimate Method respectively, categorised in the non-probabilistic and probabilistic approach, which are equally applicable to the finite element analysis of geotechnical problems, with particular references to tunnel engineering.

## 2 On approaches dealing with uncertainty

### 2.1 Uncertainty

As a comprehensive reference, Walley (1991) has mathematically and verbally elaborated many statistical and probabilistic terms, especially regarding imprecise probability and type of uncertainties in general. In addition, Baecher and Christian (2003) have devoted one chapter to categorise uncertainty and clarify frequently used terms particularly in the context of risk and reliability analysis of geotechnical problems. In brief, two kinds of uncertainty associated with geotechnical problems exist, for which in the technical literature the terms ‘*aleatory*’ and ‘*epistemic*’ are commonly used. Aleatory uncertainty represents the natural randomness of a property. As an important feature, this kind of uncertainty is irreducible and is also known as natural variability or spatial variability in the case of soil parameters, which vary over space (not over time). Epistemic uncertainty is a type of uncertainty that originates from the lack of knowledge. Consequently this type of uncertainty can potentially be reduced by means of abundant observations and collecting information. There are also other types of uncertainties concerning construction, manufacturing, maintenance and human errors (Lacasse and Nadim, 1996) that are not included in the latter categories and are usually not considered in models of engineering performance.

### 2.2 Uncertainty model

In dealing with uncertainties in any system, an uncertainty model is required. Figure 1 illustrates how uncertainty propagates through a mechanical system within an uncertainty model. An uncertainty model consists of a collection of input uncertainty, model uncertainty, and the technique by which the system response is evaluated. Thus, two main sources of uncertainty, namely model uncertainty and parameter uncertainty are identified. In geotechnics, the input or parameter uncertainties are affected by both types of uncertainty. For instance, the inherent variability of soil/rock materials is well-recognised as a random phenomenon (Lacasse and Nadim, 1996) and regarding the lack of knowledge, it is difficult to determine the borders of soil layers or to exactly characterise the loads acting on the structure. Model uncertainty concerns the degree of accuracy of a chosen mathematical model that is capable of describing a real physical behaviour of the mechanical system. This comes from our inability to exactly model the actual system; therefore, model uncertainty falls in the epistemic category. The uncertain model will lead to uncertain model responses even if crisp input values have been used. Accounting for such an uncertainty is of



interest in the area of numerical analysis when a reliability or risk analysis is being performed to observe the impact of model uncertainty as a mapping function on the system responses in any non-deterministic approach. In this dissertation, both sources of uncertainty are addressed and considered.

Regarding the representation of system responses in terms of probability, it is worth mentioning that in almost all geotechnical problems, engineers face a mixture of both types of uncertainties and therefore the outcomes of the probabilistic calculations or uncertainty analyses are signifying some sort of degree of belief (Bayesian approach) about the obtained results rather than the exact value of e.g. probability of a system failure as understood in the frequentist approach (Baecher and Christian, 2003). This notion and perception of probability is more consistent with geotechnical phenomena and practice.

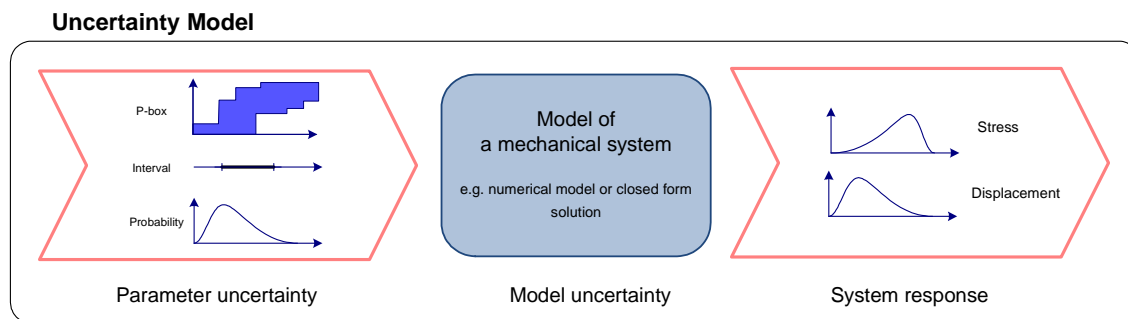


**Fig. 1:** Uncertainty model and propagation of uncertainties through a model

The uncertainty model of a mechanical system is built up for different purposes, mainly categorised in the following three types of analysis (Schweckendiek, 2006):

1. *Uncertainty analysis*, aims to estimate the extent of the system responses based on the uncertainties inherent in the model. In a comprehensive analysis a distribution is obtained, and if such a thorough analysis would not be feasible, at least some statistical characteristics are produced.
2. *Reliability analysis*, is concerned with finding the reliability or the probability of failure of a system using defined failure criteria expressing the undesired events. According to US Army Corps of Engineers (1997) "The term 'failure' is used to refer to any occurrence of an adverse event under consideration, including simple events such as maintenance items. To distinguish adverse but non-catastrophic events (which may require repairs and associated expenditures) from events of catastrophic failure (as used e.g. in the dam safety context), the term probability of unsatisfactory performance is sometimes used."

3. *Risk analysis*, aims to identify the hazards pertinent to a project and to determine the risk of one taking the potential adverse consequences of the hazards and its relevant probability of their occurrence into account (Baecher and Christian, 2003).

The current dissertation is concerned with the first two purposes. In engineering, risk analysis relates mainly to the consequences (financially) of the uncertainty and is beyond the scope of this work. However, performing uncertainty and reliability analysis can be considered as an introduction or as primary steps for such an analysis. As an example, Pöttler et al. (2007) have shown the application of Random Set Finite Element Method in risk analysis.

In the following, the techniques recently developed for analysing uncertainty in mechanical systems are outlined with the aim of identifying the position of the methods used in the current dissertation with respect to others.

### 2.3 Approaches of uncertainty analysis

In order to perform uncertainty analysis on a mechanical system, the uncertainty present in the system's characteristics have to be mathematically quantified. Probability theory has a long tradition in characterising uncertainty and the majority of the approaches in uncertainty analyses stem from this theory. Some shortcomings addressed by researchers should however be overcome e.g. in handling all types of uncertainty or when the credibility of the probabilistic approach is questionable when data are insufficient (e.g. Ben-Haim, 1994). Contrary to classical probability theory, the probability of failure computed in engineering practice cannot be interpreted as a frequency of failure; and regarding tail problems in reliability analysis using probabilistic methods in which the probability of failure may vary by orders of magnitude when fitting different distributions to the same input data obtained from laboratory tests (Oberuggenberger and Fellin, 2002). Elishakoff (2000) has collected comments of a number of experts about possible shortcomings of probabilistic methods in engineering, and opinions of current researchers about the application of probabilistic methods in practice. Thus, to overcome the shortcomings, some other mathematical theories have been recently emerged to handle epistemic or multiple types of uncertainty such as random set theory (Kendall, 1974; Goodman and Nguyen, 1985), evidence theory (Dempster, 1967; Shafer, 1976), fuzzy set theory (Zadeh, 1965), possibility theory (Zadeh, 1978), imprecise probabilities (Walley, 1991), interval approach (Moore, 1966), and convex model (Ben-Haim and Elishakoff, 1990) among others. Therefore, regarding non-deterministic analysis a classification can be made in which the current approaches for dealing with uncertainties are divided into two major methods: 1) probabilistic methods and 2) non-probabilistic methods (Moens and Vandepitte, 2005). Probabilistic methods are those supported by probability theory and the

non-probabilistic methods incorporate the other theories or probability theory is only partly involved. Figure 2 depicts tree-diagram illustrating the most commonly used approaches stemming from probabilistic and non-probabilistic methods in uncertainty and reliability analysis.

### 2.3.1 Probabilistic methods

The existing probabilistic methods can be categorised in various ways from different points of view. For instance, in a geotechnical context, Suchomel and Mašín (2010) distinguish between probabilistic methods based on considering the spatial variability of soil parameters. Generally, one possible classification of the probabilistic methods is portrayed in Figure 2.

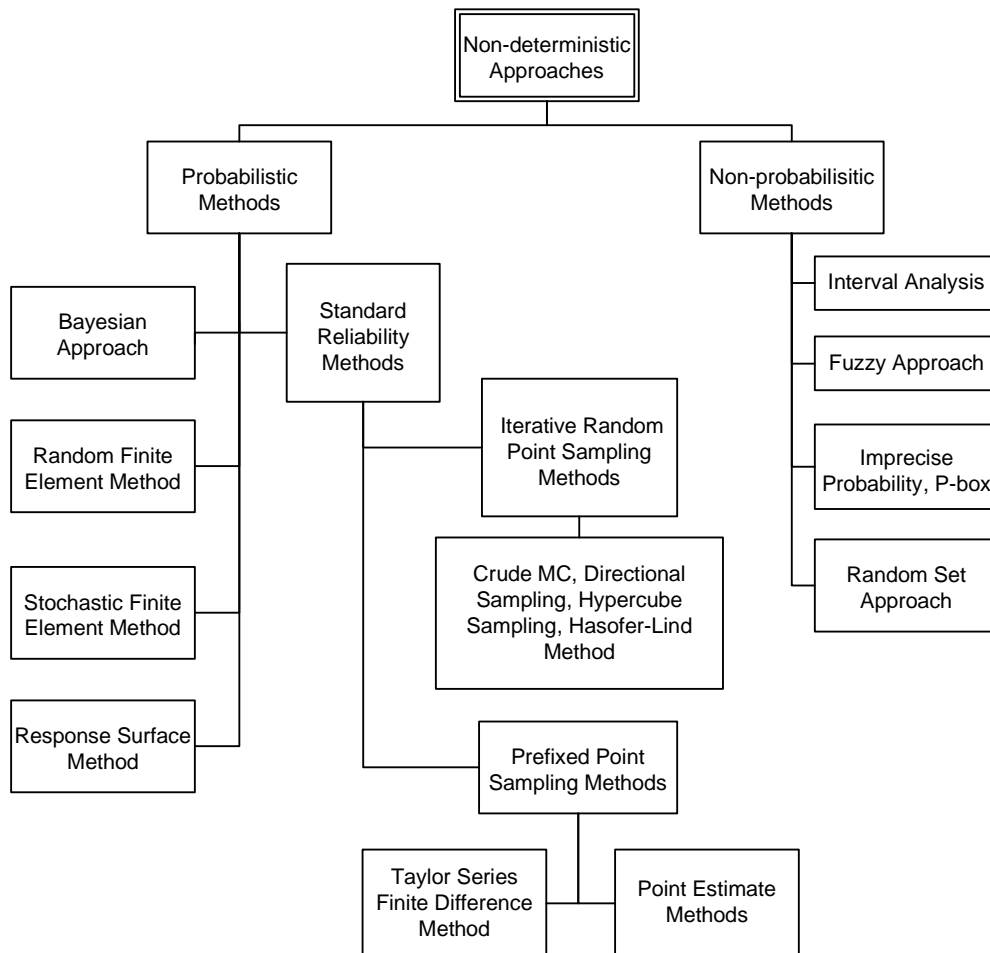


**Fig. 2:** Classification of non-deterministic approaches

There are many probabilistic methods, a selection of which is briefly mentioned herein. Standard reliability methods and procedures such as MC (Monte Carlo simulation) or First Order Second Moment approximation (FOSM), First Order

Reliability Method (FORM), Second Order Reliability Method (SORM), and the Taylor series expansion can be found in standard text books (e.g. Ang and Tang, 1975; Harr, 1996, Haldar and Mahadevan, 2000).

### **2.3.1.1 Bayesian approach**

In many cases, the required information for probabilistic analysis is missing or limited. Those researchers who are interested in using probabilistic methods tend to overcome the main disadvantage (i.e. when insufficient data are available, subjective assumptions should be made about the probability distribution of the input random variable) by applying the Bayesian theory. Thus, first a subjective probability is assumed and with the help of prospective observations and test results (whenever more data become available) using the Bayesian theory, the probability distribution is amended and improved. It is clear that if no reliable information is added to the analysis, the Bayesian method does not yield better results or predictions of the system response. Regarding the Bayesian approach in reliability analysis of geotechnical problems see Baecher and Christian (2003). Very recently, Stille et al. (2010) have utilized the Bayesian approach in the design of underground structures in combination with the observational method, since there is compatibility between these two methodologies and as the design can be modified, if necessary, as more information is obtained during the tunnelling progress. See also Zhang et al. (2009) in characterising geotechnical uncertainty models based on the Bayesian approach.

### **2.3.1.2 Response surface method**

The response surface method can be considered as an uncertainty analysis methodology in which the impact of the input parameters and their interactions on the system responses are evaluated and comes up with a relationship between the significant factors and the desirable system response in order to reduce the analysis complexity of the mechanical system (Cornel, 1990). The function obtained by this method can replace the original model in an uncertainty analysis. Then one of the probabilistic methods is employed (e.g. Monte-Carlo simulation) in order to evaluate the system with significantly smaller analysis time, maintaining the same number of simulations. Zangeneh et al. (2002) have employed this methodology in numerical geotechnical analysis, e.g. the displacement analysis of slopes subject to earthquake. The idea is simple and attractive but from a practical point of view, it has a shortcoming because it is necessary to estimate the response function using regression methods for each individual response and it is valid only in the selected ranges of the input variables. For cases that many system responses are of interest a great deal of statistical analyses and computational efforts are required.

### **2.3.1.3 Stochastic finite element method**

In the stochastic finite element method (see e.g. Ghanem and Spanos, 1991) the ‘stochastic process’ (time dependent characteristics of random variables) and ‘random field’ (variability of a parameter over space, i.e. spatial variability) characteristics of input parameters are engaged in the governing partial differential equations, which are to be discretised and numerically solved by means of the finite element method. The discretisation of random fields is usually accomplished by means of series expansions or by Monte Carlo strategies. An extensive review of such strategies has been carried out by Keese (2003). All system responses are given in terms of random field vectors, incorporating all possible outcomes based on the random field characteristics of input parameters. The method can be considered as one of the most sophisticated probabilistic methods that require significant changes to a standard finite element code. This method has been mainly utilised in structural applications.

### **2.3.1.4 Random field finite element method**

Usually in probabilistic numerical methods, the spatial variability of the soil parameters is not taken into account. In other words, the inherent soil characteristic, indicating a correlation between soil properties of an element with respect to the surrounding elements in a certain distance, is ignored. Instead, a soil layer is considered homogeneous with a relevant probability distribution which represents the stochastic behaviour of the layer, i.e. at each realisation using one of the existing sampling methods (e.g. Monte Carlo sampling) the respective soil property is identical within the layer’s elements. However, in the Random Finite Element Method (RFEM), soil parameters are modelled by random fields. The soil layer is divided into small elements by means of finite element discretisation and the sampling is implemented for each individual element. Considering the spatial correlation length (which depends on soil characteristics) the soil property of the  $i^{\text{th}}$  element in the random field is assigned using the local average subdivision technique. A series of papers presented by Griffiths and Fenton have demonstrated the applicability of the method in several geotechnical problems (see Griffiths and Fenton, 2007) such as bearing capacity, slope stability, footing settlement, and passive earth pressure of spatially random soils. Phoon and Cheng (2009) used the random field finite element method for the uncertainty analysis of a circular tunnel, modelling the Young’s modulus of the soil layer as a random field. Providing the parameters required in RFEM needs adequate information about the soil layers which are hardly obtained from standard site investigation schemes. This issue reduces the popularity of the method in practice; however, it has accommodated a great insight into the real soil behaviour from a scientific point of view.

## 2.3.2 Non-probabilistic methods

### 2.3.2.1 Interval Analysis

Moore (1966) introduced *interval analysis*, interval vectors, and interval matrices as a set of techniques that provide error analyses for computational results. The interval approach is used to describe parameter uncertainties either in geometry and loadings or in soil model parameters as interval quantities. The uncertainty is assumed to be unknown, but bounded; it has lower and upper bounds without assigning a probability structure.

One interpretation of an interval number is a random variable whose probability density function is unknown but non-zero in the range of the interval. Another interpretation includes intervals of confidence for  $\alpha$ -cuts of fuzzy sets. In general, the interval concept serves as a basis of other non-probabilistic uncertainty models (Muhanna et al., 2007). For example, in the fuzzy set approach a continuous membership function of input parameters can be split into several  $\alpha$ -levels with corresponding intervals and the fuzzy set approach turns into several analyses on different  $\alpha$ -cuts (Kaufmann and Gupta, 1991; Peschl and Schweiger, 2003). It will also be shown in chapter 3 that in the procedure of the random set analysis of a system, a series of interval analyses are performed to obtain the worst and best case on the Cartesian product of focal elements of the system parameters. Accordingly, knowledge of interval arithmetic is of great significance in applying modern uncertainty analysis methods like the Fuzzy Analysis, Random Set approach and Interval Analysis in connection with numerical models.

In the interval analysis of a mechanical system, the hull of the solution set ( $S$ ) is defined as the narrowest interval containing the results of a system response resulting from uncertainties available in the input system parameters. In other words, the hull of the solution set contains the set of the solutions. Suppose that by interval analysis set  $X$  has been obtained as a solution set. Set  $X$  is referred to as the enclosure of the solution set containing the hull of the solution set. It is called a sharp enclosure if the obtained solution (i.e. set  $X$ ) is practically useful and not significantly conservative. The inner bound of the exact solution is any interval (i.e. excluding the endpoints of the interval) that is contained in  $S$  and the outer bound is any interval that contains  $S$ .

The objective of interval analysis is to obtain the hull of a solution set or at least a rigorous sharp enclosure (outer bounds) for the ranges of system responses. From the mid-nineties many researchers have developed methods focusing on solving interval system equations for applications in Interval Finite Element Analysis (IFEA) including the most common ones:

1. **Combinatorial method** (e.g. Rao and Berke, 1997)
2. **Perturbation method** (e.g. Qiu and Elishakoff, 1998)
3. **Sensitivity analysis method** (e.g. Jasiński and Pownuk, 2000)
4. **Optimization method** (e.g. Möller et al., 2000)
5. **Monte Carlo sampling method** (e.g. Kulpa et al., 1998)
6. **Interval arithmetic FEM** (e.g. Muhanna et al., 2007)

**Combinatorial method:** If  $f(x_1, \dots, x_n)$  denotes a monotonic function of the parameters within the intervals  $X_1, \dots, X_n$ , the range of  $f$  can be determined by considering all possible combinations of the bounds of the interval parameters. Let the interval parameters  $X_i$  be denoted as  $X_i = [\underline{x}_i, \bar{x}_i] = [x_i^l, x_i^u]$ . Introducing all possible combinations of the bounds of the interval parameters into the analysis, the range of function  $f$  can be represented as an interval number as:

$$[f, \bar{f}] = [\min(f_r), \max(f_r)]: r = 1 \dots 2^n \quad (1)$$

The primary advantage of this method is that it is straightforward in its application to interval FEA. Any existing deterministic finite element code can be used for evaluating the considered function  $f$ . However, it must be noted that the combinatorial method yields the exact response range only if the system response is monotonic with respect to each parameter in its interval range. The computational cost increases exponentially with the number of interval parameters. For  $n$  interval parameters, there are  $2^n$  combinations for which the deterministic FEA has to be performed. The exponential complexity limits the applicability of the combinatorial method to systems with a rather small number of uncertain variables.

**Perturbation method:** This method is used when the uncertain parameters vary in a very small range. In fact in this method the considered function to be evaluated, should be expanded around the mid-point of the parameter interval with very small differentials. In the expanded equation higher order parts are neglected and other differential parts are substituted by a first-order Taylor series. The disadvantage of this method is that the bounds obtained are not guaranteed to enclose the true response range since the higher order terms are neglected in the equations. More details about this method can be found in Qiu and Elishakoff (1998).

**Sensitivity analysis method:** The sensitivity analysis method determines the bounds of the structural responses based on the obtained knowledge about the

monotonicity of the responses with respect to the system parameters. Jasiński and Pownuk (2000) introduced the method to achieve not only the bounds on the system response of a linear interval equation, but also an algorithm in testing the system's monotonicity over the entire interval ranges of the parameters. Although the method is able to check the monotonicity of the problem, its usability is limited in practice since it requires significant computational effort when a large number of interval variables exist.

**Optimization method:** Another way to find the bounds of the response is to perform two optimizations to compute the minimal and maximal responses when each parameter  $x$  is constrained to belong to an interval  $X$ . Möller et al. (2000) developed an optimization algorithm combining the evolution strategy, the gradient method, and the Monte-Carlo method. The optimization algorithm was applied to both static and dynamic linear/nonlinear structural analyses. This also has a disadvantage from a practical point of view, because for each response quantity, the function has to be optimized twice, in order to find the minimal and maximal values. Thus, when a small problem with limited uncertain parameters is involved this method becomes more practical.

**Monte Carlo sampling method:** The Monte Carlo sampling method involves sampling from intervals of input parameters expecting that the samples will fall sufficiently close to the values accommodating extremal system responses. If the number of samples is large enough, the lower and upper bounds of the solution set of the simulations could be a good approximation for the actual response range. Since the interval parameters do not contain the probability information, a probability distribution over the interval should be assumed for the sampling purpose. The distribution can be chosen arbitrarily. In practice, a uniform distribution over the interval is often chosen for convenience. It should be noted that this method, in spite of requiring a great amount of realisations always gives the inner bounds for system responses.

**Interval arithmetic finite element method:** Substituting variables in system equations with interval quantities leads to a severe overestimation due to a dependence problem addressed by several publications (e.g. Moore, 1966 and Neumaier, 1990). Muhanna et al. (2007) enhanced the method of solving the interval system equations in order to improve the computational efficiency of the interval approach as well as overcoming the severe overestimation of the system response ranges using the Element-By-Element technique. This methodology is referred to as the "interval arithmetic FEA". The finite element equations are reformulated seeking two objectives: 1) to reduce the repetition of the same interval variables in the computations 2) to delay the use of interval arithmetic as late as possible in the computations, in order to avoid overestimation in solution sets. In a recent development, a new formulation in IFEA has been introduced by Rama Rao et al. (2010) in which both primary (e.g. nodal displacements) and



derived unknowns (e.g. normal stress in truss elements) in the finite element formulation can be estimated sufficiently accurate, which are comparable with precise methods such as the combinatorial approach. This approach is able to handle a high degree of uncertainty (e.g. 10%) and find the worst case in a truss problem with over 10000 interval parameters efficiently and with considerably less computational effort in comparison with the combinatorial method.

The Random Set Finite Element Method (RS-FEM) is emphasised in this study and as its procedure is explained in the next chapter, a combinatorial method is used to handle the required interval analysis. Since this method is recognized as a computationally expensive method, it is convenient as long as the number of random variables is low. On the other hand, it gives an inner bound solution if the system is not monotonic with respect to the input random variables (RVs). This issue will be addressed next. Furthermore, employing interval arithmetic FEM such as those used for structural problems requires manipulating geotechnical software codes and also demands an algorithm dealing with a non-linear equation system, which is not such a straightforward task and seeks for an extensive research in this topic. Therefore it seems that the combinatorial method is a practical solution for carrying out the interval analysis inside the RS-FEM procedure. Nevertheless, the monotonic behaviour of the system should be checked.

As a conclusion, IFEM alone has a limited usage in reliability analysis since the resulting computations are in a form of simple intervals lacking probability assignments. Thus a probability statement about the results cannot be drawn (e.g. probability of failure). On the other hand, the developments lately carried out and associated with IFEM can be used to dramatically reduce the computational efforts of other non-probabilistic approaches (e.g. fuzzy set analysis and RS-FEM) that are based on interval analysis.

### **Monotonicity check**

It is not a straightforward task to prove the monotonicity condition for a geomechanical boundary value problem, especially in large scale problems involving many parameters. For instance, tangential stresses surrounding a circular tunnel might be monotonic with respect to the variation of model input parameters such as the elastic modulus, cohesion and relaxation factor, while another system response like the crown displacement of the tunnel may not demonstrate monotonic behaviour. Although such results hardly happen in geotechnical problems, prior to performing any interval analysis using the combinatorial method, one should make sure that the mechanical system behaves monotonically. However, in the author's opinion, from a practical point of view it suffices to check the monotonicity of a geotechnical boundary value problem with a simple sensitivity analysis (Peschl, 2004). Alternatively, a more rigorous

sensitivity analysis such as the monotonicity tests given by Rama Rao and Pownuk (2007) or an optimisation scheme (Moeller et al., 2000) could be employed. Of course the latter methods are more time consuming and demand higher computational effort.

In the case of truss problems, however, it can be mathematically shown (see Neumaier and Pownuk, 2007) that the monotonicity properties exist only when the stiffness parameters are involved and vary independently. This can be proven because a special form of linear system of equations arises in truss modelling. In a highly nonlinear complex geotechnical problem the monotonicity proof however, is so complicated that it demands a separate investigation which is beyond the scope of this study.

According to Pownuk (personal correspondence) many problems are monotone with respect to many parameters, however, unfortunately it cannot be generalised to all mechanical problems and their respective parameters. For instance, in the general case of FEA, when the stiffness matrix involves intervals, the monotonicity is not guaranteed (McWilliam, 2000), and the interval obtained for the system response is only an inner bound of the true response range. Therefore, prior to performing any interval analysis using the vertex method (e.g. Dong & Shah, 1987) one should make sure by one of the current methods (e.g. monotonicity test given by Rama Rao and Pownuk, 2007) that the system is monotone to obtain the hull of the solution set for the desired system responses.

### 2.3.2.2 Fuzzy Method

The overall approach of the fuzzy method may be subdivided into three main stages: 1) fuzzification 2) fuzzy analysis 3) defuzzification. The mapping of the fuzzy input values onto the result space is based on the extension principle in combination with the Cartesian product. In fuzzy analysis, the theory of possibility for fuzzy sets is used, which considers epistemic uncertainty. The fuzzy approach to uncertain problems is to mathematise the model parameters including geometrical, loading and soil model parameters as fuzzy quantities (Zadeh, 1965).

A fuzzy set is defined by its membership function whose domain is  $\mathfrak{R}$  while its range is bounded between  $[0,1]$ . The domain of the membership function is known as the interval of confidence and the range is known as the degree of membership. Therefore, each degree of membership  $\alpha$  ( $\alpha$ -cut membership,  $\alpha \in [0,1]$ ) has a unique interval of confidence  $A_\alpha = [a_\alpha, b_\alpha]$ , which is a monotonically decreasing function of  $\alpha$  (Fig. 3).

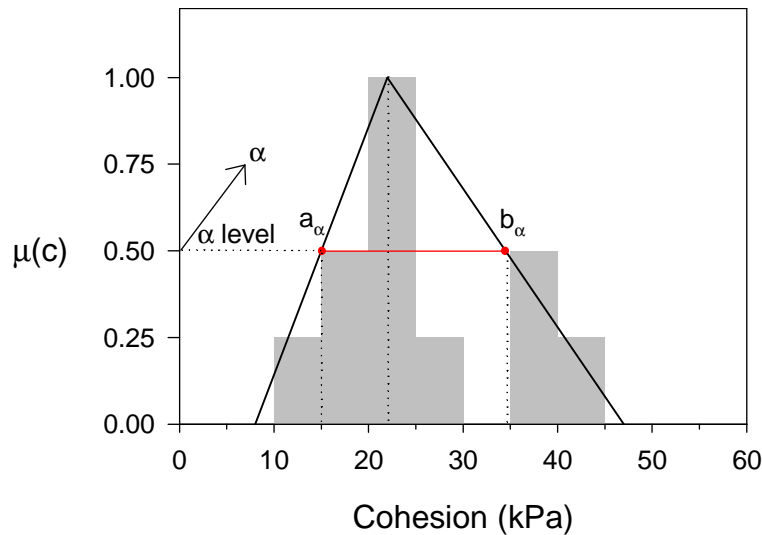


**Fig. 3:** Membership function of the cohesion of a soil layer as a fuzzy number, constructed from a histogram

The construction of a fuzzy set describing input variability may be based on an expert's opinion of possible ranges of e.g. the angle of internal friction. Of course, in this method a subjective shape should be chosen for the membership function (e.g. a triangle). Another approach based on the existing data comprised of samples, may be utilized in the form of normalised histograms. An example of a triangular fuzzy number is given in Fig. 3. Assigning a membership function to the available data is called **fuzzification**. In this stage simplifications and approximations are introduced. In this example, it can be interpreted that the expert had assigned the degree of possibility 0.5 that the cohesion is in the range of [15, 35] and a possibility of 1 that it has the value of 22 kPa. The computation of the fuzzy set approach can be performed based on the rules of the fuzzy set theory by adopting the  $\alpha$ -level discretisation of input variables to obtain the corresponding output of the same possibility level (**fuzzy analysis**). Finally, deterministic parameters of the system responses are extracted from the fuzzy results, which are presented in numbers (**defuzzification**).

Some researchers have attempted to apply the fuzzy approach in reliability analysis but using different terminology and interpretations concerning the resulting reliability. For instance, Peschl and Schweiger (2003) utilise the possibility of failure,  $\Pi_f$  for describing the safety level of a geotechnical structure. Dodagoudar and Venkatachalam (2000) studied the reliability analysis of slopes using the term 'fuzzy probability of failure'. Shrestha and Duckstein (1998) defined a kind of fuzzy reliability index and in the framework of fuzzy set theory, computed the probability of a fuzzy failure by introducing the fuzzy reliability measure that satisfies the necessary properties of the probabilistic reliability measures.

Probability of failure given by possibilistic methods e.g. Fuzzy Point Estimate Method (e.g. Dodagoudar and Venkatachalam, 2000) can be considered as the upper bound for the probability. For instance, Smith et al. (2002) exemplified a case in which the fuzzy membership function for a random variable is constructed based on the mean value and standard deviation of a random variable, and showed that the possibility of failure obtained by fuzzy analysis is 1.0 while the probability of failure is only 0.5. In general, a high degree of possibility does not necessarily mean a high value of probability (Dodagoudar and Venkatachalam, 2000). On the other hand, when an event is not possible it also implies the event is improbable.

The random set approach and fuzzy set method are similar to each other in the sense of their concept, although the former takes benefits of probability concepts and the latter is backed by possibility theory. According to Tonon (2000a) random sets are able to deal with imprecise data as a special kind of ‘ambiguity’ that is properly formalised by the concept of fuzzy sets introduced by Zadeh. In addition, a special case of random set, namely the consonant sets (discussed in Chapter 3) in which each focal element contains each other, can be interpreted as  $\alpha$ -cuts of a fuzzy set and consequently, the plausibility and belief function in the random set conform with the possibility and necessity function in possibility theory respectively.

### 2.3.2.3 Imprecise probability method based on p-box representation

A probability-box or p-box (Ferson et al. 2003) is a pair of CDFs which represent the imprecise probability distribution of a random variable as depicted in Figure 4. It is able to consider all possible distribution types that might lie within these two bounds. This representation of uncertainty is very similar to the random set representation but they are structurally different, as will be discussed in Chapter 3. Using the p-box representation, two methods can be applied alternatively in combination with finite element analysis or any other computational tool for reliability analysis; 1) Monte Carlo-based solution (Zhang et al. 2010a) 2) discretised p-box (Zhang et al. 2010b).

In the **Interval Monte Carlo method**, as graphically illustrated in Figure 4a, one can randomly generate intervals for each RV of the problem using a standard uniform random number  $u_i$ . Upon each sampling, the problem is turned into an ordinary Interval Finite Element Analysis. Therefore, the system responses are obtained in the form of intervals and after a large number of realisations, the frequency distribution of the response’s intervals can be plotted, which look like input p-boxes.

In the **discretised p-box approach**, a uniform discretisation as depicted in Figure 4b is employed to split the p-box structure into several sets (the discretisation method is arbitrary) with equally associated probability assignments. From this stage on, the problem is treated like a random set analysis. Therefore, a Cartesian product of the generated sets or intervals is to be constructed for obtaining input intervals for all required realisations. Obviously in this method, the number of realisations depends on the number of subdivisions carried out in the discretisation method.

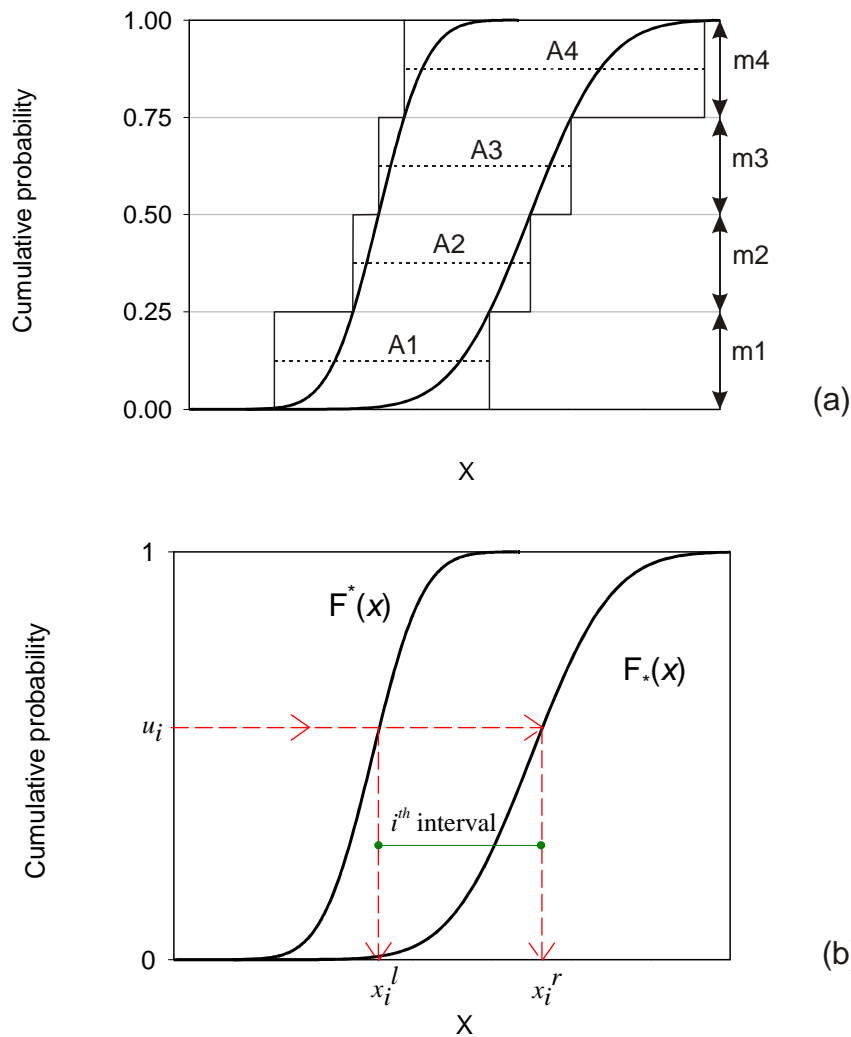


**Fig. 4:** Imprecise probability method based on p-box representation  
a) discretised probability-box, A1 to A4 are the produced focal elements with the respective probability assignments  $m_1$  to  $m_4$   
b) Monte Carlo-based random intervals (after Zhang et al. 2010b)

One of the disadvantages regarding this method is that basically imprecise probabilities are of interest, when scarce information is available and consequently two probability distributions required for upper and lower bounds are to be defined on the basis of subjective assumptions unless abundant set-

based observations would have been carried out. Secondly, a large amount of simulation is needed like any Monte-Carlo sampling method to give a correct answer.

## 2.4 Adopted approaches in this study

In this Chapter, a short summary of common methodologies for the evaluation of an uncertainty model in mechanical systems has been presented along with their main advantages and disadvantages. Basically the non-deterministic methods are divided into two main categories, non-probabilistic and probabilistic methods. In this work one method from each branch of the non-deterministic methods shown in Figure 2 has been selected. Although due to the characteristics of information usually available in tunnelling problems, in this study the Random Set Approach is proposed to deal with the uncertainties involved and the main emphasis has been given to this approach. On the other hand, Point Estimate Method is still appealing for engineering practice and therefore one chapter is devoted to evaluating the shortcomings and benefits of this probabilistic method in tunnelling.

The Random Set Finite Element Method (RS-FEM) and the Point Estimate Method will be explained further in detail in Chapters 3 and 6. In the following, a summary of arguments in employing these methods are mentioned.

### Random Set Approach

In short, in random set, set valued information (focal elements) with given probability measures (probability assignments) are combined together leading to probability bounds in terms of discrete cumulative distribution functions (CDF). The bounds comprise any distribution compatible with the existing data including the actual distribution. The Random set procedure maps the inputs onto the system response, also in terms of probability bounds. This approach has many similarities to other aforementioned non-probabilistic methods such as the fuzzy set and p-box approach. For instance, both random set and fuzzy set approaches are supported by set theory and interval analysis would be an integral part of their solution procedure. However, in Random Set the independence of the individual information sources are preserved while in the p-box approach a set is randomly taken by the Monte-Carlo process at each simulation. Random set is concerned with the probability of events while in fuzzy set, the possibility of events are measured.

Random Set Theory provides a powerful framework in which different sources of information may be combined, whereas it will be shown in the next section that fuzzy sets can convolute different information only when special conditions exist

(consonant sets are available). In this respect, random sets are more general than fuzzy set.

The random set is attractive in the sense that it enables engineers to consider both aleatory and epistemic types of uncertainty. On the other hand in tunnel engineering due to the linear nature of tunnel projects usually very limited investigation programs are available at the beginning of the design stage, which leads to very sparse and scarce data. Consequently, the geotechnical properties mostly appear in ranges without probability measures attributed across the ranges. In such conditions, the random set approach is proposed and preferable.

### **Point Estimate Method**

Point Estimate Method is one of the probabilistic methods. In brief, the probability distribution of input parameters is substituted by single values and their respective predefined weights. The uncertainty model is evaluated with the predefined sampling points and as a result, the statistical moments of system responses that are of interest, are estimated.

This method in the sense of simplicity (from a practical point of view) as well as its relatively low number of simulations is favourable, although there are disadvantages whose details are discussed in Chapter 6. Part of the study has been devoted to identify the possible limitations and merits of such a method in tunnel problems by comparison with the results of the random set approach.

## 3 Random Set Finite Element Method in Tunnelling

The random set theory developed by several authors (e.g. Kendall 1974, Matheron 1975, Goodman 1985, and Dubois 1991) has provided an appropriate mathematical model to cope with uncertainty while overcoming some of the drawbacks of "classical" probability theory, which is not well suited to deal with imprecise data. In practical geotechnical engineering, subjective assumptions about the probability density function of parameters are often made because in many cases the results of geotechnical investigations are set valued rather than being precise and point valued. Tonon et al. (1996, 2000a, b) used Random Set Theory (RST) to deal with the uncertainty in geomechanical classification of jointed rock masses and reliability analysis of a tunnel lining. Peschl (2004), Schweiger et al. (2007) have combined Random Set Theory with the finite element method, developing the Random Set Finite Element Method (RS-FEM), which is practiced in this Chapter. They illustrated the applicability of the developed framework to practical geotechnical problems and showed that in early design phases RS-FEM is an efficient tool for reliability analysis in geotechnics, being complementary to the observational method.

For tunnel excavation problems, numerical methods are frequently employed to assess both the stability and deformation behaviour. Material parameters for modelling the behaviour of the ground and the support measures are based on geotechnical investigations and frequently derived from experience. In order to account for uncertainties in material parameters, which are inevitable due to heterogeneities and the limitations of site investigation schemes, the scattering of in-situ behaviour is reflected in geotechnical design reports by defining values within a certain range. However, in numerical calculations this is commonly replaced by deterministic analysis with characteristic values and a limited variation of different parameter combinations. In order to do that, ground conditions are usually divided into homogeneous sections. It is shown in this chapter that the Random-Set-Finite-Element-Method (RS-FEM) provides a convenient tool to account for the scatter in material and model parameters (Tonon et al. 2000b) and thus can significantly increase the validity of numerical analyses. In addition, a comparison between calculation and field measurements allows an assessment of the quality of the geotechnical model whereas it has to be emphasized that in-situ measured values will also vary within a "homogeneous" section and thus are also available in ranges. The basic concepts of RST and RS-FEM procedures have been presented by Tonon (1996) and Peschl (2004), however, a summary of the most important aspects will be provided in the following section for continuity.



### 3.1 Concept of random set theory

Random set theory provides a general framework for dealing with set-based information and discrete probability distributions. It yields the same results as interval analysis, when only range information is available and under certain conditions similar to result of Monte-Carlo simulations (Peschl 2004).

Let  $X$  be a non-empty set containing all the possible values of a variable  $x$ . Dubois & Prade (1990, 1991) defined a random set on  $X$  as a pair  $(\mathfrak{S}, m)$  where  $\mathfrak{S} = \{A_i : i = 1, \dots, n\}$  and  $m$  is a mapping,  $\mathfrak{S} \rightarrow [0, 1]$ , so that  $m(\emptyset) = 0$  and

$$\sum_{A \in \mathfrak{S}} m(A) = 1 \quad (2)$$

$\mathfrak{S}$  is the support of the random set, the sets  $A_i$  are the focal elements and  $m$  is the basic probability assignment. Each set,  $A \in \mathfrak{S}$ , contains some possible values of the variable,  $x$ , and  $m(A)$  can be viewed as the probability that  $A$  is the range of  $x$ . As an example, each set  $A_i$  could be the result of an interval valued measurement and  $m(A_i)$  its relative frequency in a sample (see Tonon et al. (2000a) for an example of such a situation in rock engineering). Alternatively, the sets  $A_i$  could be ranges of a variable obtained from source number  $i$  with relative credibility  $m_i$ . Because of the imprecision, it is not possible to calculate the probability of a generic  $x \in X$  or of a generic subset  $E \subset X$ , but only lower and upper bounds on this probability. Random set theory is one of the theories that deal with *imprecise probabilities* (Walley 1991); in this case, imprecise probabilities are expressed by the intervals  $[Bel(E), Pl(E)]$  where the belief function,  $Bel$ , of a subset  $E$  is a set function obtained through the summation of basic probability assignments of subsets  $A_i$  included in  $E$ ; and the plausibility function,  $Pl$ , of subset  $E$  is a set function obtained through the summation of basic probability assignments of subsets  $A_i$  having a non-zero intersection with  $E$ . They are bounds for all possible probabilities of the event  $E$ .

#### 3.1.1 Bounds on the system response

Random set theory provides an appropriate mathematical framework for combining probabilistic as well as set-based information, in which the extension of random sets through a functional relation is straightforward (Tonon et al. 2000a). Let  $f$  be a mapping  $X_1 \times \dots \times X_N \rightarrow Y$  and  $x_1, \dots, x_N$  be variables whose values are incompletely known. The incomplete knowledge about the vector of basic variables  $\mathbf{x} = (x_1, \dots, x_N)$  can be expressed as a random relation  $R$ , which is a random set  $(\mathfrak{S}, m)$  on the Cartesian product  $X_1 \times \dots \times X_N$ . The random set  $(\mathfrak{R}, \rho)$ , which is the image of  $(\mathfrak{S}, m)$  through  $f$  is given by (Tonon et al. 2000b):

$$\mathfrak{R} = \{R_j = f(A_i), A_i \in \mathfrak{S}\}; \quad f(A_i) = \{f(\mathbf{x}), \mathbf{x} \in A_i\} \quad (3)$$

$$\rho(R_j) = \sum_{A_i: R_j = f(A_i)} m(A_i) \quad (4)$$

If  $A_1, \dots, A_n$  are sets on  $X_1 \times \dots \times X_N$  respectively and  $x_1, \dots, x_N$  are stochastically independent, then the joint basic probability assignment is given by

$$m(A_1 \times \dots \times A_n) = \prod_{i=1}^n m_i(A_i), \quad A_1 \times \dots \times A_n \in \mathfrak{R} \quad (5)$$

If the focal set  $A_i$  is a closed interval of real numbers:  $A_i = \{x \mid x \in [l_i, u_i]\}$ , then the lower and upper cumulative probability distribution functions, respectively  $F_*(x)$  and  $F^*(x)$ , can be obtained given by Equations 6 and 7 at some point  $x$  which are illustrated in Figure 5.

$$F_*(x) = \sum_{i: x \geq u_i} m(A_i) \quad (6)$$

$$F^*(x) = \sum_{i: x \geq l_i} m(A_i) \quad (7)$$

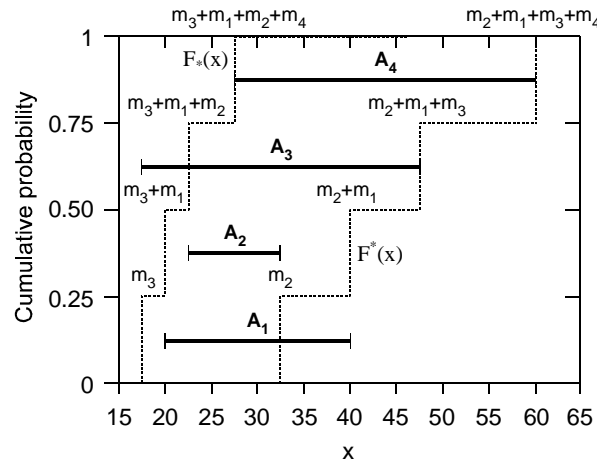


**Fig. 5:** Upper and lower bounds of random set input (after Peschl, 2004)

The basic step is the calculation of the image of a focal element through the function  $f$  by means of Equations 3, 4. The requirement for optimisation in order to locate the extreme elements of each set  $R_j \in \mathfrak{R}$  (Equ. 3) can be avoided if it can be shown that the function  $f(A_i)$  is continuous in all  $A_i \in \mathfrak{S}$  and also no extreme points exist in this region, except at the vertices, in which case the methods of interval analysis are applicable, e.g. the Vertex method (Dong & Shah 1987).

$$f(A_i) = [l_i, u_i] \quad (8)$$

Assume each focal element  $A_i$  is an  $N$ -dimensional box, whose  $2^N$  vertices are indicated as  $v_k$ ,  $k = 1, \dots, 2^N$ . If the vertex method applies, then the lower and upper bounds  $R_{j*}$  and  $R_j^*$  on each element  $R_j \in \mathfrak{R}$  will be located at one of the vertices:

$$R_{j*} = \min_k \{f(v_k) : k = 1, \dots, 2^N\} \quad (9)$$

$$R_j^* = \max_k \{f(v_k) : k = 1, \dots, 2^N\} \quad (10)$$

Thus function  $f(A_i)$ , which represents a numerical model in the RS-FEM framework, has to be evaluated  $2^N$  times for each focal element  $A_i$ . The number of all calculations,  $n_c$ , required for finding the bounds on the system response is:

$$n_c = 2^N \prod_{i=1}^N n_i \quad (11)$$

Where  $N$  is the number of basic variables and  $n$  the number of information sources available for each variable.

In order to combine these sources an appropriate procedure is required if more than one source of information is available for one particular parameter. Suppose there are  $n$  alternative random sets describing some variable  $x$ , each one corresponding to an independent source of information. Then for each focal element  $A \in X$

$$m(A) = \frac{1}{n} \sum_{i=1}^n m_i(A) \quad (12)$$

### 3.1.2 Types of random set and visualisation

A random set, evidence or sets of information can be represented in three different formats as follows:

1. Random intervals with their respective basic probability weights
2. Contour function or plausibility of singleton.
3. Lower and upper cumulative distribution functions or p-box

The first type of random set format preserves the most information in itself, whereas the other two formats, despite having some advantages, lose some

information relating to the original sets. For instance, an infinite number of random sets containing different focal elements can be fitted into certain  $Pl(E)$  and  $Bel(E)$  functions given in the format of a contour function or p-box, where  $E$  is an arbitrary event.

An alternative to the visualisation of a random set can be presented through its contour function (Shafer, 1976) over the basic variable  $x$ , assigning each singleton  $x$  its plausibility;  $x \rightarrow Pl(\{x\})$ . This contour function is obtained by summing up the probability assignments  $m_i$  of those focal elements  $A_i$  to which  $x$  belongs. Figure 6 depicts a random set composed of 4 focal elements and the corresponding contour function which in some references are called the plausibility of singleton  $x$ .

A random set is presented in terms of contour functions when it is either composed of a family of confidence intervals (Fetz and Oberguggenberger, 2009) using Tchebycheff's inequality or all focal elements are nested. From the contour function, one can readily derive the possibility function or membership function of a fuzzy set equivalent to the random set.

Four types of random set are considered from multiple sources that one might encounter in practice: 1) consonant sets, 2) consistent sets, 3) arbitrary sets, and 4) disjoint sets.

**Consonant sets** can be represented as a nested structure of sets where the elements of the smallest set are included in the next larger set, all of whose elements are included in the next larger set and so on. This can correspond to the situation where the information obtained over time increasingly narrows or refines the size of the sets. On the other hand, if the configuration of the random set lies within the next three categories, it is called a dissonant type of random set.

**Consistent sets** insinuate that there is at least one focal element that is common to *all* sets.

**Arbitrary sets** correspond to the situation where there is no focal element common to *all* sets, though some sets may have elements in common. One possible configuration has been illustrated in Figure 7.

**Disjoint sets** imply that any two focal elements have no common elements in any other set.

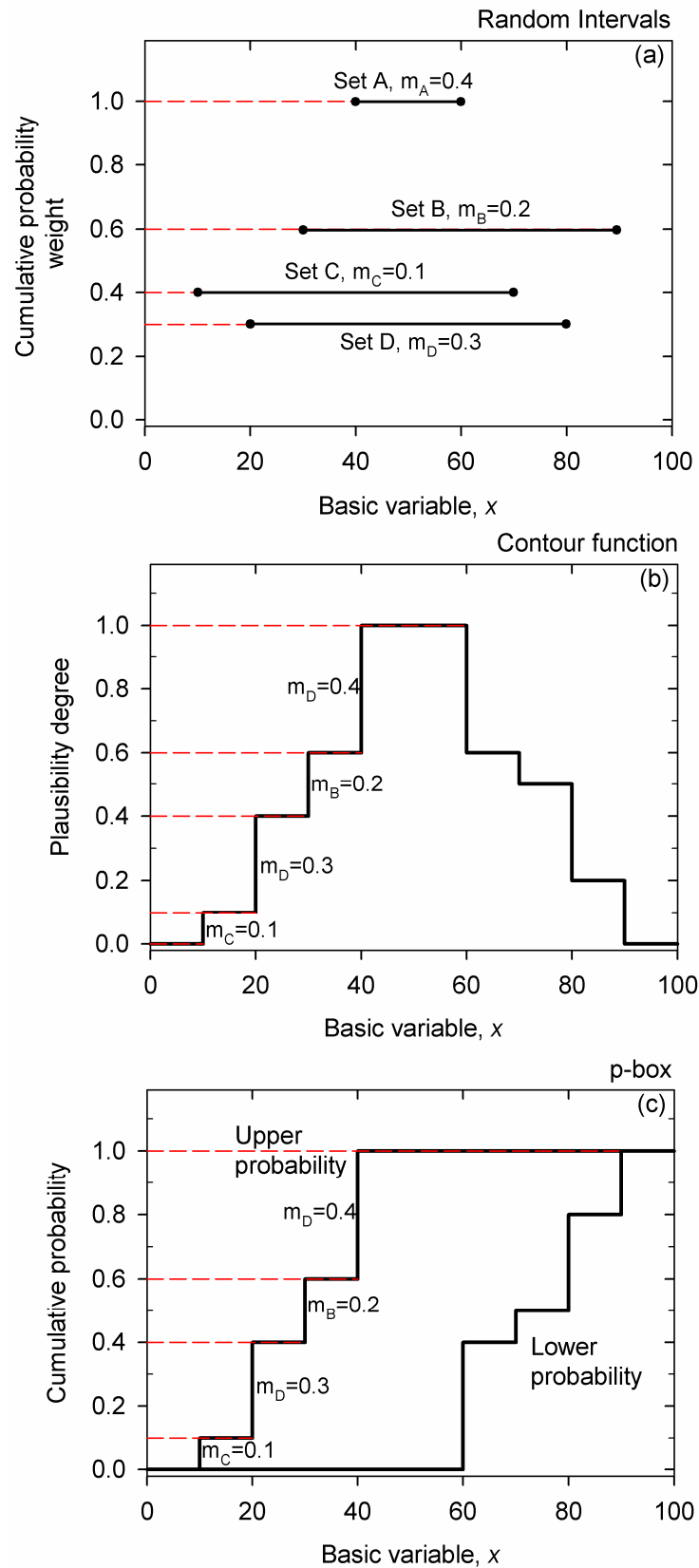


**Fig. 6:** Types of random set visualisation: a) random interval b) contour function c) p-box

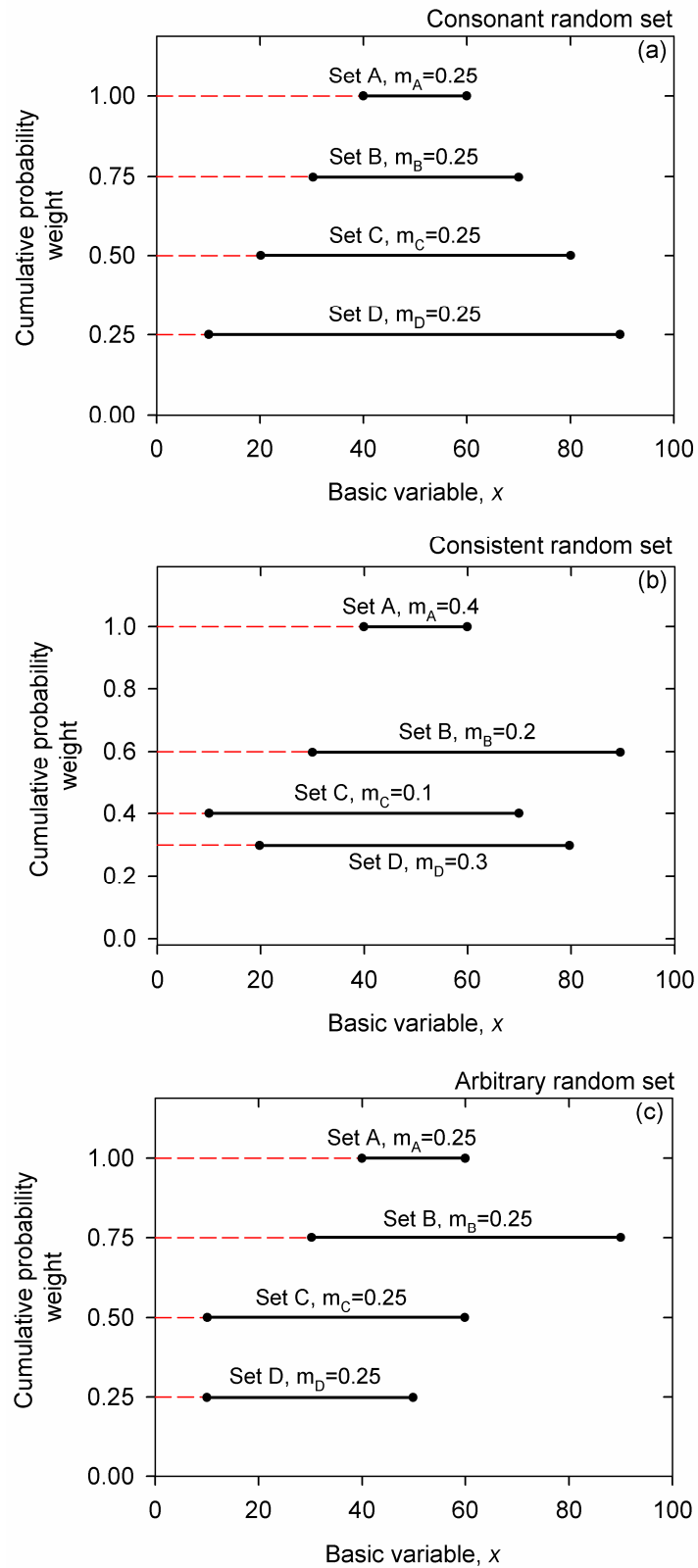


**Fig. 7:** Types of random set: a) consonant b) consistent c) arbitrary

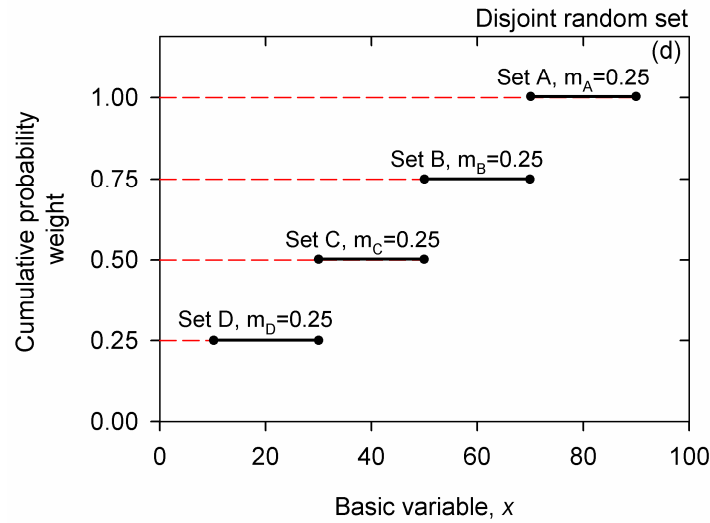


**Fig. 7:** continued, Types of random set: d) disjoint

### 3.2 Procedure of the RS-FEM

The merits of numerical modelling using the Finite Element Method in estimating deformations and internal forces of complex geomechanical structures are evident. The Finite Element Method has obtained considerable reputation over the last decades in solving practical problems by introducing advanced constitutive models, which can describe the material behaviour more accurately. Particularly in tunnelling problems -which in this work are the main concern- a very limited number of closed form solutions are available. They are very simplified and valid only under specific conditions (e.g. unsupported circular deep tunnel surrounded by a single layer homogeneous material) and also they are not capable of considering all aspects of underground structures' behaviour. Moreover, other methods such as limit equilibrium and limit analysis theorems have limitations in assessing all aspects of ground behaviour and accordingly have limited usability in reliability analysis. This study takes advantage of both FEM and the concepts of random set analysis to accommodate a procedure in which a reliability analysis can be performed. Reliability analysis is of great importance especially in the case of scarce data, where a sufficiently accurate probability distribution function cannot be provided to perform a full probabilistic reliability analysis. Another advantage of RS-FEM is that there is no need to modify the available Finite Element Codes, and any commercial FE software can be used for performing the required deterministic calculations. Figure 8 graphically illustrates the items that should be followed in the RS-FEM and are summarized in the steps below:

1. Defining the geometry or geometries of the problem, the preparation of the respective master files and the FE model, selecting an appropriate constitutive model for material and support elements.
2. Selecting the input parameters that should be considered as basic variables in the random set analysis and providing the expected ranges from different sources of information (random sets).
3. Uncertainty reduction over the selected random sets, which show spatial variability considering the length of the possible failure mechanism in the model. This step requires the determination of spatial correlation length as well as an estimation of the length of the possible failure line.
4. RS-FEM has exponential complexity, which means the computational cost increases proportional to  $2^N$  ( $N$  is the number of basic random variables). This entails employing a sensitivity scheme to identify the variables that have negligible effect on desired results even if there is a wide uncertainty on them, in order to reduce the computational effort.
5. Computation of the calculation matrix, which includes the defined parameter combinations, the preparation of deterministic FE files and the relevant probability share of the individual calculation considering the dependencies (correlation coefficients) between the basic random variables involved (see Peschl 2004).
6. Finite element calculations and determination of results such as stresses, strains, displacements and internal forces in support elements in terms of bounds on discrete cumulative probability functions, which may be compared to measured data once they become available. Subsequently fitting the resulted CDF's using the best-fit methods, in order to achieve a continuous distribution function. For this step, commercial software such as the package @RISK<sup>®</sup> (Palisade, 2008) can be employed.
7. Definition of suitable performance functions. This definition is of paramount importance and is a crucial step in the analysis. For example a function can be defined over the critical deformations such as tunnel crown displacement to control the required clearance of the tunnel and/or maximum stresses carried by shotcrete lining. The performance function can be evaluated with results (bounds on continuous distribution functions of the evaluated system parameters) from the finite element calculations, in order to obtain a range for the probability of failure or unsatisfactory performance.



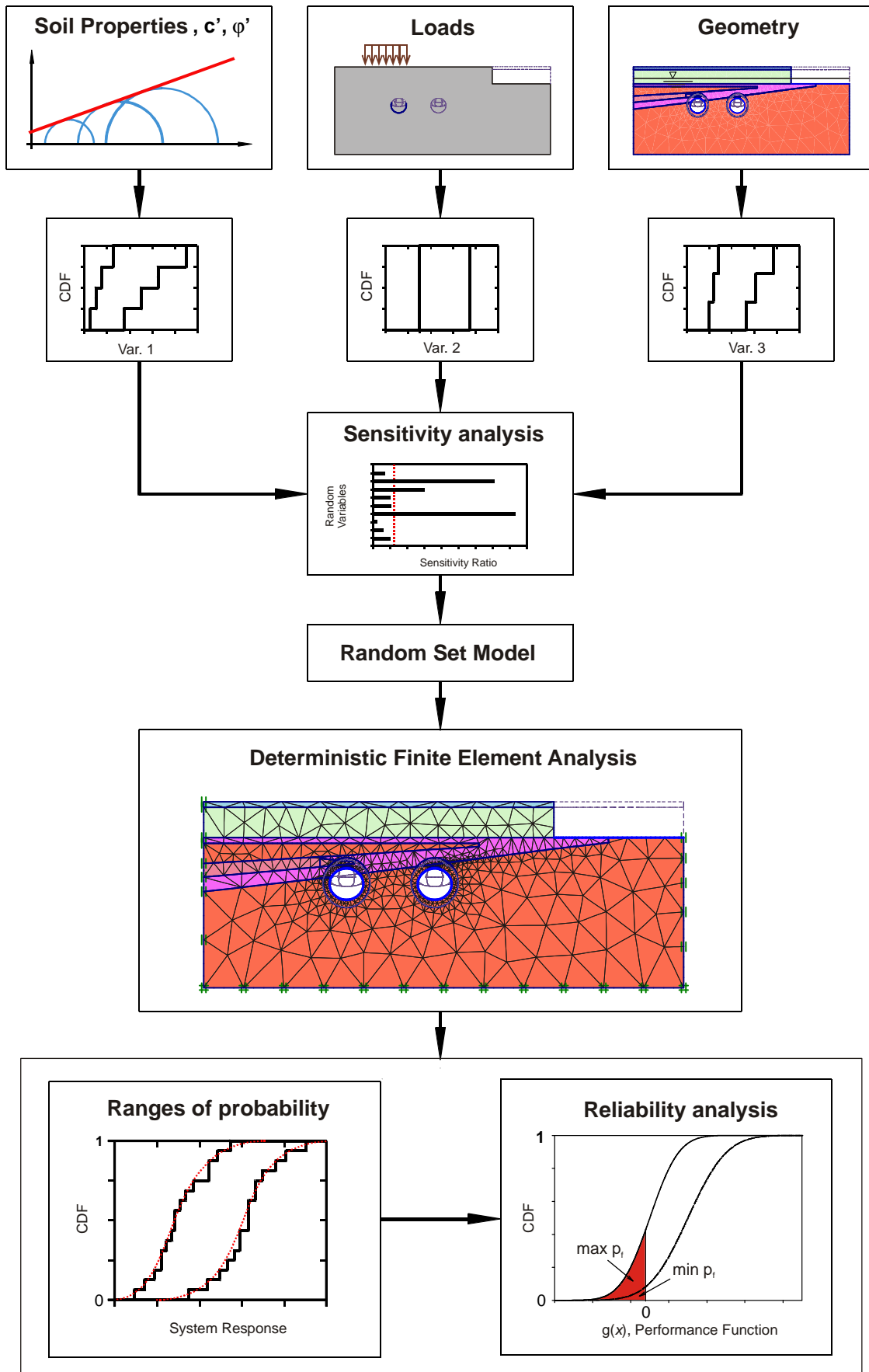


**Fig. 8:** RS-FEM procedure (Modified from Peschl, 2004)

Basically preparation of a master file is required to incorporate all the important specifications of the tunnel problem. The master file should be evaluated before start of the duplication in order to construct all the deterministic FE files, to be assured that it can numerically model the actual behaviour of the system as accurately as possible. Next, this master file is duplicated as required according to the calculation matrix. If a geometry uncertainty is involved, several master files must be prepared based on different geometry models. The finite element code Plaxis V9 (Brinkgreve & Broere, 2008) is utilised for all the random set finite element calculations given in this thesis. An appropriate pre- and postprocessor is required for the preparation of input files and retrieving the FE results, to minimize manual labour time. To do so, one can take benefit of the calculation manager and sensitivity option in the calculate menu of Plaxis, which facilitates performing successive calculations and extracting the desirable FE results for further reliability analysis. In addition, appropriate Excel files have been generated to prepare the calculation matrix, the material needed for input files and to present the results in terms of lower and upper discrete cumulative distribution functions.

The application of RS-FEM analysis in tunnelling is illustrated through a case study in the following section. The objective of this chapter is to demonstrate efficiency, applicability and convenience of such analysis prior to tunnel construction. Furthermore, in combination with the observational method the current procedure can be considered a tool using information -that is constantly being updated by newer observations- to control the efficiency of support elements.

### **3.3 Principles of NATM and historical background**

When excavating tunnels according to the principles of the New Austrian Tunnelling Method (NATM), it is aimed to preserve and improve the potential of the ground to support itself by utilising an arching effect in the surroundings of the tunnel as much as possible. Therefore, a certain amount of deformation of the tunnel cross section has to be allowed, while on the other hand, too large deformations that lead to the loosening of the ground have to be avoided to arrive at an equilibrium.

Following the NATM principles in poor or difficult ground conditions, to provide sufficient stability at construction stage, the tunnel cross section is frequently divided into several phases. Various excavation sequences have been applied in practice to provide the required stability and to avoid excessive settlement and disintegration of ground material surroundings of the excavation area. One of the typical NATM construction sequences for middle-size cross

sections in which the tunnel's width is not so wide, consists of three major phases namely top-heading, bench, and invert.

For the first time Rabcewicz (1962) introduced a new concept and philosophy of tunnelling in a lecture at the Geomechanics Colloquium in Salzburg and 2 years later he published the English version of that in 1964 entitled "The New Austrian Tunnelling Method", and emphasised the role of the surrounding rock as a part of the tunnel support system which is believed to be the key principle of NATM. Rabcewicz, Müller and Pacher are often referred to as the "fathers" of the NATM. Since 1972, the hypothesis of Pacher (1964) concerning the trough shaped ground response curve, the minimization of the rock pressure, and the lining thickness based upon it has become more and more central to the concept of the NATM (Karakus and Fowell 2004). Müller had also large contribution to NATM in his professional career by publishing several papers to establish the NATM principles, avoiding misunderstandings in NATM concepts, and removing the misconceptions (e.g. Müller 1978 and 1990).

The three most important design principles of NATM, which can be derived from many references, e.g. Health and Safety Executive (1996), Müller (1990), Schubert et al. (2000), can be summarized in the following concepts:

1. The tunnel lining and the construction sequence should be designed in such way that ground around the excavation could carry the overburden as much as possible, on the basis of arching effects and plastic stress redistribution, which naturally occurs due to excavation in the ground; and a relative light primary lining consists of sprayed shotcrete in combination with rock bolts (if required) should carry the rest and provide a safety required for performance of the tunnel structure.
2. The displacements should be controlled and be kept within two limits to accommodate the following two purposes:
  - The lower limit of displacement is set in a manner to purposely designate the ground a major contribution of the overburden - before the installation of the lining- in order to achieve a lighter retaining structure and subsequently an economical tunnelling. In addition, it implies that deformations should not be completely stopped by the support right after installation and the structure needs to be relatively flexible. The case of shallow tunnels situated in urban areas is an exception, in which even small amounts of displacement are not allowed to occur in order to control the surface settlement trough.
  - The upper limit of displacement is required to avoid the deformations going beyond a critical level, where disintegration (loosening) of the rock mass/soil occurs. The deformation

constraints regarding the performance of the structure or allowable surface settlement should be satisfied.

A systematic deformation measurement is required to evaluate the assumed or predicted behaviour of the rock mass and the retaining system, to observe the stabilization process and provide information for optimisation of supports and measures. Despite the development of analysis tools the reliability of the preliminary design is still low because of 1) the existence of a number of uncertainties in the ground model 2) the difficulties to assess the ground properties in an appropriate manner. Therefore, observation during construction should be considered as an integral part of the method to appropriately adjust the excavation method and support to the ground conditions.

### **3.4 Application of RS-FEM to tunnel excavation case study**

To demonstrate the applicability and efficiency of RS-FEM in geotechnical practice, a real case study has been chosen, namely a tunnel excavation located in the south of Germany. The original design has been accomplished by means of a conventional deterministic approach on the basis of characteristic material properties. Random set approach was carried out to estimate the most probable ranges of results considering the existing uncertainty based on the state of knowledge prior to the start of the construction. In this analysis, particular attention is given to two important issues in tunnelling; first, tunnel closure or convergence for the matter of maintaining the clearance of the tunnel section; and second, satisfactory performance of shotcrete lining regarding safety issues. Ultimately in this Chapter, the advantages of the current approach will be identified by performing these analyses and comparing them to the standard design approaches and the measured values.

The tunnel has a cross section of 15×12.3 m width and height respectively, and has a total length of 460 m. The overburden along the tunnel axis varies between 7.5 to 25 m. It is excavated according to the principles of the New Austrian Tunnelling Method (NATM) with three main construction phases to be considered in the analysis: excavation of top heading, excavation of bench and finally the invert. NATM principles and historical background are briefly introduced in the next section. In general, the tunnel is situated in a hard rock mass except for the portal areas (zone I) and a limited zone located about 130m away from the portal of the tunnel where the rock mass has been faulted (zone III) and weathered rocks are prevailing. Considering these differences in ground conditions, three homogeneous zones, indicated as I, II and III in Figure 9 can be identified. In this chapter focus is on zone I where ground conditions are less favourable and the overburden is low (7.5 m). For this section it is justified to consider the rock mass as homogeneous material. Due to the fact that the original

design has been made employing a simple Mohr-Coulomb constitutive model, this has been preserved in the RS-FEM analysis.

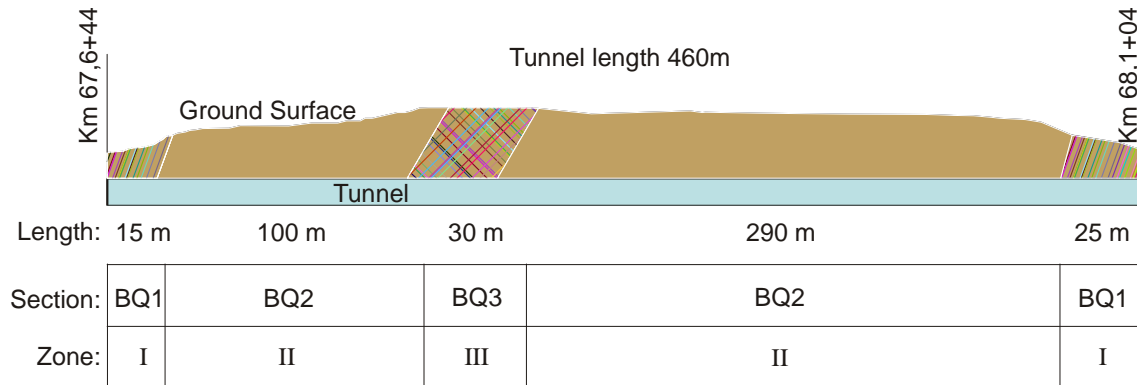


**Fig. 9:** Longitudinal profile of the tunnel

The geometry and finite element mesh including some model specifications are illustrated in Figures 10 and 11. Approximately 670 15-noded triangular elements have been used.

In the geotechnical report the material parameters have been specified in ranges, which are summarized in Table 1. The design of section BQ1 has been based on a deterministic finite element analysis using the parameters presented in Table 1, which are within the aforementioned range. Elastic beam elements and elasto-plastic geomembrane elements were used to model the shotcrete lining and anchors respectively. The specifications of the structural elements are summarized in Table 2.

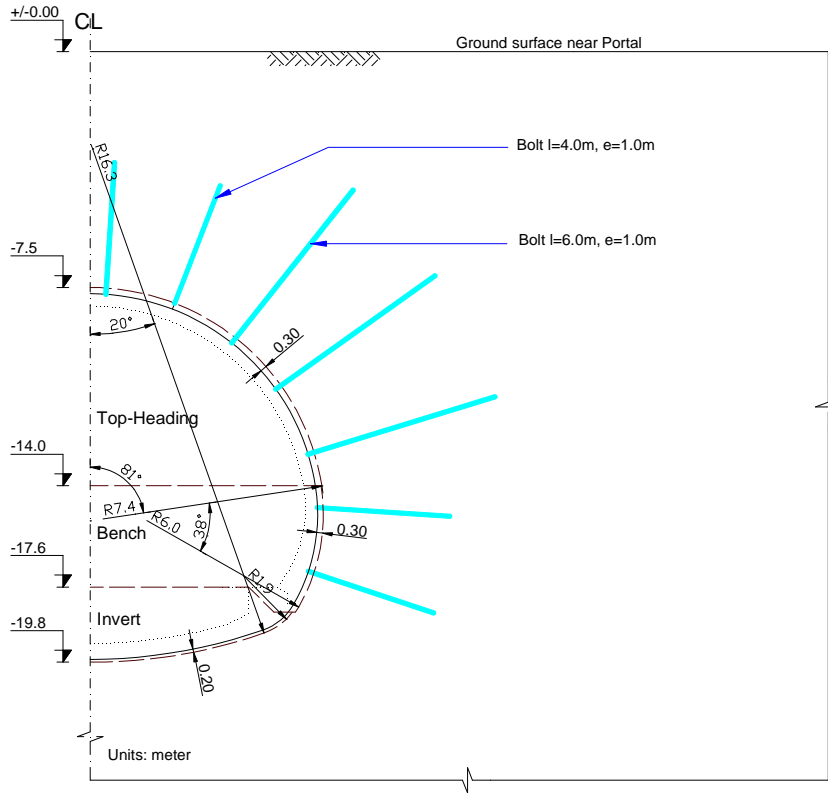


Fig. 10: Geometry of the tunnel

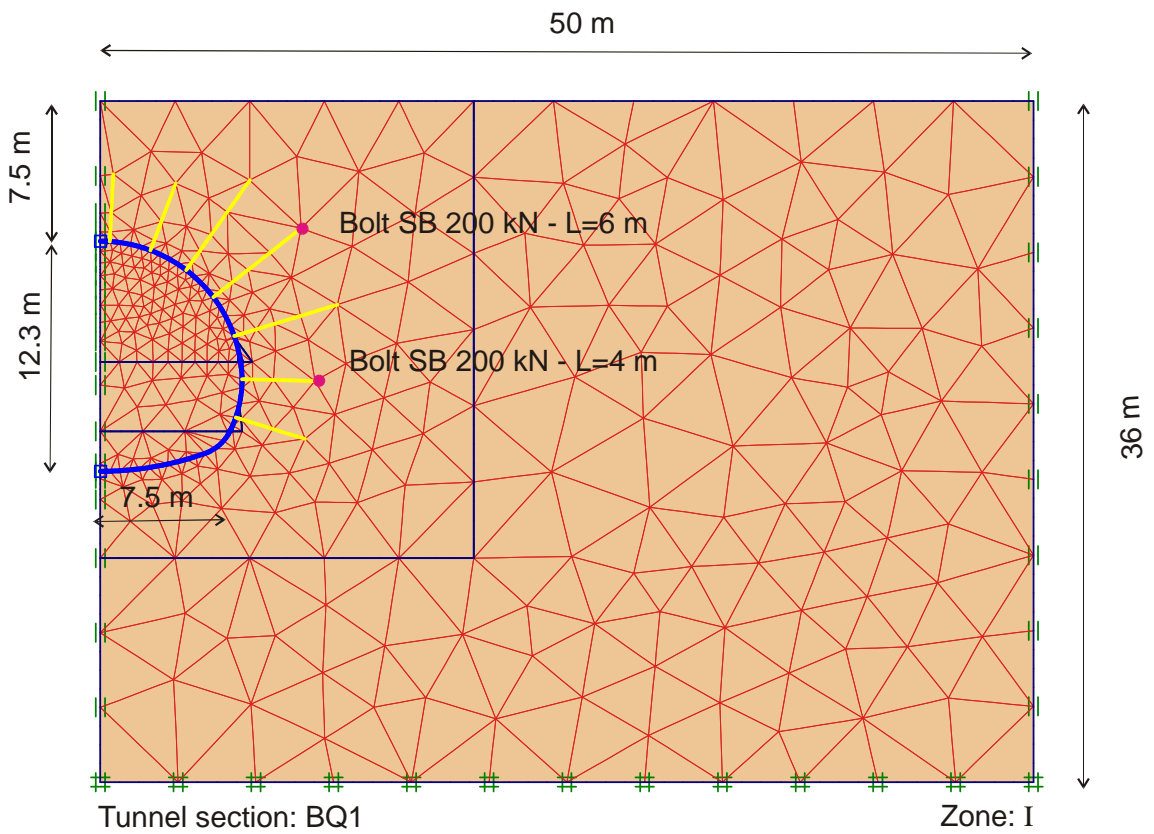


Fig. 11: Tunnel section BQ1 in 2D finite element mesh

**Tab. 1:** The range and reference value of MC-model parameters extracted from geotechnical report for zone I

Parameter	Zone	$\gamma$	$E_{ref}$	$c$	$\varphi$	$K_0^{nc}$	$\nu$
		[MN/m <sup>3</sup> ]	[MN/m <sup>2</sup> ]	[kPa]	[°]	[-]	[-]
Range	I	24	75-150	50-80	20-22	0.4-0.6	0.35
Ref. value	I	24	125	70	21	0.5	0.35

**Tab. 2:** Parameters for structural elements

Support element	Location	Type	$E$ -modulus		Plastic Limit Force	Thickness /Diameter
			young	old		
			[MPa]		[kN]	[cm]
Shotcrete	Top-heading	Elastic	5000	15000	-	30
Shotcrete	Bench	Elastic	5000	15000	-	30
Shotcrete	Invert	Elastic	5000	15000	-	20
Anchor	T.H., B., I.	Elasto-plastic	210000		200	2.2

### 3.4.1 Procedure for determining basic variable sets in a random set model

In order to determine the required sets used in the random set analysis, the following four steps have to be considered:

#### 3.4.1.1 Determination of basic variables

First, all model parameters and material properties that are considered to have a pronounced effect on the system response have to be identified by engineering judgement and this is not always done easily. In the present study, 6 important parameters were selected for further analysis, namely the angle of internal friction  $\varphi$ , the effective cohesion  $c$ , the coefficient lateral earth pressure  $K_0$ , the stiffness modulus from one-dimensional compression tests  $E_s$ , the Young's modulus of young shotcrete  $E_{sh}$  as well as the relaxation factor  $R_f$  which takes the 3D effects of the construction process into account in an approximate manner in the 2D model. The choice depends on the problem at hand and if in doubt whether or not a particular parameter plays a significant role, it should be

included at this stage because as will be shown in the section 3.4.1.3, a rigorous assessment of the influence of each parameter is carried out.

The random sets are collected for each basic variable in form of ranges from reliable sources such as geotechnical reports, expert opinion, comparison of similar projects, and the literature. At least two sets are desirable for the basic variables in order to produce results in the form of reasonable probability distributions; otherwise the outcome will appear as a simple interval.

**Tab. 3:** Basic variables of rock mass, relaxation factor,  $R_f$ , lateral earth pressure coefficient at rest,  $K_0$ , shotcrete elastic modulus of young,  $E_{sh}$

Set No.	Probability assignment	$E_s$ MN/m <sup>2</sup>	$c$ kPa	$\phi$ °
1	0.5	75-150	50-80	20-22
2	0.5	100-200	60-90	18-24
Design value	-	125	70	21

**Tab. 3:** Continued

Set No.	Probability assignment	$E_{sh}$ GPa	$K_0^{nc}$ -	$R_f$ Phase No.		
				1	2	3
1	0.5	3-6	0.4-0.6	0.4-0.6	0.3-0.5	0.2-0.4
2	0.5	4-7	0.5-0.7	0.3-0.5	0.2-0.4	0.1-0.3
Design value	-	5	0.55	0.5	0.25	0.25

Here, the basic variables are obtained from two sources, first, from the geotechnical report, which is based on a number of laboratory and in-situ tests and second, from expert knowledge that is derived from previous experiences of similar projects. They are summarised in Table 3. In principle, a different probability assignment to each set can be defined in case one recognises that some sources are more reliable in comparison with others. In this case, probability assignments of both sources are equal to 0.5, which means there is no preference and both data sources have equal influence on results.

The basic variables are illustrated in Figure 12 and 13 in terms of upper and lower cumulative distribution for both original data sets and spatially correlated ones. To allow for spatial variability of the soil parameters, a modification is carried out on primary data sets using variance reduction technique, which is explained in the next section.



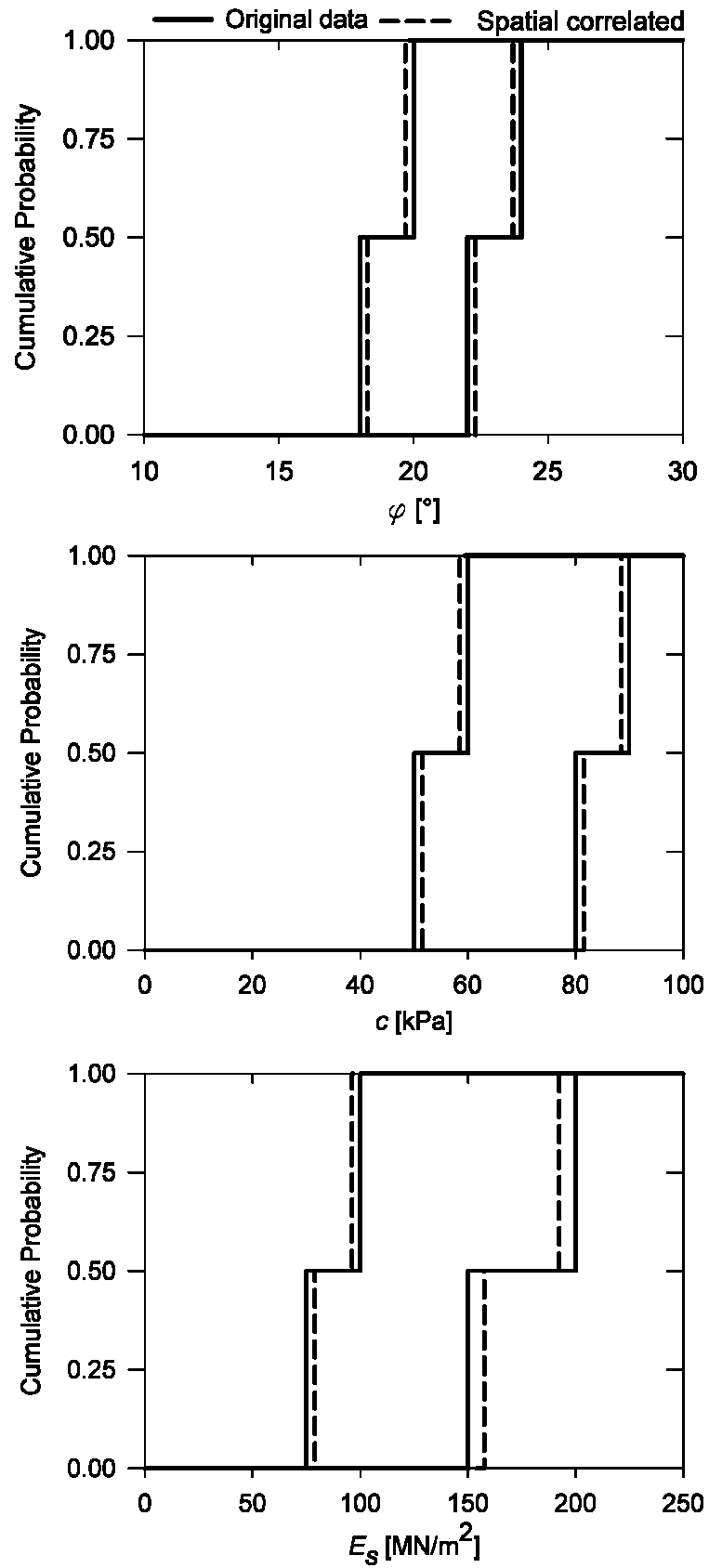


**Fig. 12:** Random sets of input parameters: friction angle,  $\varphi$ , cohesion,  $c$  and elastic modulus of rock mass,  $E_s$

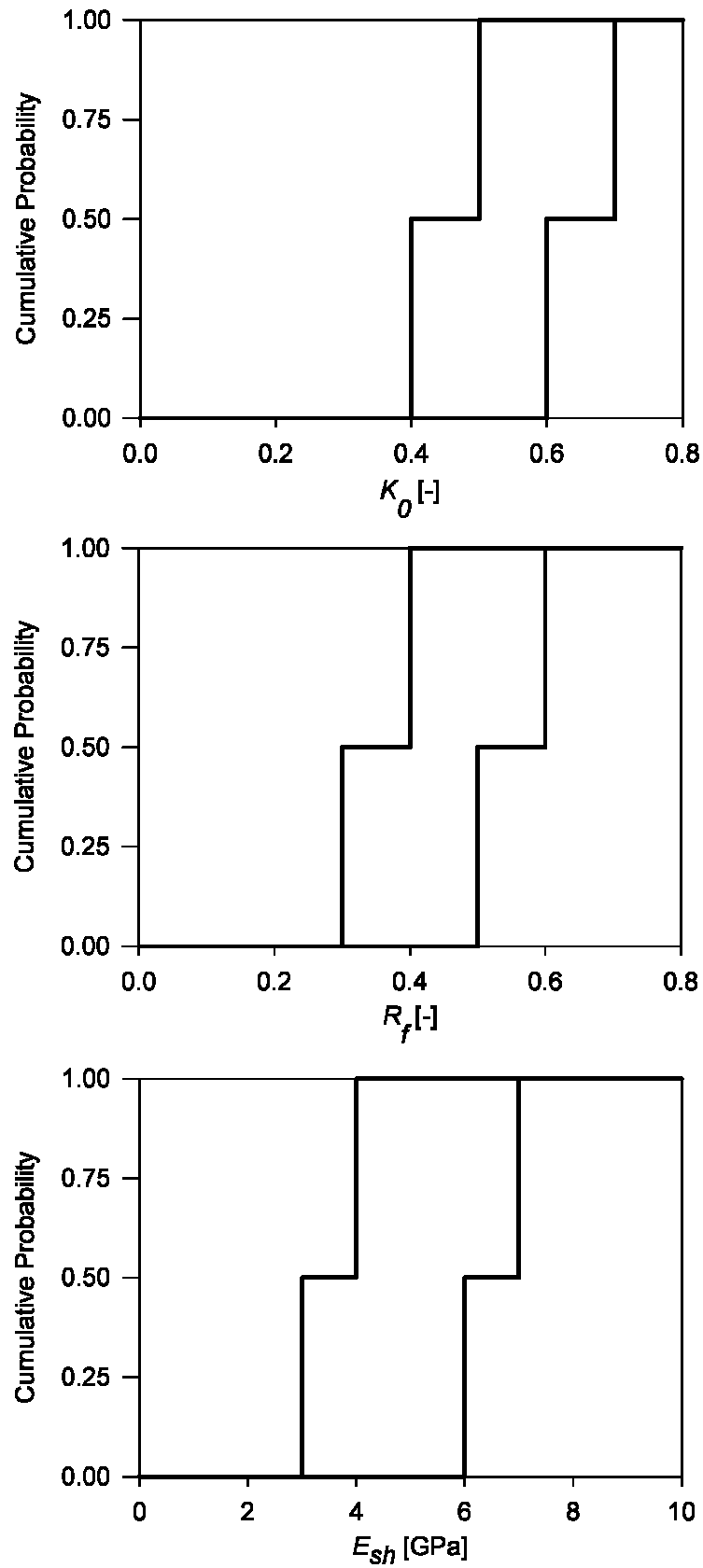


**Fig. 13:** Random sets of input model parameters: earth pressure coefficient at rest,  $K_0$ , Relaxation factor,  $R_f$  and shotcrete elastic modulus of young,  $E_{sh}$

### 3.4.1.2 Variance reduction technique

It is well-known that the variance of soil properties of large specimens or in-situ tests that mobilise a large volume of soil is less than that of small specimens or in-situ tests that mobilise only a small soil volume. Accordingly, it is possible to reduce the uncertainty of soil properties in a boundary problem value by means of the variance reduction technique. Vanmarcke (1983) proposed the variance reduction factor which can be estimated by a simple formula leading to a relation between the reduction factor and the distance over which the soil parameter is averaged (Equ. 13).

$$\Gamma^2 = \left[ \frac{\Theta}{L} \left( 1 - \frac{\Theta}{4L} \right) \right] \quad \text{for} \quad \frac{\Theta}{L} \leq 2 \quad (13)$$

Here  $\Gamma$  = variance reduction factor;  $\Theta$  = spatial correlation length;  $L$  = length of a potential failure surface.

In this study, an alternative approach based on the Vanmarcke method, suggested by Schweiger & Peschl (2005) has been adopted that applies the variance reduction technique for the random set theory. If  $n$  sources of information are assumed, the function of the spatial average of the data  $x_{i,\Gamma}$  can be calculated from the discrete cumulative probability distribution of the field data  $x_i$ , using  $\Gamma$  from Equation 13 as given in Equations 14 and 15.

$$x_{i,\Gamma} = x' - (x' - x_i) \cdot \Gamma \quad (14)$$

$$x' = \frac{1}{n-1} \cdot \sum_{i=1}^{n-1} \frac{(x_{i+1} + x_i)}{2} \quad (15)$$

**Tab. 4:** Basic variables used in RS-FEM considering spatial variation

Set No.	$E_s$	$c$	$\varphi$
	MN/m <sup>2</sup>	kPa	°
1	79-158	52-82	19.7-22.3
2	96-192	58-88	18.3-23.7

Typical values of spatial correlation lengths,  $\Theta$ , for soils as given e.g. by Li & White (1987) are in the range 0.1 to 5 m for  $\Theta_y$  and from 2 to 30 m for  $\Theta_x$ . The spatial correlation length for this study is assumed to be 10 m. Applying the described procedure leads to a slight change in the parameters of the basic

variables, which are summarised in Table 4 and depicted in Figure 12 in the form of discrete cumulative probability distributions.

### 3.4.1.3 Sensitivity analysis

The main purpose of the sensitivity analysis the following:

1. Identifying the most influential input parameters governing the desirable system responses.
2. To investigate the monotonic behaviour of the mechanical system

The reduction of the number of basic variables, which are actually considered in the formal RS-FEM analysis, is accomplished by means of a sensitivity analysis. This is essential in order to reduce the number of required finite element runs. For instance 1024 finite element runs are required if 5 basic variables with two sets each are taken into account (see Equ. 11) while this amount is decreased to 256 runs in case of 4 basic variables.

A relatively simple sensitivity method given by U.S. EPA: TRIM (1999) is used, which has been extended and made compatible with the random set approach by Peschl (2004). In this method three major coefficients, namely *sensitivity ratio* (Equ. 16), *sensitivity score* (Equ. 17) and *relative sensitivity* (Equ. 18) of each input variable with respect to any system response are calculated. Figure 14 illustrates the parameters used in the formulas 16-18. The ratio of the change in model output per unit change of an input variable is called sensitivity ratio. In the process of random set analysis, sensitivity analysis is recommended to be carried out over both a small and a large amount of change in input variables which are called local and range intervals respectively (Fig. 14). For instance, in the calculation of range sensitivity ratio, an input variable,  $x_R$ , is varied across the entire range of the random set. As it can be seen from Figure 14, the results can be also used to some extent in recognizing the monotonicity of the system response. The total number of  $4N+1$  calculations are needed to accomplish the sensitivity analysis.

$$\eta_{SR} = \left| \frac{\left[ \frac{f(x_{L,R}) - f(x)}{f(x)} \right]}{\left[ \frac{x_{L,R} - x}{x} \right]} \right| \quad (16)$$

When the sensitivity ratio is weighted by some characteristic of the input variable (e.g. standard deviation over mean,  $\sigma/\mu$ ) the sensitivity score will be obtained, which makes the sensitivity ratio independent from the units of the variable. In this work, the ratio of total range over reference value,  $x$ , is used instead of  $\sigma/\mu$ .

$$\eta_{SS} = (\eta_{SR, x_R^{lo}} + \eta_{SR, x_R^{up}} + \eta_{SR, x_L^{lo}} + \eta_{SR, x_L^{up}}) \cdot \frac{(x_R^{lo} - x_R^{up})}{x} \quad (17)$$

After the calculation of the sensitivity score of each variable,  $\eta_{SS,i}$ , on respective results  $A, B, \dots$  (e.g. displacements, forces, factor of safety and etc.) the sensitivity matrix is constructed as shown in Table 5. The sensitivity score of each input variable on a system response (e.g. displacement,  $A$ ) at all construction steps can simply be added up to be representative  $\eta_{SS,Ai}$  for the whole construction sequence. Then the relative sensitivity of the system response  $A$  is obtained as follows:

$$\alpha_A(x_i) = \frac{\eta_{SS,Ai}}{\sum_{i=1}^N \eta_{SS,Ai}} \quad (18)$$

Finally, the total relative sensitivity,  $\alpha(x_i)$ , for each input variable is given by

$$\alpha(x_i) = \frac{\sum \eta_{SS,i}}{\sum_{i=1}^N \sum \eta_{SS,i}} \quad (19)$$

Depending on what kind of performance function is going to be evaluated, a respective relative sensitivity should be taken into account. For instance, the relative sensitivity of a certain variable,  $\alpha(x_1)$ , concerning the displacement of the tunnel crown is negligible while the same variable has significant influence (high relative sensitivity) on another result e.g. the safety factor of the top-heading. Thus, considering merely the total relative sensitivity could be misleading in evaluating the influential parameters, although utilizing the sensitivity score can reduce the effect of input variable units. In order to make a sound decision concerning the parameters that are of significance, it is suggested to look at both the total relative sensitivity and relative sensitivity of an individual system response.

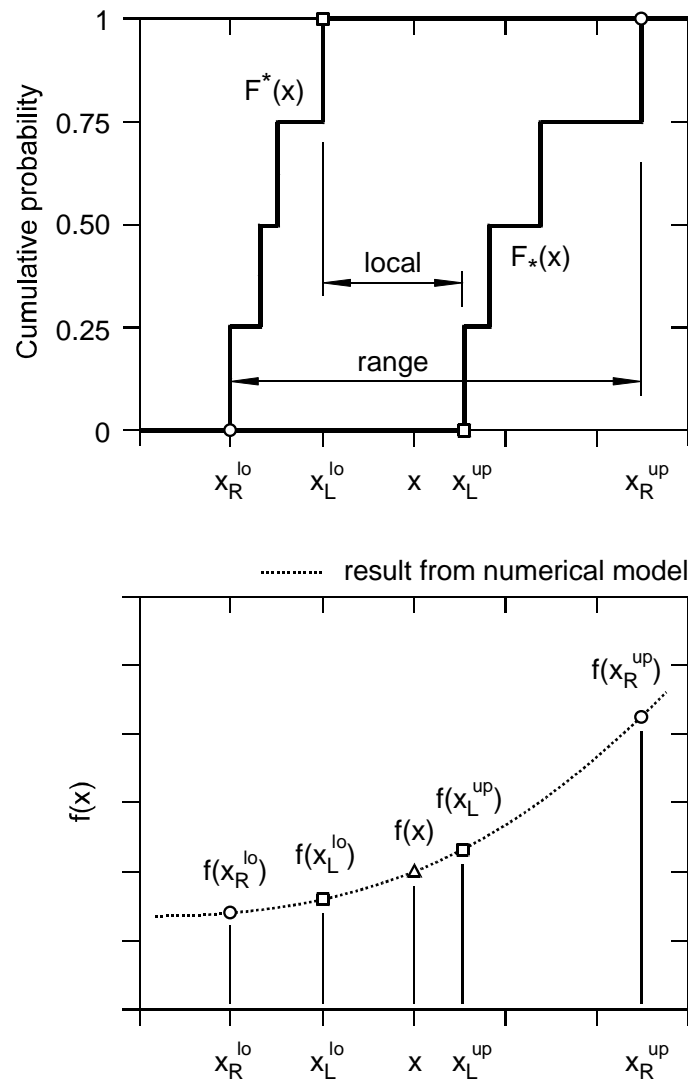


**Fig. 14:** An illustration of target functions with different sensitivities with respect to input variable  $x$  (after Peschl, 2004)

**Tab. 5:** Sensitivity matrix

Input variables	System response results						Total sensitivity $\alpha$ [%]
	A	$\alpha_A$ [%]	B	$\alpha_B$ [%]	...	$\Sigma$	
$x_1$	$\eta_{SS,A1}$	$\alpha_A(x_1)$	$\eta_{SS,B1}$	$\alpha_B(x_1)$	...	$\Sigma\eta_{SS,1}$	$\alpha(x_1)$
$x_2$	$\eta_{SS,A2}$	$\alpha_A(x_2)$	$\eta_{SS,B1}$	$\alpha_B(x_2)$	...	$\Sigma\eta_{SS,2}$	$\alpha(x_2)$
$\vdots$	$\vdots$	$\vdots$	$\vdots$	$\vdots$	$\vdots$	$\vdots$	$\vdots$
$x_N$	$\eta_{SS,AN}$	$\alpha_A(x_N)$	$\eta_{SS,BN}$	$\alpha_B(x_N)$	...	$\Sigma\eta_{SS,N}$	$\alpha(x_N)$

The sensitivity scheme described above was applied to the tunnelling problem. The input parameters with the ranges given in the previous section have been used in evaluating the most influential parameters. The average of the lower and upper values of random sets serves as reference values in sensitivity analysis. It is quite informative to display the relative sensitivity of individual results in order to observe the impact of each input parameter. In such manner, the designer gains a better understanding of the system behaviour prior to starting a sophisticated probability analysis. In this case, three major system responses such as the factor of safety at the stage of the top-heading, tunnel crown displacement, and maximum normal force of the lining have been considered in the calculations. Figure 15 depicts the respective results along with the total relative sensitivity. If one wishes to select the most effective variables regarding each response based on a threshold value, different sets of parameters would be chosen. For instance, if only the safety factor of the top-heading is taken into account,  $K_0$ ,  $c$ ,  $E_s$  and  $\varphi$  are identified, whereas if the normal force in the lining is considered the set of parameters  $K_0$ ,  $c$ ,  $E_s$ ,  $R_f$  and  $E_{sh}$  are identified as most influential parameters. The total relative sensitivity will help to choose a compromise of most important parameters. In addition, the  $\alpha_{(Total)}$  of  $R_f$  and  $\varphi$  are very close to the threshold value which makes it more difficult for the final decision. Each of them has the same impact on different responses (i.e.  $\alpha_{(Normal\ force)}$  of  $R_f$  is identical to  $\alpha_{(FOS)}$  of  $\varphi$ ) but finally  $\alpha_{(total)}$  of  $R_f$  is higher than that of  $\varphi$ , and correspondingly  $R_f$  falls into the set of important parameters. The reason is the large discrepancy between the magnitude of dimensionless  $\eta_{SS}$  of FOS and crown displacement. This discrepancy amounts to the order of magnitude, in the case of  $\eta_{SS,FOS}$  and  $\eta_{SS,Crown-displacement}$ . Thus, it is reasonable to assign weights to sensitivity scores based on their significance, to obtain a representative total relative sensitivity which can equally consider all required indices for a sound decision making. However, in the current calculations, no weighting is involved.

A threshold value has to be introduced to separate highly sensitive variables from low ones. Usually, depending on the problem, a threshold value between 5 to 10 percent can be considered appropriate. Here, a threshold value of 7% was chosen. As depicted in Figure 15 with the acceptance of the 7% threshold value, four major basic variables  $E_s$ ,  $c$ ,  $K_0^{nc}$ ,  $R_f$  are identified and these were chosen for the RS-FEM analysis. From experience follows that usually 3 to 4 basic variables are sufficient to obtain relatively smooth cumulative probability distribution functions of output variables, which on the other hand maintain the number of calculations within acceptable limits.

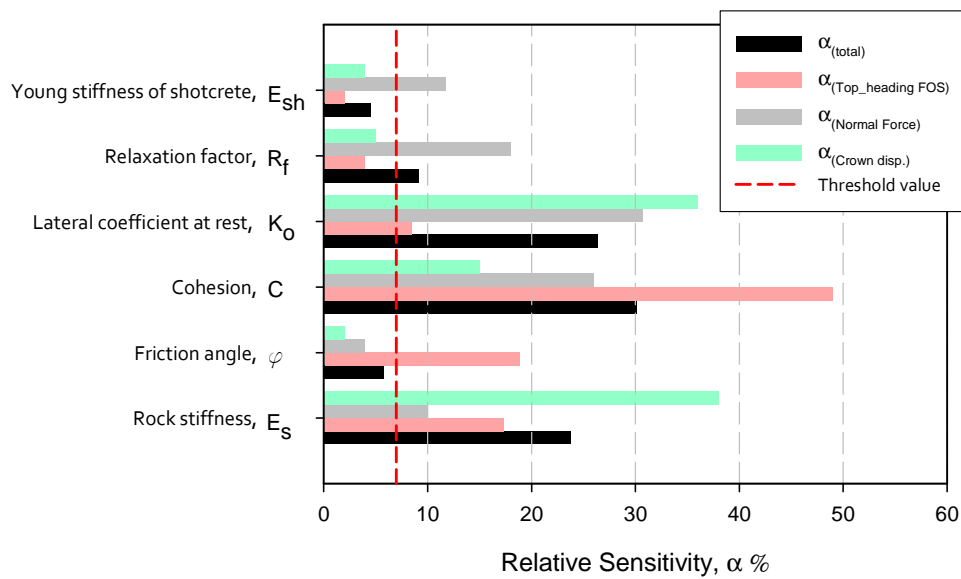


**Fig. 15:** Results of sensitivity analysis

## 3.4.2 Calculation results and system response

### 3.4.2.1 Construction sequences

In accordance with the actual construction sequence 8 calculation phases have been modelled:

1. Initial stresses
2. Pre-relaxation phase of top heading excavation
3. Installation of anchors and primary lining in top heading
4. Pre-relaxation phase of bench excavation
5. Installation of anchors and primary lining in bench
6. Pre-relaxation phase of invert excavation
7. Completion of primary lining and anchors
8. Application of the strength reduction technique in order to obtain a factor of safety after phase 3



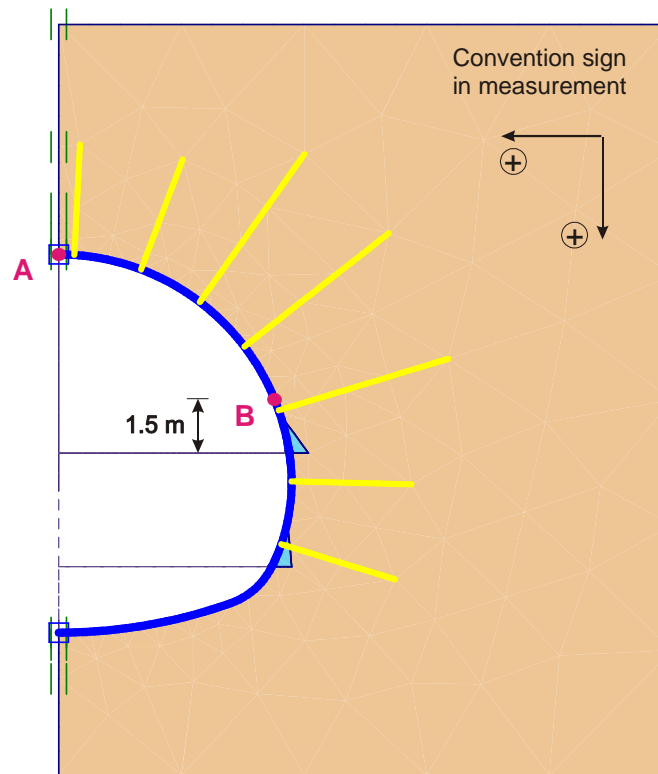


**Fig. 16:** Position of nodes for evaluating results

As elaborated in section 3.4.1.3, four basic variables have been considered for the RS-FEM analysis resulting in 256 different input sets for the finite element model. The following results of the analysis have been evaluated in terms of cumulative probability distributions and will be depicted in Figure 20 and following.

1. Vertical displacement of the crown (Point A in Fig. 16)
2. Vertical and horizontal displacement of the side wall (Point B in Fig 16)
3. Maximum normal force in the lining
4. Maximum moment in the lining
5. Safety factor after the top-heading excavation

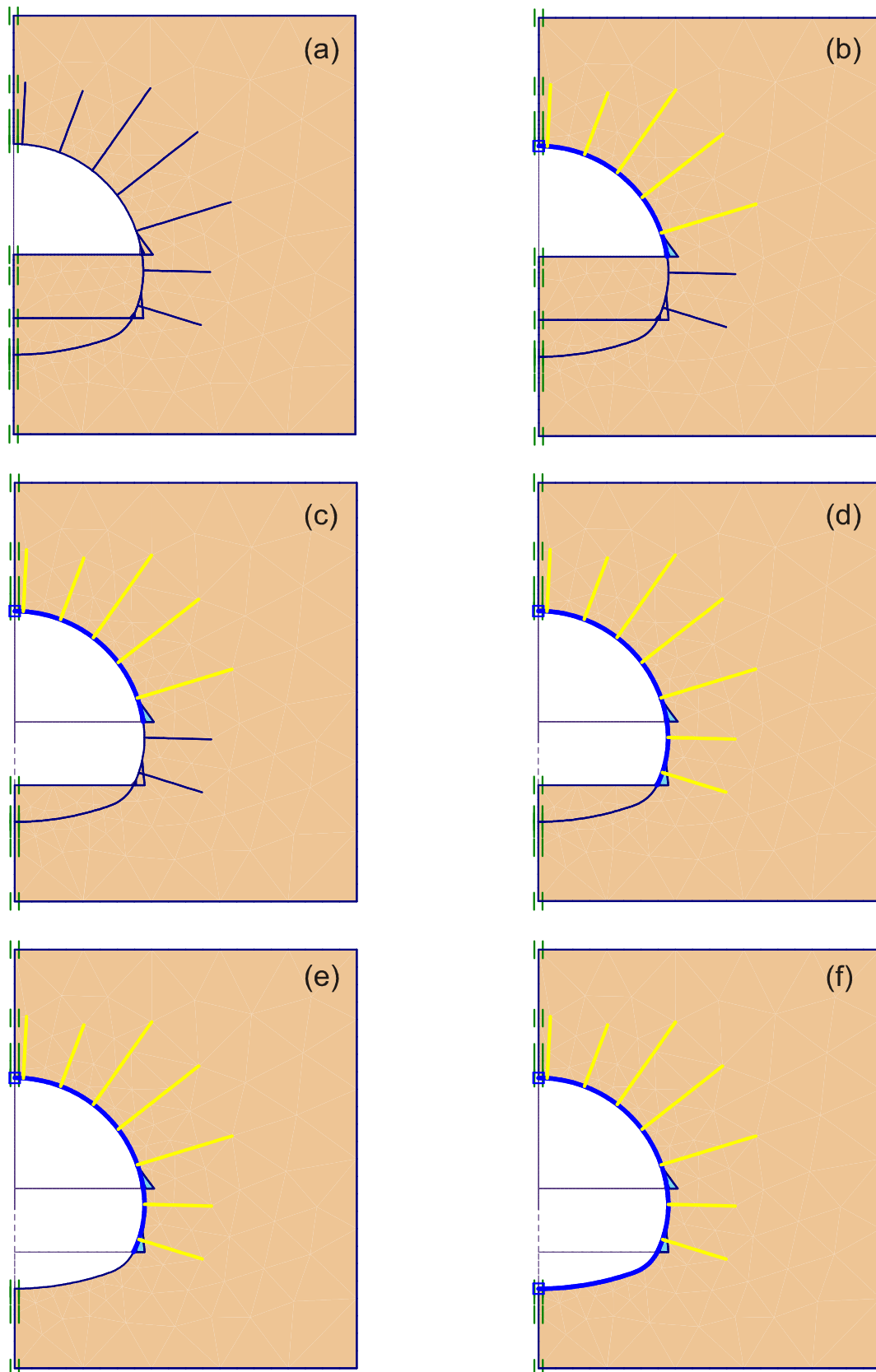


**Fig. 17:** Tunnel construction sequences: (a) Pre-relaxation of top-heading (b) Excavation of top-heading, anchors and shotcrete lining installation (c) Bench pre-relaxation (d) Bench excavation and support installation (e) Invert pre-relaxation (f) Invert excavation and shotcrete lining

### 3.4.2.2 Probability share of each deterministic FE realisation

After the identification of input variables, the combination of different sources and extremes of the parameters based on a random set model have to be calculated. Thus, data files for deterministic finite element calculations have to be provided and as mentioned before, spread sheet files may facilitate the calculation process, which have been developed for this purpose. The concept of constructing a random set relation according to Tonon et al. (2000a & 2000b) for the case considered here is as follows.

Let  $x \in X$  be a vector of set value parameters, in which:  $x = (E, c, K, R_f)$ , and a random relation is defined on the Cartesian product  $E \times C \times K \times R$ . As a result, according to combination calculus, the pairs generated by the Cartesian product are given in the following vector:

$$E \times C \times K \times R = \{(E_1, C_1, K_1, R_1)_1, (E_2, C_1, K_1, R_1)_2, (E_1, C_2, K_1, R_1)_3, \dots, (E_2, C_2, K_2, R_2)_{16}\} \quad (20)$$

Here the index of parameters denotes the relevant set number and the index of pairs signifies one combination of basic variables. Because there are two sets for each basic variable, 16 combinations will be produced. For each combination, an interval analysis is required, by which the deterministic input parameters of the worst and the best case of each combination are being realised. As an example, the deterministic input values of such analysis for the case of  $(E_1, C_1, K_1, R_1)$  are presented in Table 6.

**Tab. 6:** Inputs relating to  $(E_1, C_1, K_1, R_1)$  variables used in deterministic finite element calculations

Run number				1	2	3	4	5	6	7	8	9	10	11	12	13	14	15	16
<i>Run</i>	<i>Mass prob.</i>	<i>Var.</i>	<i>Set No.</i>	<i>LLLL*</i>	<i>LLLU</i>	<i>LLUL</i>	<i>LLUU</i>	<i>LULL</i>	<i>LULU</i>	<i>LUUL</i>	<i>LUUU</i>	<i>ULLL</i>	<i>ULLU</i>	<i>ULUL</i>	<i>ULUU</i>	<i>UULL</i>	<i>UULU</i>	<i>UUUL</i>	<i>UUUU</i>
1-16	0.5	$E^\dagger$	1	79	79	79	79	79	79	79	79	158	158	158	158	158	158	158	158
	0.5	$C$	1	52	52	52	52	82	82	82	82	52	52	52	52	82	82	82	82
	0.5	$K$	1	0.4	0.4	0.6	0.6	0.4	0.4	0.6	0.6	0.4	0.4	0.6	0.6	0.4	0.4	0.6	0.6
	0.5	$R_f$	1	0.4	0.6	0.4	0.6	0.4	0.6	0.4	0.6	0.4	0.6	0.4	0.6	0.4	0.6	0.4	0.6

\*  $L$  denotes the lower extreme of a random set variable and  $U$  denotes the upper extreme.

† units of  $E$ , MPa ;  $c$ , kPa ;  $\varphi$ , degree

Similarly the construction of all 256 required realisations (see Equ. 11) and relevant input files for a deterministic finite element analysis are accomplished. The next step is to determine the probability of the assignment of each realisation. Assuming that the random variables are stochastically independent with reference to Tonon et al. (2000b), the joint probability of the response focal element obtained through function  $f(x)$  (in this case, the finite element model) is the product of the probability assignment  $m$  of input focal elements by each other. For instance, in the above case since the mass probability of each set equals to 0.5 it results in:

$$\begin{aligned} m(f(E_1, C_1, K_1, R_1)) &= m(E_1) \cdot m(C_1) \cdot m(K_1) \cdot m(R_1) \\ &= 0.5 \times 0.5 \times 0.5 \times 0.5 \\ &= 0.0625 \end{aligned} \quad (21)$$

### 3.4.3 Validity of the model

#### Construction of the random set results in the form of p-box:

To construct the *Belief* and *Plausibility* distribution function (i.e. lower and upper bounds) of a required response from deterministic FE calculations, the following procedure is pursued. Suppose that it is required to build up the p-box of the tunnel crown displacement. The crown displacement values pertinent to all 16 realisations, given in Table 6, are sorted out to obtain the minimum and maximum of crown displacements which determine the focal element extremes of crown displacements corresponding to the combination  $(E_1, C_1, K_1, R_1)$ . The displacement values of those realisations between the extremes are discarded. According to Equ. 21, the probability assignment of this focal element is 0.0625, which constitutes one step in the cumulative distribution function depicted in Figure 20. Similarly, this process is repeated for other combinations e.g.  $(E_1, C_2, K_2, R_1), \dots$  to calculate the extremes of all focal elements of crown displacement. Finally, the left and right extremes of all focal elements are arranged in ascending order to obtain the upper and lower bounds for  $U_y$ -A respectively.

As depicted in Figure 18, measured values of a series of cross sections within an assumed homogeneous region can be expressed in terms of a discrete cumulative distribution in which the probability assignments of individual sections are equal. In this way, measurements are comparable with the results of the random set bounds. A single value measurement similar to Figure 20 is illustrated with the vertical line because only one observation is available within the considered region.

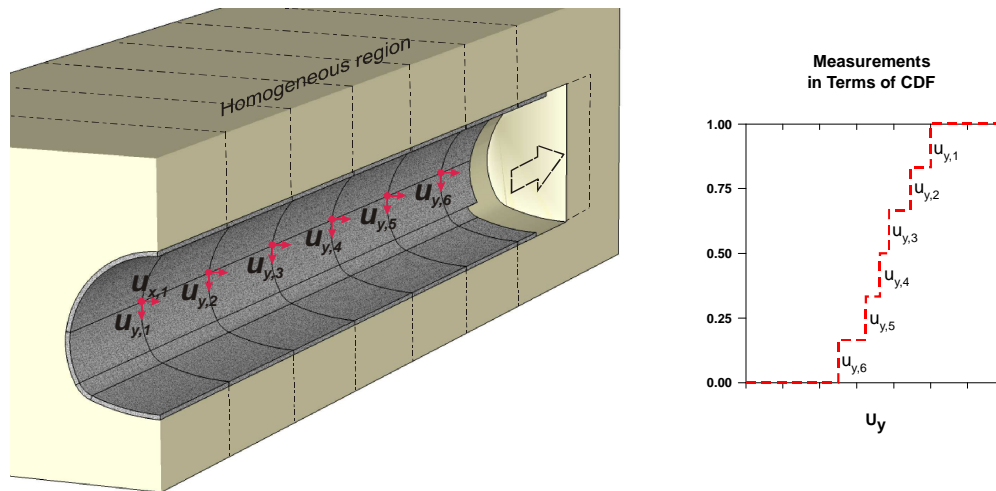


**Fig. 18:** Representation of the measurement in terms of a cumulative distribution function within a homogeneous region

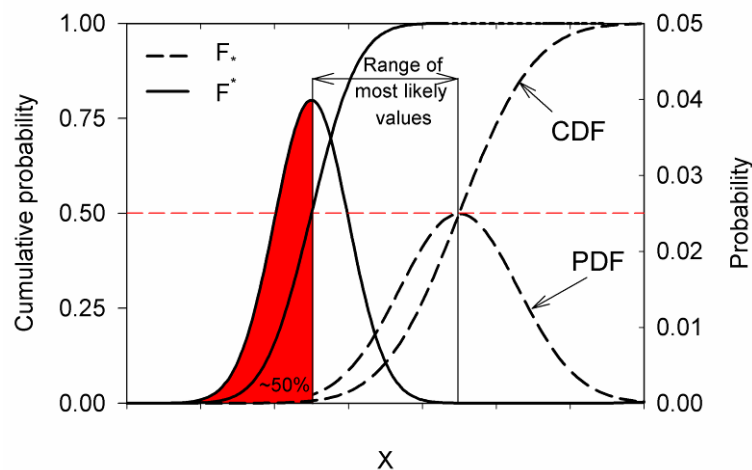


**Fig. 19:** Range of most likely values,  $F^*$  and  $F_*$  denote upper and lower probability for respective system response, respectively

Figures 20 and 21 illustrate upper and lower bounds of the cumulative distribution function for the selected points A and B respectively. The results obtained from the deterministic design analysis as well as measured values have been overlaid on the figures for comparison. RS results can be generated for any desirable target value at any construction stage; for instance, Figure 20 compares vertical crown displacement at two different stages 1) after top-heading and 2) after completion of the shotcrete lining. It displays almost the same trend for bounds of result at both stages with a slight difference in the absolute values.

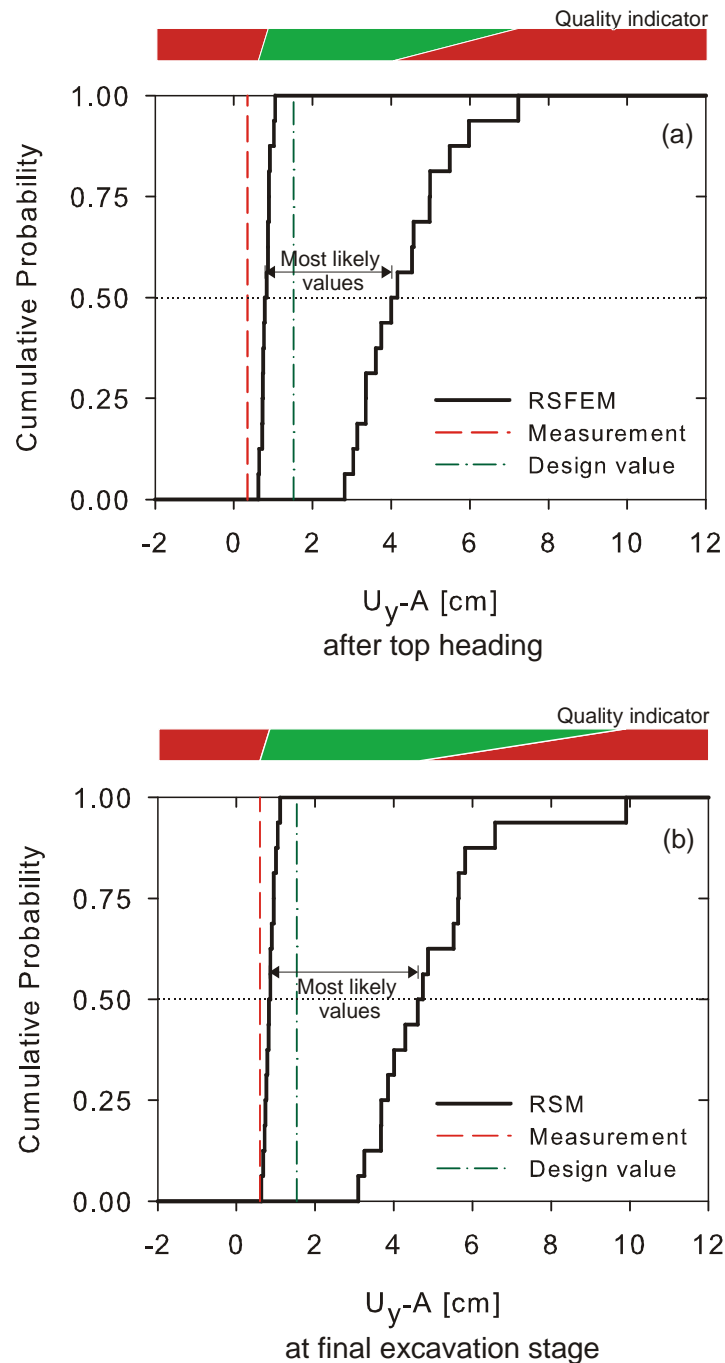


**Fig. 20:** Lower and upper bounds on vertical displacement of the tunnel crown for two construction stages, a) after top heading excavation b) after completion of the invert

Generally, the most likely values are defined as values with the highest probability of occurrence, where the slope of the corresponding cumulative distribution function is steepest. For the purpose of simplification, it is assumed that the most likely results are those values, whose measure of their belief degree are less than 50% and their corresponding plausible likelihood of occurrence are larger than 50% as shown in Figure 19.

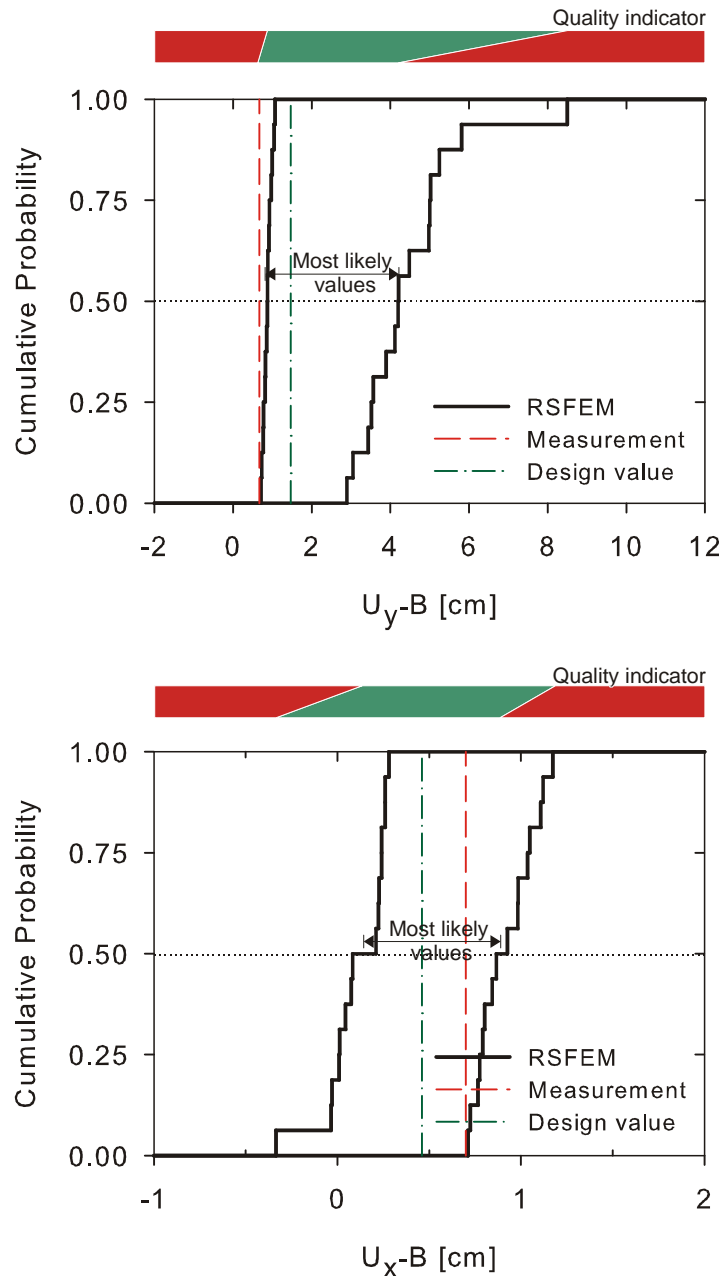


**Fig. 21:** Lower and upper bounds on vertical and horizontal displacement of the tunnel side wall after the final excavation stage

For instance, the most likely settlement of the tunnel crown at the final stage is in a range from 8 to 46 mm. In the same way, the most probable values of the side wall displacement in the vertical and horizontal direction are in a range approximately [9, 42] mm and [2, 9] mm, respectively.

#### Mean value of the true system response:

The mean value of the true system response obtained by random set bounds is within the following range given by Tonon et al. (2000a):

$$\mu = \left[ \sum_{i=1}^N m_i \cdot \inf(A_i); \sum_{i=1}^N m_i \cdot \sup(A_i) \right] \quad (22)$$

where  $\inf(A)$  and  $\sup(A)$  denote lower and upper extremes of focal element  $A$ , respectively. The intervals obtained from both the most likely range definition and those calculated from Equ. 22, indicate a good conformity and they have been tabulated below (Tab. 7).

**Tab. 7:** Lower and upper mean values of true system response

<i>Results</i>		$U_{y-A}$	$U_{y-B}$	$U_{x-B}$	<i>FOS</i> <i>T.H.</i>	<i>Max</i> <i>Moment</i>	<i>Max</i> <i>Normal</i> <i>Force</i>
		[cm]	[cm]	[cm]	[-]	[kN.m/m]	[kN/m]
<i>Interval of true mean values (Equ. 22)</i>	<i>Lower</i>	0.85	0.87	0.1	1.46	14.5	462
	<i>Upper</i>	4.95	4.5	0.9	1.82	38.1	787
<i>Interval of most likely values</i>	<i>Lower</i>	0.8	0.9	0.2	1.46	14.4	461
	<i>Upper</i>	4.6	4.2	0.9	1.80	38.5	779

### **Interpretation:**

One can demonstrate the validity of the numerical calculations against the observations using the quality indicator shown in Figures 20 and 21. The quality indicator consists of three parts: first in the middle, the green colour shows the area of the most likely values of the system response. The full red colour identifies the theoretical zone of an unlikely system response. Outside the most likely values zone, the green colour zone in the quality indicator starts to fade and convert into the red one. This transition zone can be called an alarm zone because it indicates that the actual ground condition is gradually moving away from the assumed conditions invoked in the RS analysis. It should be noted that this alarm zone is different than that alarm threshold value used in the observational method (see e.g. Olsson and Stille, 2002). In that context, defining the alarm value is very difficult and controversial. It varies from case to case and depends on the significance of the project, range of the absolute values, the extent of the expected uncertainties involved in the problem, and many other indices that are defined based on engineering judgment. However, the results generated by RS-FEM along with the quality indicator defined in this manner can be considered as a useful tool for decision making. In addition, when the measured displacements of the tunnel lining are within the acceptable predicted range (e.g. green zone) one can assume (at least from a practical point of view) that the design of the support elements are also reliable albeit the internal forces of tunnel structure have not been monitored.



Strictly speaking if the numerical model is appropriate and the parameters chosen cover the "true" uncertainty in-situ measured values must fall inside the range of RS-FEM results, if not, this would be a clear indication that either the model itself (e.g. assuming a continuum for a jointed rock mass) is not appropriate or the range of parameters is not representative for the ground conditions.

Figures 20 and 21 indicate that the predicted vertical displacements at tunnel crown and side wall comply with the lower bound of the RS-FEM results, while the horizontal displacement of the side wall lies within the range of the most likely values. The measured value of  $U_y$ -A is slightly outside the random set range but from a practical point of view this can be considered to be within an error tolerance.

### 3.4.4 Determination of performance function

The performance function is selected to numerically characterise a mode of performance of the tunnel structure. For each performance mode one or more performance functions may be considered. For instance, possible performance modes considered for a tunnel design would be:

1. Shotcrete failure (large cracks or complete damage)
2. Failure of the temporary footing at the top-heading excavation stage
3. Over-break of the surrounding rock mass
4. Face instability during construction

To evaluate the potential for rock-fall or over-break a discrete element code is required and the current finite element model is not appropriate for assessing this type of failure mode. The problem of face stability is also not discussed here because a 3D analysis would be required. The presented example is concerned with shotcrete failure and the likelihood of footing damage only, but in a complete design procedure the other possible failure mechanisms have to be taken into account as well. Figure 22 shows the possible failure mechanism at the stage of top-heading excavation by means of incremental shear strain contours using the so called strength reduction technique. It indicates that the failure mechanism can take place due to inadequate bearing capacity of the temporary lining footing. Assuming that the safety factor of the ground failure at the top heading stage should be higher than 1.3, a performance function is set and by using the random set results, the probability of a safety factor below 1.3 is estimated. According to the normal distribution fitted to the lower bound of the RS result, the upmost probability of the safety factor being less than 1.3 is approximately 0.0005 (Fig. 24).

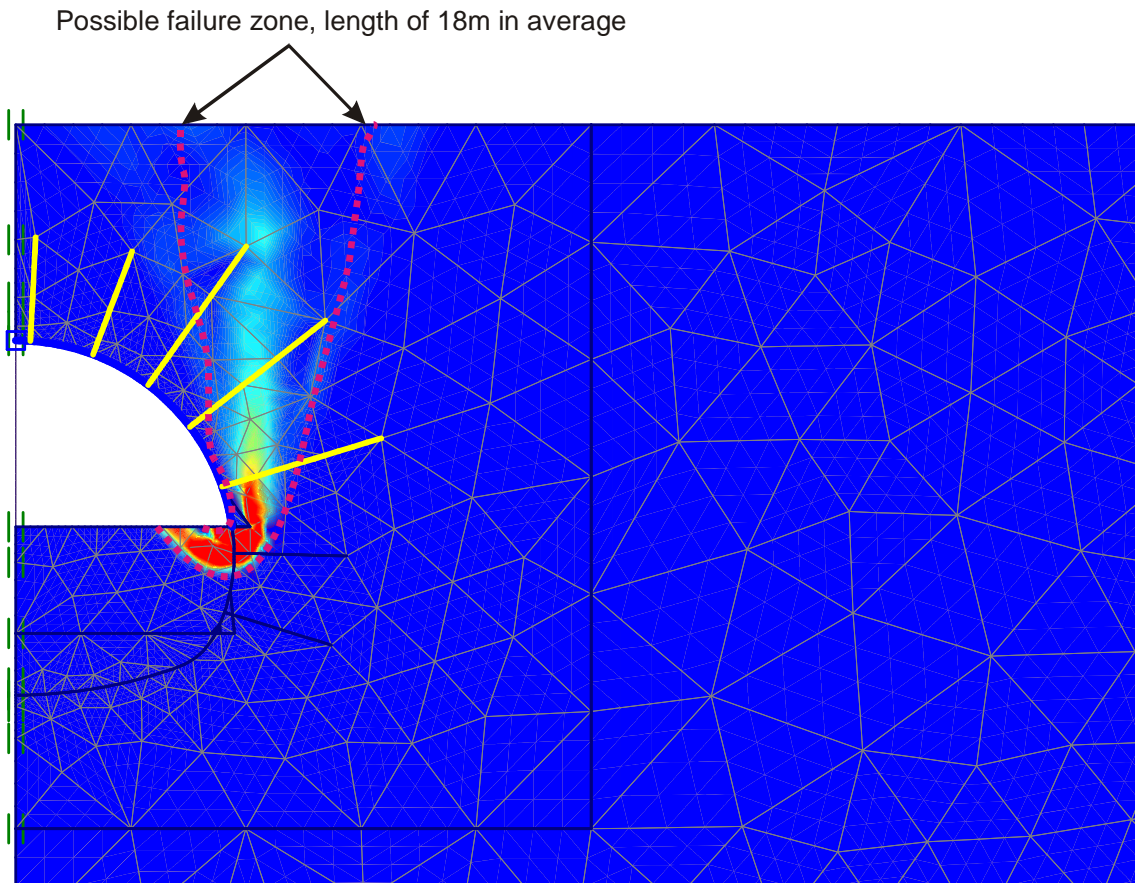


**Fig. 22:** Contour plot of incremental shear strain illustrating possible failure mechanism at top-heading excavation

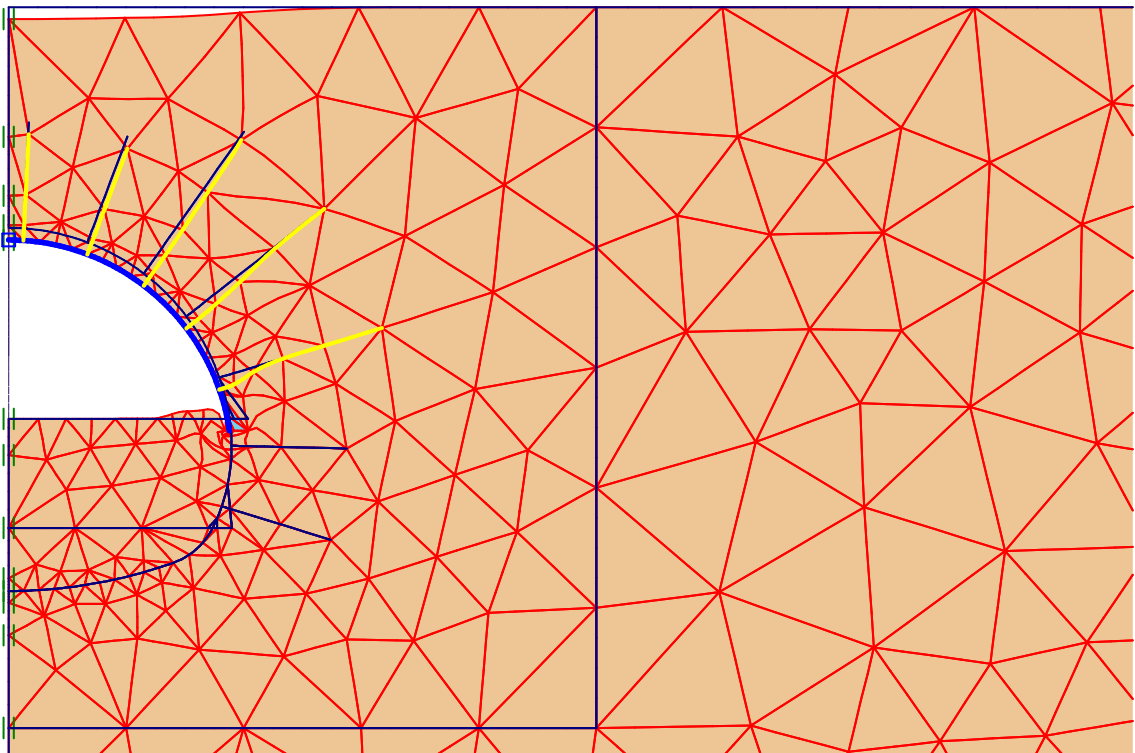


**Fig. 23:** Top-heading failure mechanism and deformed mesh

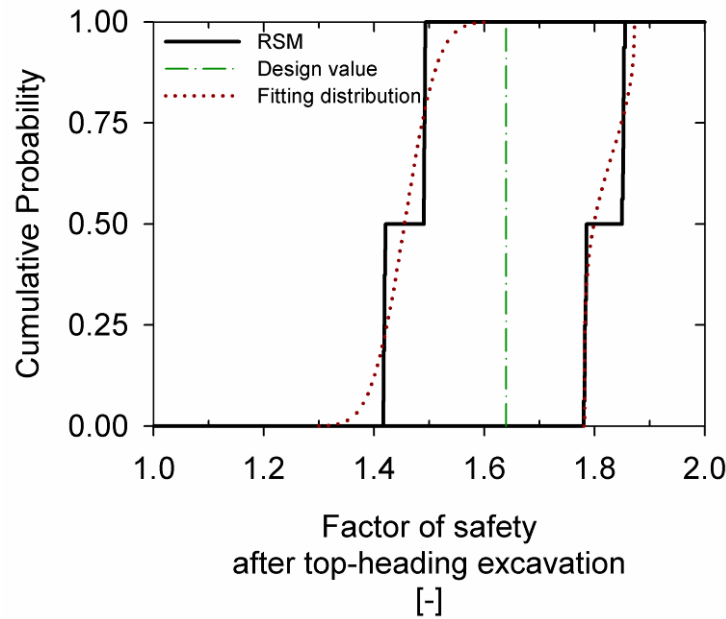


**Fig. 24:** p-box representation of safety factor after top-heading excavation

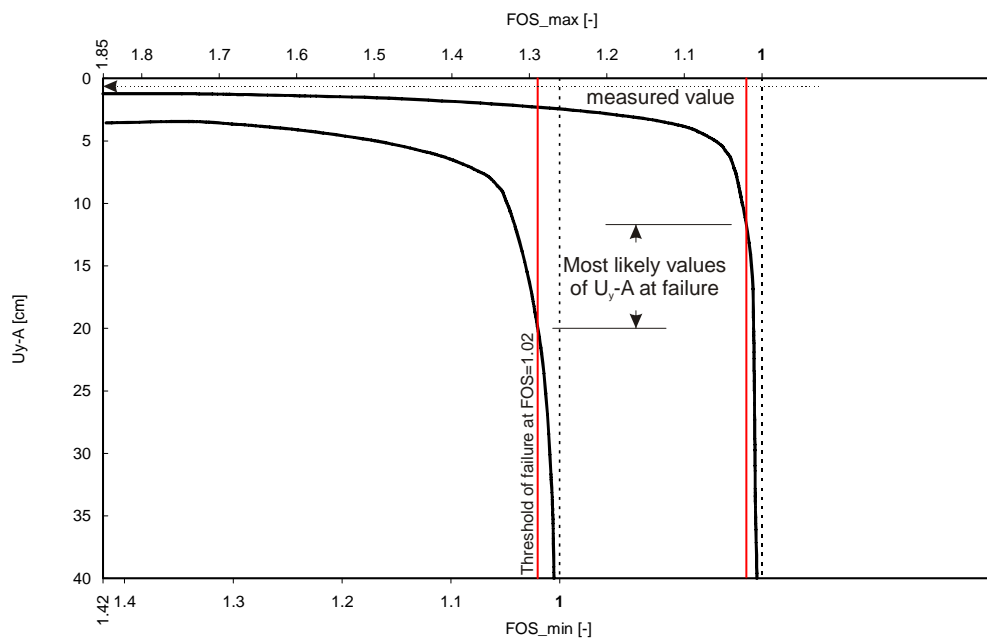


**Fig. 25:** Bounds of maximum and minimum of safety factor in terms of vertical crown displacement

The lower and upper probability values of top-heading FOS being less than 1.0 are almost zero. It has to be acknowledged that this value is not very accurate because it depends considerably on the type of distribution fitted to the discrete data but it is sound enough as an estimate from a practical point of view. The most probable values of the safety factor are in a range of approximately 1.46 up to 1.8.

The minimum and maximum of safety factors given in Figure 24 can be plotted versus the vertical displacement of the tunnel crown since such a result depicted in Figure 25 can be used for assessing the behaviour of the tunnel structure including soil-structure interaction (ductile or brittle behaviour). Two points can be inferred from Figure 25. Firstly, when the measured values of vertical tunnel crown displacement are about entering the range between 12 and 20 cm a failure mechanism can be expected and secondly, due to the current measurement status the actual safety after the excavation of the top-heading is more than 1.85. Figure 25 provides helpful information, for instance, the range of displacement in which the failure can be expected. This can be considered as a warning range or alert value required for the Observational Method (Nicholson et al., 1999).

### 3.4.5 Evaluating the serviceability limit state of the shotcrete lining

To illustrate the applicability of RSM in reliability analysis, a serviceability limit state function was considered. The serviceability limit state of the shotcrete lining is based on the damage of the lining due to cracking after the tensile capacity of the material is exceeded. The admissible value of the normal force  $N_{lim}$  as a function of the eccentricity  $e(x)$  as given by Schikora & Ostermeier (1988) is:

$$N_{lim} = \frac{f_c d}{F_s} \left( 1 - 2 \frac{e(x) + e_a}{F_s d} \right) \quad (23)$$

Where

- $f_c$  uniaxial strength of shotcrete
- $e_a$  imperfection
- $d$  thickness of lining
- $e(x)$  eccentricity  $M/N$
- $M$  bending moment
- $N$  axial force
- $F_s$  factor of safety

The  $x$  indicates the position of the point in the shotcrete lining whose moment and normal force is considered.

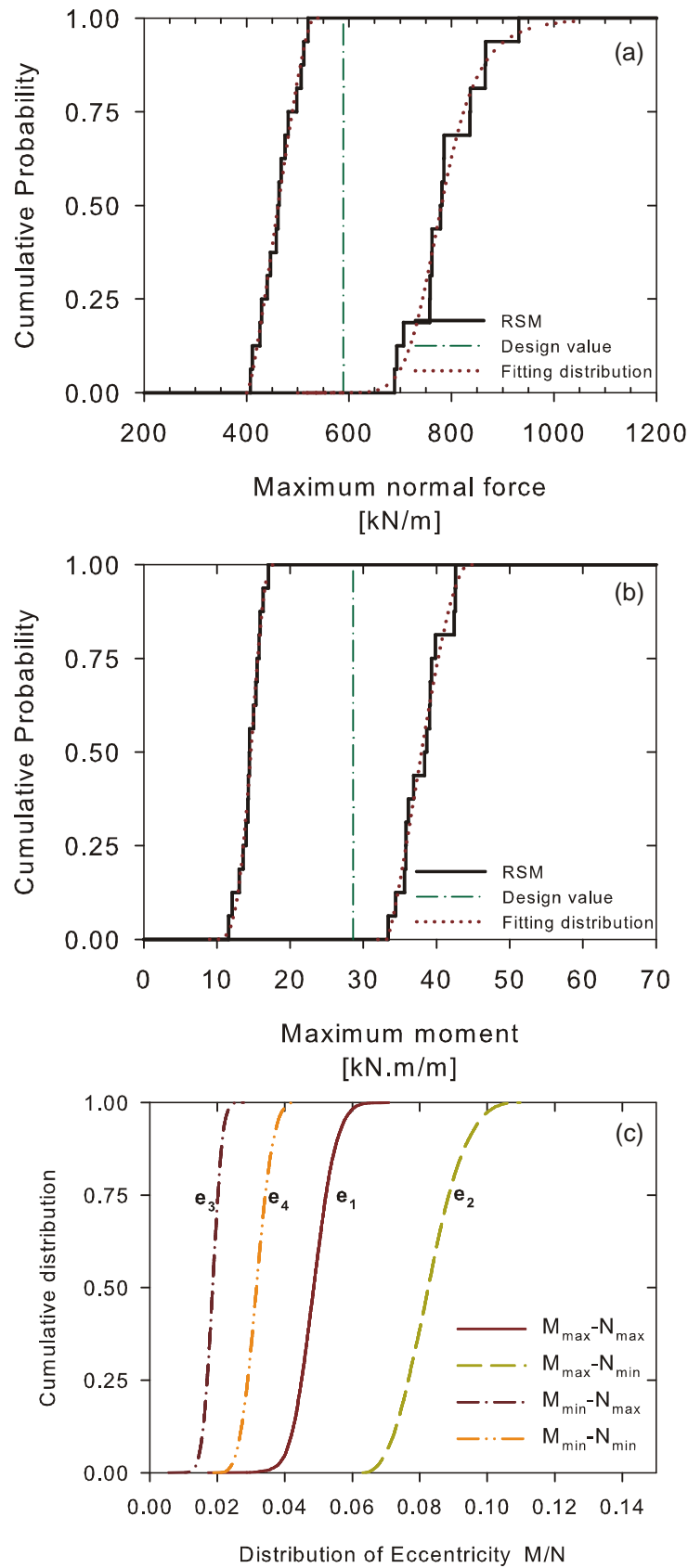


**Fig. 26:** Tunnel internal forces results of RS-FEM analysis in terms of cumulative distribution functions

Thus, the serviceability limit state function which should be evaluated is defined in Equation 24.

$$g(x) = N_{lim} - N \quad (24)$$

A Monte Carlo simulation was executed using the Latin Hypercube sampling technique and employing @Risk<sup>®</sup> (Palisade, 2008) software to carry out a reliability analysis for serviceability conditions of the shotcrete lining at the final stage of construction. The uncertainty of uniaxial strength of shotcrete and thickness of the lining as well as the eccentricity of the internal forces were considered. For the shotcrete a C20/25 with a uniaxial strength of about 17.5 MPa is used and its uncertainties are modelled assuming a Lognormal distribution for the strength as LN(17.5,0.25) MPa and for the thickness as LN(0.25,0.017) m. To cover imperfections an eccentricity of  $e_a = 2.0$  cm and for the serviceability limit state a factor of safety of  $F_s = 2.1$  is considered according to Schikora & Ostermeier (1988). Based on the fitted cumulative distribution functions of the normal force, the bending moment and the respective eccentricity illustrated in Figure 26, the limit state function has to be evaluated four times in order to obtain bounds on the probability of exceeding the admissible normal force in the lining, leading to the four distributions shown in Figure 27. The range of the probability of exceeding the admissible normal force in the lining,  $N > N_{lim}$ , where cracking takes place, is given in Table 8.

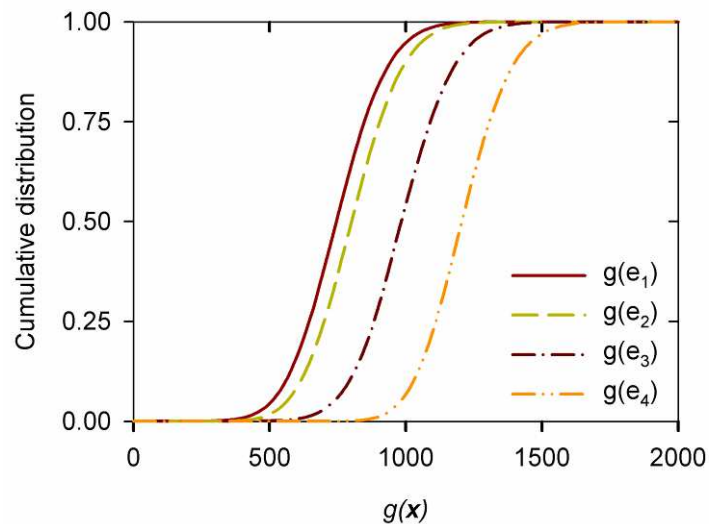


**Fig. 27:** Cumulative distribution of  $g(x)$  obtained from four eccentricity functions

The value of the probability of failure indicates that the shotcrete satisfies the serviceability criteria and it is expected not to observe major cracks in the lining.

**Tab. 8:** Range of probability that  $N/N_{lim}$  ( $F_s=2.1$ )

Construction Phase	Fitted distribution				max $P_f$	min $P_f$
	$N_{max}$	$N_{min}$	$M_{max}$	$M_{min}$		
Final stage	Log-logistic	Beta	Beta	Beta	3E-4	1.4E-5

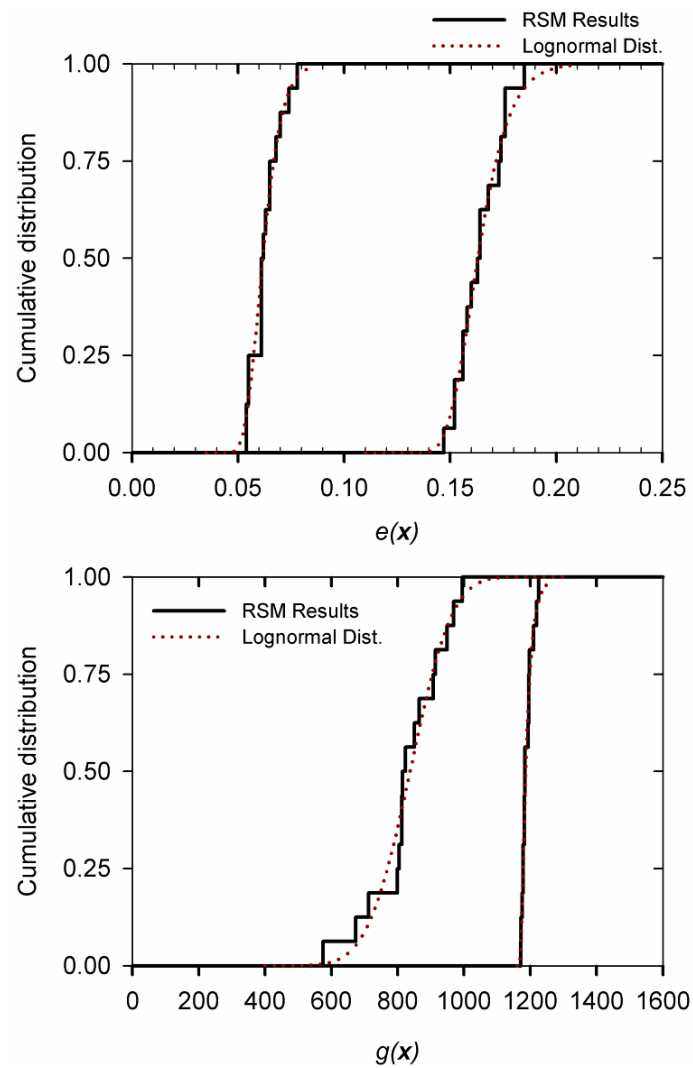
Alternatively, it is possible to compute the performance function,  $g(x)$ , directly from random set analysis results. The advantage is that the performance function is evaluated over all elements of the tunnel cross section with the normal force and its corresponding bending moment and in contrast to the previous method, the coincidence of maximum normal force and maximum moment is avoided in the calculation. For each individual deterministic calculation, eccentricity  $e(x)$ , normal force and thickness of shotcrete are known at any section of the lining. Thus, Equation 23 can be evaluated assuming the other required parameters such as shotcrete strength and thickness values are constant. In this way,  $g(x)$ , is evaluated like other primary system responses (e.g. normal force) and can be presented in terms of discrete cumulative probability with upper and lower distribution. Figure 28 depicts such results for the current example for both eccentricity and serviceability limit state functions. Obviously, the latter method results in a narrower band for  $g(x)$  than the first method. The range obtained by the first method varies between 400 and 1600 while in the respective result yielded by the latter method, varies between 580 and 1220. The Lognormal distribution fitted to the discrete upper and lower distribution of the results (Fig. 28) indicates that the likelihood of  $g(x)$  being less than zero is almost zero.

The disadvantage of this method is that it is not possible to take the existing uncertainty in the thickness and strength of the shotcrete into account. Although the first method of evaluating  $g(x)$  is simple and capable to consider the uncertainty existing in shotcrete strength, variation of shotcrete thickness and so on, but it results in a conservative reliability assessment. Therefore, in the cases that the performance function is sufficiently distant from failure conditions, the result of the first method is acceptable and can be applied, if not, the second method should be used to check whether the performance is satisfactory or not. According to US Army Corps of Engineers (1997) qualitative evaluation of performance level based on reliability index and probability measure obtained from reliability analysis has been given in Table 9. On the basis of this table the level of shotcrete performance is assessed as good performance.

In addition, if in the Equation 23  $F_s$  is set to zero, the serviceability limit state function is converted to the ultimate limit state function. Thus, simultaneously both types of performance functions can be assessed.

**Tab. 9:** Expected performance level

Expected Performance Level	Reliability index ( $\beta$ )	Probability of Unsatisfactory Performance
Hazardous	1.0	0.16
Unsatisfactory	1.5	0.07
Poor	2.0	0.023
Below average	2.5	0.006
Above average	3.0	0.001
Good	4.0	0.00003
High	5.0	0.0000003

**Fig. 28:** The p-boxes of both the eccentricity and the shotcrete limit state function obtained directly from RS-FEM results



### 3.5 Summary and conclusion

The application of an RS-FEM analysis to a real tunnel project has been presented. Based on engineering judgement, important model parameters have been identified and their influences on results have been evaluated quantitatively by means of a sensitivity analysis. Based on the sensitivity, the basic variables for the RS-FEM calculations have been chosen. The RS-FEM results for the selected responses were given in form of lower and upper probability bounds. One of the important features of Random Set analysis is that once in-situ measurements are available, the quality of the numerical model can be judged. The measurements that fall outside the range of calculated displacements imply that either the numerical model itself was not appropriate or the range of parameters did not reflect the in-situ behaviour. This result may have important consequences in cases where e.g. the ground investigation programme was insufficient and therefore design and construction has been based on incorrect assumptions. A review process of the design based on a random set model is depicted in Figure 29. For a management review process of a typical tunnel monitoring the readers are referred to CIRIA report 185 presented by Nicholson et al. (1999).

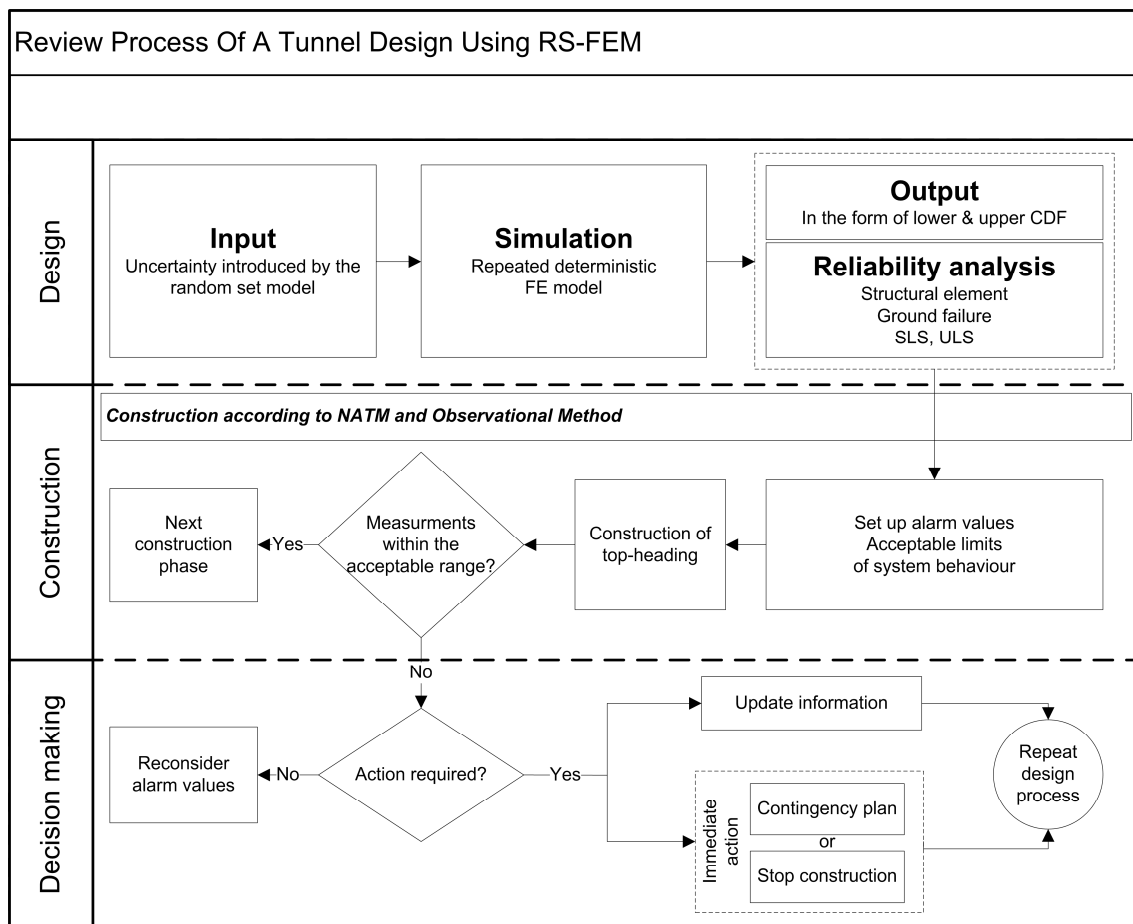


**Fig. 29:** Process of design based on random set model

Advantages of applying RS-FEM were demonstrated in this chapter and are summarized as follows:

1. RS-FEM provides a user-friendly and practice-oriented framework that can take advantage of the advanced constitutive models available in FE programmes. Complex tunnel geometry, subsurface conditions, nonlinear structural elements and etc. can be taken into account in order to predict the behaviour of an underground structure within the ranges of upper and lower probability distributions without assuming subjective distributions of input model parameters. In other words, all advantages of a complex numerical model are preserved.
2. With relatively small number of simulations (in this example, 256 realisations) relatively smooth bounds on the system responses were obtained, and as a result, a satisfactory reliability analysis was accomplished. The application of RE-FEM requires less computational effort as compared to fully probabilistic methods such as the Monte-Carlo simulation.
3. Applicability of the RS-FEM was demonstrated by a tunnel example in which the field measurements were in reasonable agreement with the primary RS-FEM results without any updated data and information during construction.
4. When providing all required FE calculations, the p-box of any desirable result in any construction phase can be generated and the serviceability and ultimate limit states can be evaluated with the same model.
5. It provides a framework by which it is possible to check the validity of the numerical model and corresponding design. In tunnel projects constructed corresponding to NATM principals, displacement measurements of at least 3 points in the cross section are recorded regularly. Thus, the required measurements are available at each construction stage. As it was shown in this Chapter, the results of a random set model can be provided in all construction stages. When finishing the first construction phase (e.g. top-heading), the random set model can be validated against the measurements. If the measurements are in the predefined acceptable range, construction proceeds to the next phase, otherwise the obtained information from the first stage is used to update the uncertainty model. The whole procedure is repeated and the required design variations are applied for the next construction phase. The design revision can be carried out within the lagging time available between different construction stages (e.g. top heading and bench). Therefore, RS results of the intermediate

construction stages accommodate a chance for early stage recognition of a model error.

## 4 Limitations of RS-FEM

In the foregoing chapter, the procedure of the RS-FEM was reviewed and application of RS results in reliability analysis was demonstrated for a tunnel problem. As it was shown, all the required deterministic finite element calculations should be performed to construct the lower and upper bounds of the desired system responses. If some of the calculations would have failed e.g. due to non convergence of the finite element analysis, it would have been impossible to determine the probability bounds on the system response because result points would have been missing. Therefore, applying RS-FEM for such cases would be problematic. In addition, in cases where the range of displacements is very large the results would become meaningless and a reliability analysis based on those results would not provide any help for decision making. Therefore some shortcomings of the method will be addressed in this chapter. This issue will be illustrated by an example and possible solutions are discussed in the next sections.

### 4.1 Tunnel example in faulted zone

For the purpose defined above, a section with an overburden of 25 m within in the faulted zone (zone III-Figure 9) of the tunnel described in Chapter 3 was selected to apply the random set method. The tunnel geometry and its relevant 2D finite element model mesh including some model specifications are depicted in Figures 30 and 31 respectively. Approximately 900 15-noded triangular elements were employed in the model.

Due to similarities in rock mass characteristics of the portal area (zone I) and the faulted zone (Zone III) the random sets for zone III adopted the same parameters as given in Chapter 3 for zone I. The range of MC-model parameters derived from the site investigation report and values used in design have been summarised in Table 10. All the required steps for performing the RS-FEM procedure have been followed in the same manner as those for section BQ1 in Chapter 3. Therefore, four basic variables,  $K_0$ , elasticity modulus of the rock mass  $E_m$ , cohesion and relaxation factor, considered in the random set analysis of section BQ3 are given in Table 12. In addition, the construction sequence followed is similar to section BQ1 including top-heading, bench and invert. The only difference between section BQ1 and BQ3 is the amount of overburden and support elements used in the design. The specifications of the structural elements are given in Table 11.

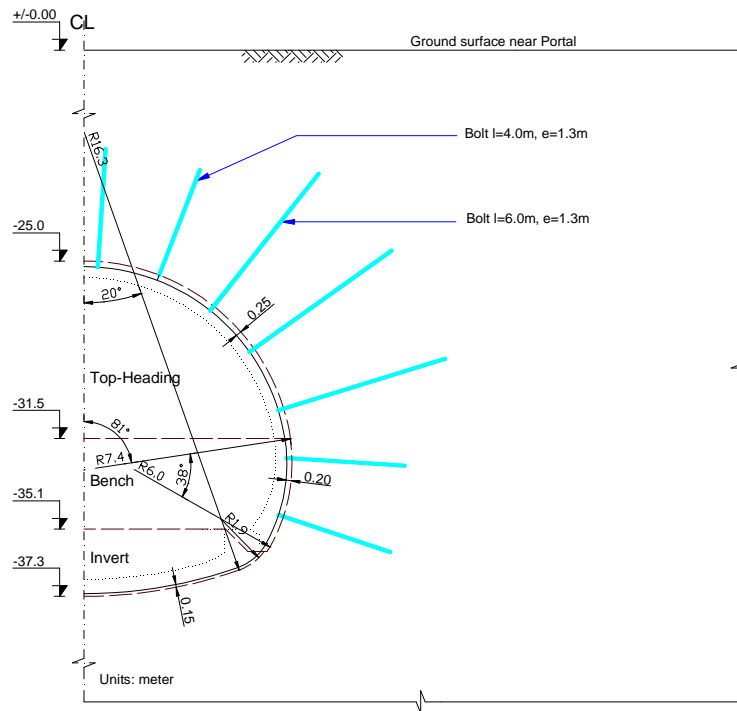


**Fig. 30:** Specifications of the tunnel geometry and bolts

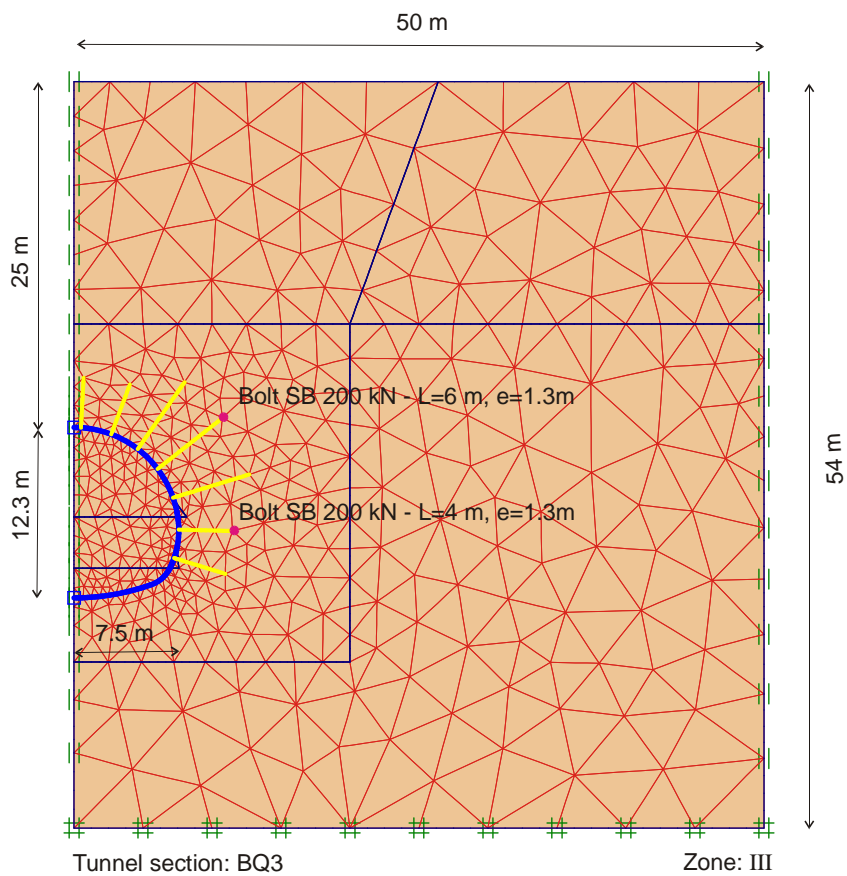


**Fig. 31** The 2D finite element mesh of the tunnel section BQ3 with 25m overburden

**Tab. 10:** The range of MC-model parameters extracted from the geotechnical report for zone III and the representative values used in design

	Zone	$\gamma$	$E_{rm}$	$c$	$\varphi$	$K_0^{nc}$	$\nu$
		[MN/m <sup>3</sup> ]	[MN/m <sup>2</sup> ]	[kPa]	[°]	[-]	[-]
Geotechnical report	III	24	100-200	60-90	21-23	0.4-0.6	0.35
Design-K6-1	III	24	200	90	23	0.6	0.35

**Tab. 11:** Parameters for structural elements used in design section K6-1

Support element	Location	Type	$E$ -modulus		Plastic Limit Force	Thickness /Diameter
			young	old		
			[MPa]		[kN]	[cm]
Shotcrete	Top-heading	Elastic	5000	15000	-	25
Shotcrete	Bench	Elastic	5000	15000	-	20
Shotcrete	Invert	Elastic	5000	15000	-	15
Anchor	T.H., B., I.	Elasto-plastic	210000		200	2.2

**Tab. 12:** The random sets used in section BQ3 considering spatial autocorrelation

Set No.	Probability assignment	$E_{rm}$ MN/m <sup>2</sup>	$c$ kPa	$K_0^{nc}$ -	$R_f$		
					T.H.	Bench	Invert
1	0.5	79-157	52-82	0.4-0.6	0.4-0.6	0.3-0.5	0.2-0.4
2	0.5	96-192	58-88	0.5-0.7	0.3-0.5	0.2-0.4	0.1-0.3

### 4.1.1 Random set finite element results

Figures 32 and 33 show upper and lower bounds of the cumulative distribution function for typical responses of a tunnel structure including the tunnel crown and side-wall displacements and the maximum moment of internal lining. The position of the points A and B are those depicted in Figure 16 of Chapter 3. The results obtained from the deterministic analysis for design (Type K6-1) are indicated in Figures 32 and 33 for comparison.

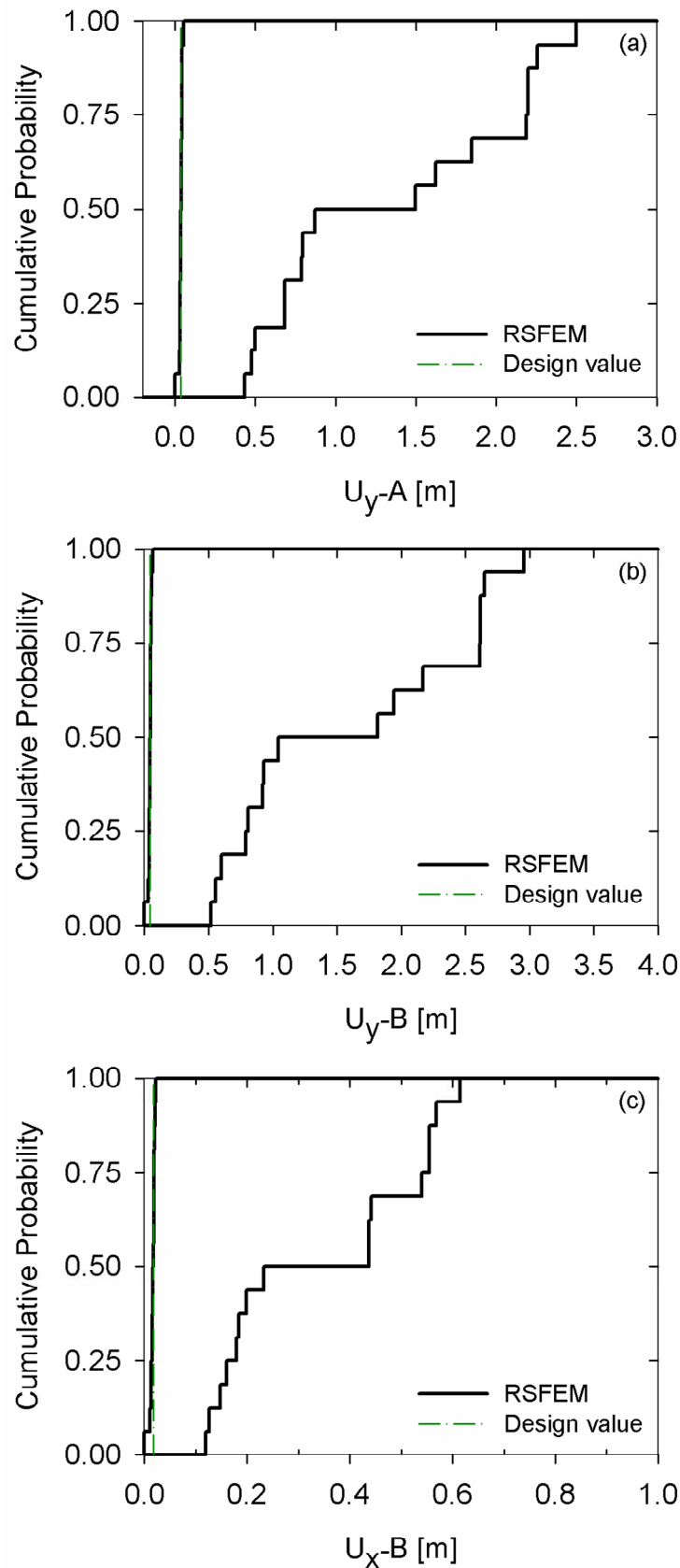


**Fig. 32:** p-box of RS results, based on random sets given in Table 3, a) vertical displacement of the tunnel crown, b) & c) vertical and horizontal displacement of point B respectively

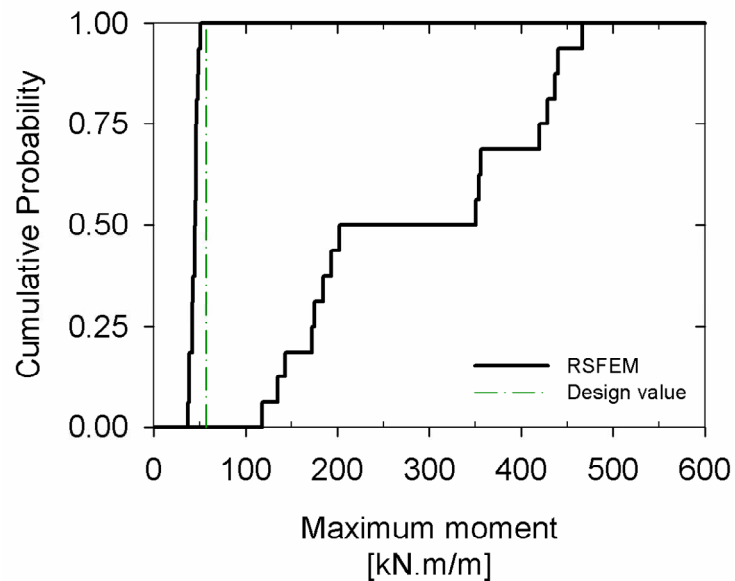


**Fig. 33:** P-box of the maximum moment in the lining, based on random sets given in Table 12

The model assumptions for the deterministic design have been given in Table 10. It follows from the figures that deformations and internal forces of the design values are very close to the lower bound, which could be envisaged because nearly all the input parameters have been chosen corresponding to the optimistic extremes of the random sets.

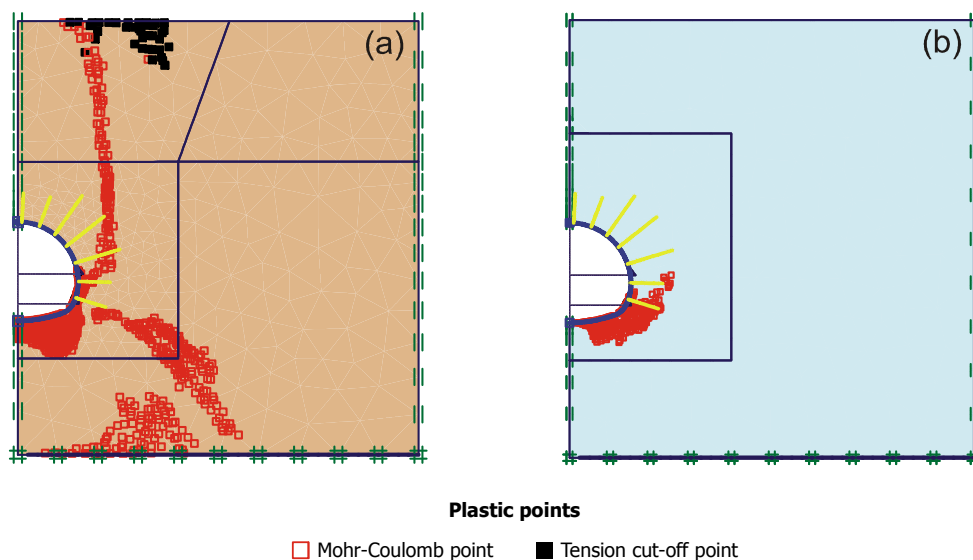


**Fig. 34:** Illustration of the plastic points in the model for the cases, a) one of the worst cases of the RS-FEM calculations, b) design analysis

When comparing the design values with the RS results, it appears that there are certain combinations of the input parameters that mobilise large plastic zones and a failure mechanism (as depicted in Fig. 34) will develop around the tunnel structure resulting in large displacements. This clearly proves the advantages of



the RS-FEM that it can systematically detect the pessimistic combination of the uncertain input parameters leading to the worst case system behaviour but on the other hand shows the disadvantage of the method in the sense that results show a very wide range which is of limited practical use.

When the results are sorted in the form of a bar chart as in Figure 35, a large difference in the results is obtained from cohesion set 1 and 2. In this way the most influential parameters can be identified. If it is not possible to narrow the range of possible values for this parameter by means of additional investigations, the extreme range in results cannot be reduced.

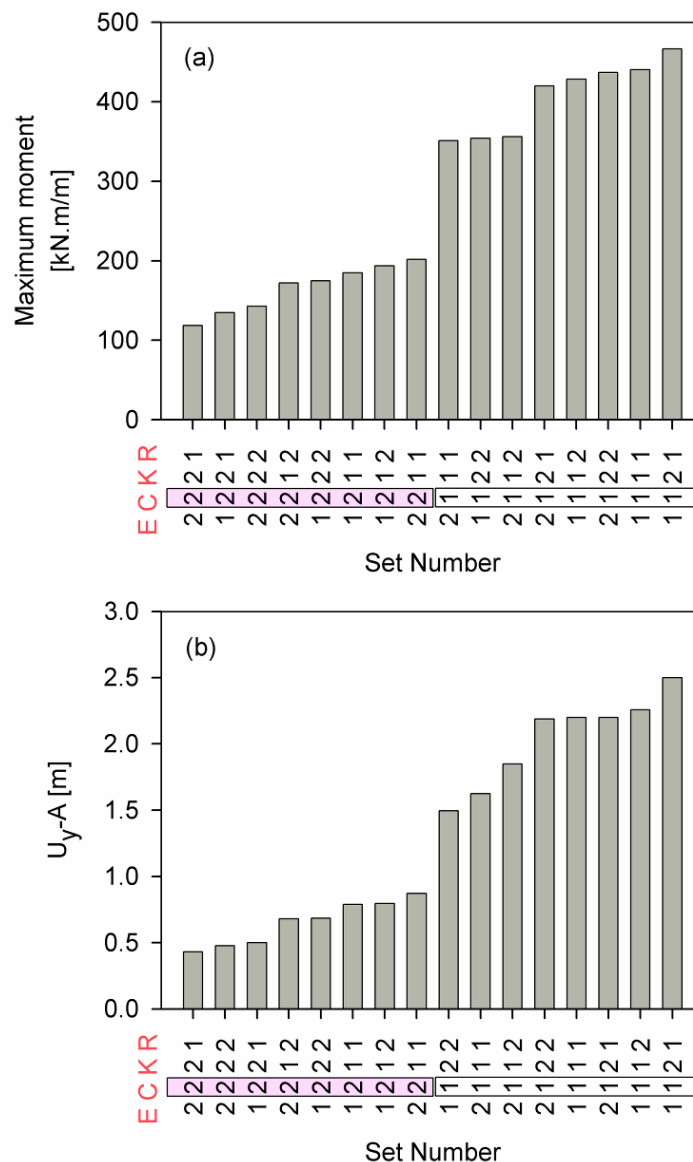


**Fig. 35:** Discrete upper bound values of RS results in terms of input set number, a) maximum moment in the lining b) vertical displacement of the tunnel crown. Each digit of a 4-figure number represents the set number of E-modulus, cohesion,  $K_0$  and relaxation factor from left to right respectively.

### 4.1.2 Scenarios concerning the unsuccessful random set results

The result of the random set method would be unsatisfactory if either one of the followings takes place:

1. The RS results show a considerably large range between the lower and upper bounds. For instance in the case shown in the previous section, the range of vertical displacement at the tunnel crown varies between a few centimetres up to 2.5 metres, which is not admissible from a design point of view.
2. Among the realisations required for the random set analysis, some FE-calculations remain incomplete because parameter combinations lead to ground or structural failure. As a result, the bounds on the system responses cannot be obtained.

The rest of the chapter attempts to show how the cases mentioned above can be dealt with and turned into a successful result.

Two scenarios might exist regarding the above mentioned issues:

#### **Scenario 1:**

On the one hand, the system response range is the reflection of the input intervals, and on the other hand the selection of the input parameter sets is prone to error. It means that a very conservative choice of input parameters involved in the uncertainty analysis may be a main cause of the unsuccessful RS results. As demonstrated in the previous example, design has been carried out on the basis of the most optimistic combination of parameters, and the design outcome was satisfactorily conforming to the construction feasibility and other design criteria. On the contrary, the pessimistic bounds (or belief) of the RS-FEM results are far away from acceptable, and raise doubts whether the design is robust. It is therefore imperative to use reliable sources, and in cases where too conservative assumptions have been made, the selected sets must be corrected and/or rectified. Thus, scenario 1 put a question mark on validity of input parameter sets.

#### **Scenario 2:**

It is likely that the scenario 1 is rejected which means that the ranges of input parameters reflect the actual uncertainty of subsurface conditions. Therefore, the large scatter of the results or failure of some realisations is a natural

consequence of the degree of the existing uncertainty in the input data. This implies that considering the existing state of knowledge, the current design is not appropriate. Scenario 2 suggests modifying the current support design since the current state of knowledge cannot be reduced unless more investigation is carried out. So the master model employed in the RSM should be modified by applying additional support measures.

In the following sections the two scenarios are practiced using the introduced tunnel project. In section 4.2, scenario 1 is followed in which the input parameters are revised and new random sets are derived which represent the actual ground conditions. Section 4.3 follows scenario 2 assuming that the current conservative random sets represent the actual subsurface condition. However, a new class of support should be provided in order to obtain a reasonable RS result.

## 4.2 Scenario 1: Revision of input random set according to Hoek-Brown parameters

Assuming that the first scenario mentioned above is adopted, in this section an attempt will be made to extract the MC parameters directly from test results performed on rock samples, which have been given in the site investigation report. It follows that in the faulted zone III mainly the rock type comprises Andesite and Rhyolithe and the characteristic parameters of the rock mass can be quantified by Hoek-Brown parameters summarised in Table 13.

**Tab. 13:** The rock mass characteristics of zone III derived from the site investigation report

Parameter Description	Rock Quality Designation	Elastic modulus of intact rock	Rock mass rating	Geological strength index	Unconfined compressive strength of intact rock	HB parameter
Symbol	RQD	$E_i$	RMR	GSI	$\sigma_{ci}$	$m_i$
Unit	-	GPa	-	-	MPa	-
Value/Range	<25%	19-25	25-35	30-40	10-50	15-25

### 4.2.1 Rock mass strength parameters

For the purpose of underground structure design, many researchers have developed characterisation and classification methods by which rock mass behaviour can be distinguished and categorised into some classes based on related criteria. Based on that empirical classification, relevant support and

excavation methods are recommended. Another philosophy is based on evaluating the rock mass behaviour and determining the appropriate support based on site specific evaluations and experience in similar conditions. Goricki (2007) has developed a hierarchical design procedure for rock mass characterisation and classification based on rock mass behaviour. He has discussed the shortcomings of empirical classification systems and a summary of well-known classification systems has been presented.

Above all, in evaluating any underground system behaviour an estimate of the rock mass strength is necessary and a failure criteria is commonly used to quantify the capability of the rock mass in bearing the applied load. A comprehensive review of failure criteria associated with intact rock materials and rock mass (e.g. Hoek & Brown 1980, Ramamurthy 1985, Shoerey 1989, Yoshida 1990) has been presented by Edelbro (2003). Among others, the most two common criteria in engineering practice are Mohr-Coulomb (MC) and Hoek-Brown (HB) for evaluating the homogeneous rock mass strength. There are a number of corresponding empirical correlations, experienced by practitioners as well as tables and graphs, which provide values for rock mass parameters according to rock type and quality. The correlations are valid provided that the rock mass does not exhibit significant anisotropy in strength and deformability (e.g. rock mass contains a dominant joint set) and the probable failure mechanism has a shear failure mode. For instance, other failure modes like buckling, ravelling, rock burst, sliding or falling of kinematically free blocks and so on cannot be evaluated by means of this criterion and should be separately checked by the respective criteria (Goricki, 2007; Steiner, 2005). Moreover, it is possible to calculate the equivalent MC parameters from HB ones (and vice versa) over a certain stress range. Both MC and HB models are classified as elasto-perfectly-plastic constitutive models with different failure criteria. Mohr-Coulomb failure criterion relates the major and minor principal stresses linearly. However, the strength of the rock mass is usually better expressed by a parabolic function which may comply more appropriately with the real behaviour of rock (e.g. Brown 1970).

#### 4.2.1.1 Hoek-Brown criterion

At failure, the generalized HB criterion (Hoek et al. 2002) relates the maximum effective stress  $\sigma_1$  to the minimum effective stress  $\sigma_3$  through the equation:

$$\sigma_1 = \sigma_3 + \sigma_{ci} \left( m_b \frac{\sigma_3}{\sigma_{ci}} + s \right)^a \quad (25)$$

where  $\sigma_{ci}$  is the uniaxial compressive strength of the intact rock, and  $s$  and  $a$  are model constants. The relationships between  $m_b/m_i$ ,  $s$ ,  $a$ , and the geological strength index (GSI) are as follows:

$$m_b = m_i \exp\left(\frac{GSI - 100}{28 - 14D}\right) \quad (26)$$

$$s = \exp\left(\frac{GSI - 100}{9 - 3D}\right) \quad (27)$$

$$a = \frac{1}{2} + \frac{1}{6}\left(e^{-GSI/15} - e^{-20/3}\right) \quad (28)$$

Hoek et al. (1995) introduced the Geological Strength Index, as a complement to their generalised rock criterion and as a way to estimate the parameters  $s$ ,  $a$ , and  $m_b$  in the criterion. This GSI estimates the reduction in rock mass strength for different geological conditions. The GSI value can be empirically estimated either from rock classification systems (e.g. Q-system given by Barton et al., 1974, and RMR introduced by Bieniawski, 1976) or directly from a table given by Hoek et al. (1995) that practically varies over a range between 10 to 100. By definition, GSI values close to 10 correspond to very poor quality rock mass, while GSI values close to 100 correspond to excellent quality rock masses. The GSI takes the geometrical shape of intact rock fragments as well as the condition of joint faces into account. Finally,  $D$  is a factor that quantifies the disturbance of rock masses. It varies from 0 (undisturbed) to 1 (disturbed) depending on the amount of stress relief, weathering and blast damage.

#### 4.2.1.2 Equivalent Mohr-Coulomb parameters

As mentioned above it is possible to estimate the equivalent MC strength parameters from HB parameters with various methods. The choice of the method for determining equivalent cohesion and friction angle is largely a matter of experience (Merifield et al., 2006). Several ways have been proposed to match the HB and MC strength parameters (Sjöberg, 1997). In general, there are two options to derive equivalent cohesion and friction angle from HB parameters; First, by fitting the MC failure line to the HB failure curve tangentially at a specific minor principal stress or normal stress. Second, a regression method can be applied over a dominant stress range of the problem, to obtain average values of MC strength parameters. However, this may lead to an underestimate of the strength for low stresses and an overestimate for high stresses. Nevertheless, the latter is the most frequently used method and is typically performed by fitting a linear relationship to the curve generated by Equation 25 for a range of minor

principal stress values defined in Equation 29 given by Hoek et al. (2002). This formula has been suggested for shallow and deep tunnel applications.

$$\frac{\sigma'_{3\max}}{\sigma'_{cm}} = 0.47 \left( \frac{\sigma'_{cm}}{\gamma H} \right)^{-0.94} \quad (29)$$

where  $\sigma'_{cm}$  is the global rock mass strength and a function of HB parameters calculated by Equation 30,  $\gamma$  is the unit weight of the rock mass, and  $H$  is the tunnel depth below the surface.

$$\sigma'_{cm} = \sigma_{ci} \cdot \frac{(m_b + 4s - a(m_b - 8s))(m_b / 4 + s)^{a-1}}{2(1+a)(2+a)} \quad (30)$$

This fitting procedure results in the following equations for the equivalent MC strength parameters:

$$\phi' = \sin^{-1} \left[ \frac{6am_b(s + m_b\sigma'_{3n})^{a-1}}{2(1+a)(2+a) + 6am_b(s + m_b\sigma'_{3n})^{a-1}} \right] \quad (31)$$

$$c' = \frac{\sigma_{ci} [(1+2a)s + (1-a)m_b\sigma'_{3n}] (s + m_b\sigma'_{3n})^{a-1}}{(1+a)(2+a) \sqrt{1 + (6am_b(s + m_b\sigma'_{3n})^{a-1}) / ((1+a)(2+a))}} \quad (32)$$

where  $\sigma_{3n} = \sigma'_{3\max} / \sigma_{ci}$

It is noted that  $\sigma'_{3\max}$  should be determined for each case individually; the stresses are likely to vary within the rock mass, which makes it more difficult to select a representative value of  $\sigma'_{3\max}$  (Merifield et al., 2006). For general geotechnical applications, another suggestion proposed by Hoek and Brown (1997) is to match the MC failure line with HB over the range  $0 < \sigma'_3 < \sigma'_{3\max} = 0.25\sigma_{ci}$ . Here both suggestions are used to obtain the new random sets for MC strength parameters.

It is aimed to derive two sets for each MC strength parameter from HB strength parameters given in Table 13 using Equations 25-32. When constructing the first set, lower values of  $m_i$  and  $\sigma_{ci}$  are taken into account while the upper values are used to make up a second set. To compute the lower bound of each set for  $c$  and  $\phi$  the lower value of both  $D$  and GSI are used and for the upper bound the higher values are taken. Thereby, considering two different assumptions about the range of  $\sigma_3$  in the fitting procedure results in two different random sets, which are illustrated in Figure 36. In the computation the depth of the tunnel has been assumed equal to 30 meters.

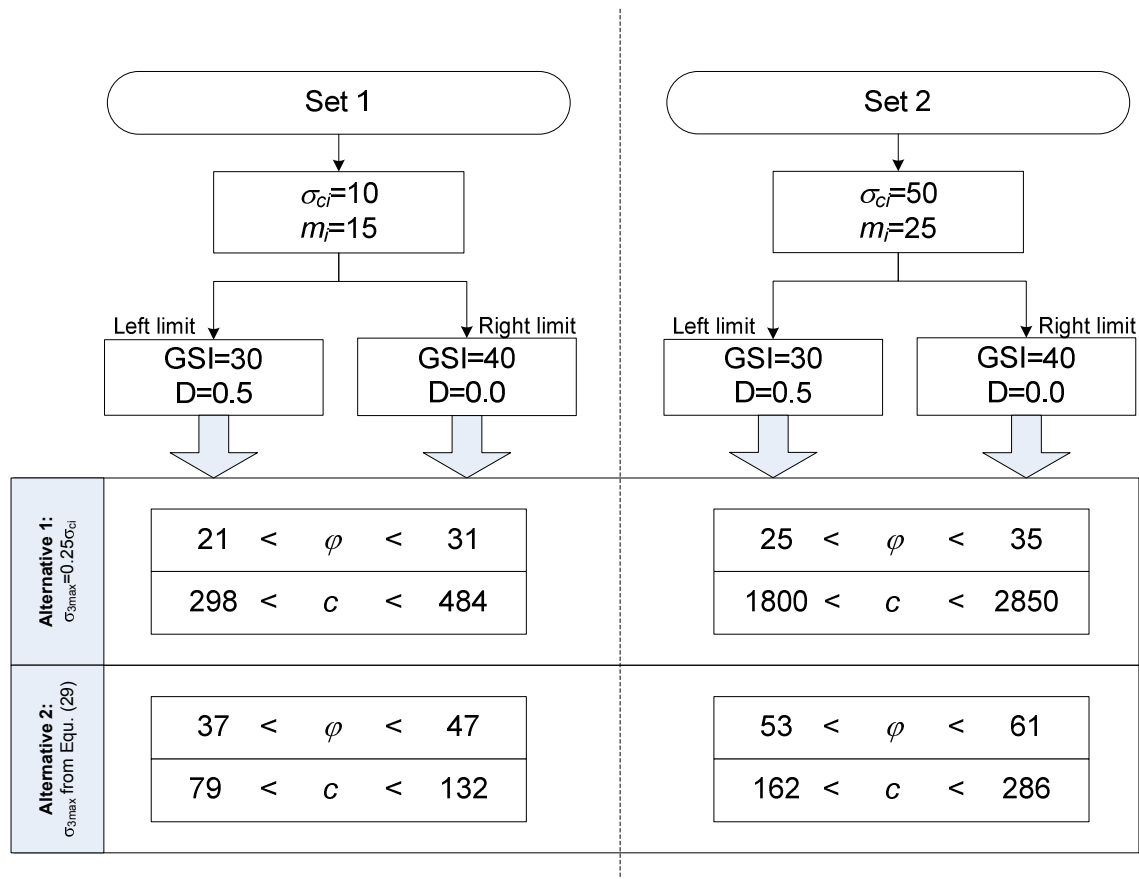


**Fig. 36:** Random set of MC strength parameters drawn from HB model parameters, unit of cohesion is kPa

Obviously, alternative 2 gives higher friction angles than alternative 1 because the corresponding  $\sigma'_{3max}$  is lower and the regression line is fitted in a lower range of  $\sigma'_3$  stress. Consequently, the fitted line becomes steeper and the corresponding cohesion is decreased. Furthermore, the random sets (alternative 1 or 2) obtained in this method give higher rock mass strength with respect to the previous random set given in Tables 10 and 12 both in terms of friction angle and cohesion.

## 4.2.2 Revised deformability modulus of the rock mass

For different reasons, it is often difficult to obtain specific design parameters directly from tests and as an alternative, empirical correlations are used. To obtain realistic values of rock mass deformation modulus ( $E_{rm}$ ), in-situ tests, such as plate bearing, flat jack, pressure chamber, borehole jacking and dilatometer tests, need to be conducted. The in-situ tests, however, are time-consuming, expensive and, in some cases even impossible to carry out. Therefore, a number of empirical methods have been developed that correlate various rock quality indices or classification systems to the deformation modulus of rock masses. The correlations are mostly between the deformation modulus and RQD (Rock

Quality Designation), RMR (Rock Mass Rating), Q (Q-System) and GSI (Geological Strength Index). The frequently used correlations are summarized in Table 14. All of these classifications are based on the assumption of isotropy and homogeneity. This means that a rock mass must contain a sufficient number of discontinuities sets so that the real deformations could be expected to exhibit sufficiently isotropic behaviour.

The scatter of the rock mass stiffness values obtained from the empirical correlations is considerable and therefore, taking all the correlations into account, the difference in results would be one order of magnitude. For the purpose of determining the new random set for the deformability parameter a choice has to be made which correlations are used. Hoek and Diederichs (2006) evaluated the common correlations against large field data and they pointed out, for instance, the  $E_{rm}$  calculated by correlation 12 has shown just 5% error in comparison with the Serafim and Pereira (1983) relation, whose error reaches 50% since correlation 12 does not consider the damage factor ( $D$ ). Zhang (2005) also found that the equation given by Serafim and Pereira (1983) overestimates the rock mass deformation modulus for poor quality rocks. Some equations use only classification indices that have not been directly in access for this project or they don't consider any characteristics of the intact rock. Therefore, correlation 11 has been used as a basis for deriving the two sets since it is consistent with those given for strength parameters in the previous section.



**Tab. 14:** Empirical correlation equations for determining rock mass deformability

Correlation equation	Development/comment	Author
1) $E_{rm} = 2RMR - 100$ [GPa]	<ul style="list-style-type: none"> <li>Drawback: It gives negative values for <math>RMR &lt; 50</math></li> <li>Data of seven projects involved in the equation</li> </ul>	Bieniawski, 1978
2) $E_{rm} = 10^{((RMR-10)/40)}$ [GPa]	<ul style="list-style-type: none"> <li>It estimates well for good quality rocks, highly overestimated for poor rock quality</li> </ul>	Serafim and Pereira, 1983
3) $E_{rm} = 0.0736e^{0.0755RMR}$ $E_{rm} = 0.1451e^{0.0654GSI}$ [GPa]	<ul style="list-style-type: none"> <li>Obtained from 115 in situ plate loading and dilatometer tests,</li> <li>Only RMR or GSI index is involved</li> </ul>	Gokceoglu et al., 2003
4) $E_{rm} = E_i(0.0028RMR^2 + 0.9e^{RMR/22.82})$	<ul style="list-style-type: none"> <li>For general use</li> </ul>	Nicholson and Bieniawski, 1990
5) $E_{rm} = E_i(1 - \cos(\pi \times RMR/100))/2$	<ul style="list-style-type: none"> <li>For general use</li> </ul>	Mitri et al., 1994
6) $E_{rm} = 10 \left( Q \frac{\sigma_{ci}}{100} \right)^{1/3}$	<ul style="list-style-type: none"> <li><math>\sigma_{ci}</math> in MPa and <math>E_{rm}</math> in GPa</li> <li>For general use</li> </ul>	Barton, 2002
7) Lower bound: $E_{rm} = 10 \log Q$ 8) Upper bound: $E_{rm} = 40 \log Q$ 9) Mean: $E_{rm} = 25 \log Q$	<ul style="list-style-type: none"> <li><math>E_{rm}</math> in GPa</li> <li>Only applicable to <math>Q &gt; 1</math> and generally for hard rocks</li> </ul>	Barton et al., 1980
10) $E_{rm} = 0.33e^{0.064GSI}$ [GPa]	<ul style="list-style-type: none"> <li>For general use</li> </ul>	Hoek, 2004-for the reference see Zhang, 2005
11) $E_{rm} = (1 - D/2) \sqrt{\frac{\sigma_{ci}}{100}} 10^{((GSI-10)/40)}$ [GPa]	<ul style="list-style-type: none"> <li><math>\sigma_{ci} &lt; 100</math> MPa</li> </ul>	Hoek et al., 2002
12) $E_{rm} = E_i \left( 0.02 + \frac{1 - D/2}{1 + e^{((60+15D-GSI)/11)}} \right)$	<ul style="list-style-type: none"> <li>Based on 494 in situ tests and back analyses comprising wide range of rock types and <math>0 &lt; GSI &lt; 100</math></li> </ul>	Hoek and Diederichs, 2006
13) $E_{rm} = 100 \left( \frac{1 - D/2}{1 + e^{((75+25D-GSI)/11)}} \right)$ [GPa]	<ul style="list-style-type: none"> <li>where only GSI data are available</li> </ul>	Hoek and Diederichs, 2006
14) $E_{rm} = E_i \times 10^{0.0186RQD-1.91}$	<ul style="list-style-type: none"> <li>RQD is significantly dependent on borehole orientation; to reduce the dependency of RQD see treatment given in Zhang 2005</li> </ul>	Zhang and Einstein, 2004
15) $E_{rm} = \alpha_E E_i$ $\alpha_E = 0.0231(RQD) - 1.32 \geq 0.15$	<ul style="list-style-type: none"> <li>Adopted by ASSHTO, 1989</li> </ul>	Gardner, 1987

Considering the ranges of GSI and  $\sigma_{ci}$  presented in Table 15, one is able to infer two sets of parameters for the geological condition of the rock mass assuming that the lower value of UCS combined with the range of GSI makes up the first set and similarly the upper value of UCS forms the second set. Consequently, in this manner two random sets given in Table 15 are derived for the elastic modulus of rock mass using correlation 11 of Table 14.

**Tab. 15:** Input random sets of elastic modulus of rock mass

Parameters	Probability of assignment	$\sigma_{ci}$ (UCS)	GSI	$E_{rm}$ (modulus of rock mass)
Units	-	MPa	-	MPa
Set No. 1	0.5	10	30-40	1000-1770
Set No. 2	0.5	50	30-40	2230-3970

### 4.2.3 Basic variables for the random set model

As described in section 4.2.1.2, assuming two different ranges for fitting MC strength parameters along the HB failure line, results in two different sets of parameters with a large discrepancy. Thus, these two alternatives are included in the following RS-FEM analyses in order to observe the differences. The random set model and procedure described in Chapter 3 was followed separately considering the two alternatives. The number of basic variables was maintained as four. Therefore, the number of FE calculations required for RSFEM remains 256 realisations. The spatial variability was taken into account for the rock mass parameters using the reduction technique except for the strength parameters of alternative 2 since the change in the set limits due to the reduction factor is negligible. To compute the variance reduction factor ( $I$ ), the spatial correlation length ( $\Theta=10$  m) was taken similar to the amount used for zone I in the previous tunnel example with 7.5 meters overburden. The length of a potential failure surface ( $L$ ) has been estimated about 30 meters from one of the calculations using the strength reduction method.

The final random set input variables utilized in further analyses are summarised in Tables 16 and 17 corresponding to alternatives 1 and 2 for strength parameters respectively. It is noted that both sets chosen for the stress relaxation factor are based on expert's opinion and the lower values are matched to the set with lower strength and deformability modulus values. In addition, the values for different stage constructions are correlated to each other, i.e. in any realisation the left or right extreme of  $R_f$  for the top-heading, bench and invert are used simultaneously. Moreover, it should be noted that high values of cohesion sets in alternative 1 have been reduced to 75% (suggestion advised by Hoek and Brown, 1997). The

values given in Tables 16 and 17 have been rounded after applying the variance reduction factor.

**Tab. 16:** Revised random set parameters (alternative 1)

Var.	$m(A)$	$E_{rm}$ (rock mass modulus)	$R_f$ T.H.	$R_f$ Bench	$R_f$ Invert	$\varphi$	$c$
Units	-	[MPa]	-	-	-	[°]	[kPa]
Set 1	0.5	1300-2300	0.4-0.6	0.3-0.5	0.2-0.4	22-32	450-750
Set 2	0.5	1900-3400	0.3-0.5	0.2-0.4	0.1-0.3	24-34	1000-1600

**Tab. 17:** Revised random set parameters (alternative 2)

Var.	$m(A)$	$E_{rm}$ (rock mass modulus)	$R_f$ T.H.	$R_f$ Bench	$R_f$ Invert	$\varphi$	$c$
Units	-	[MPa]	-	-	-	[°]	[kPa]
Set 1	0.5	1300-2300	0.4-0.6	0.3-0.5	0.2-0.4	37-47	80-130
Set 2	0.5	1900-3400	0.3-0.5	0.2-0.4	0.1-0.3	53-60	160-280

Extracting the input parameters directly from basic parameters, test results and observations reflected in the site investigation report has significantly changed the input random sets, and demonstrates that the primary sets had been chosen as too conservative.

#### 4.2.4 Validity of the RSFEM results

Considering the two alternatives for the revised random set basic variables, the bounds on selected results are illustrated in terms of discrete cumulative probability in Figures 37 to 40. To evaluate the quality of the input variables as well as the random set model a comparison has been made with available displacement measurements. The measurement points A and B have been considered at the tunnel crown and its side wall respectively, whose positions have already been depicted in Figure 16. Since two observations were available within the faulted zone (section BQ3), measurements can be presented in terms of discrete cumulative probability that comprise two steps corresponding to those measurements as depicted in Figures 37 and 39.

The new random set results not only show a significant decrease in tunnel displacements but also a success in estimating and encompassing the

measurements within its bounds. The primary random set results showed a very wide range of displacements from millimetres to meters whereas by revising the values of the sets, the displacements dropped considerably to a reasonable range. For instance, regarding the results of alternative 1, Figure 37 shows that the measured values of the vertical displacement of the tunnel crown have been located within the green zone of the quality indicator, or in other words, they lie within the range of the most likely values predicted by the random set model. Part of the measurements of the horizontal displacement at point B falls outside the most likely range; however, it is still within the green indicator. The vertical displacement at point B shows partial disagreement with the random set model although from a practical point of view it can be neglected. However, it theoretically implies that the numerical model cannot represent all aspects of ground behaviour perfectly. For instance, one hypothesis is that the rock mass behaves heterogeneously and therefore an anisotropic model should be employed instead. A second hypothesis is that the sets of strength parameters do not properly represent the rock mass behaviour. The results of the second alternative strengthen the correctness of the latter hypothesis. Figure 39 illustrates the random set results of alternative 2, which demonstrate almost a full agreement between measured values and the predicted random set range. The only difference between alternatives 1 and 2 is the equation by which the Mohr Coulomb parameters were derived. Considering the success of alternative 2 in estimating the reasonable range for all responses, one can confirm that Equation 29 used for obtaining the MC parameters of alternative 2 could be appropriate for tunnel applications.

Another example of the random set results is the safety factor of the top heading excavation after installing the shotcrete lining. The lower and upper bounds of the safety factor have been depicted in Figures 38 and 40 for alternatives 1 and 2 respectively. In an average, the factor of safety obtained in alternative 1 is twice that of alternative 2 which would be expected considering the differences in strength parameters. In addition the p-box of the internal forces of the tunnel lining is illustrated. There is a slight difference between the responses of the two alternatives.

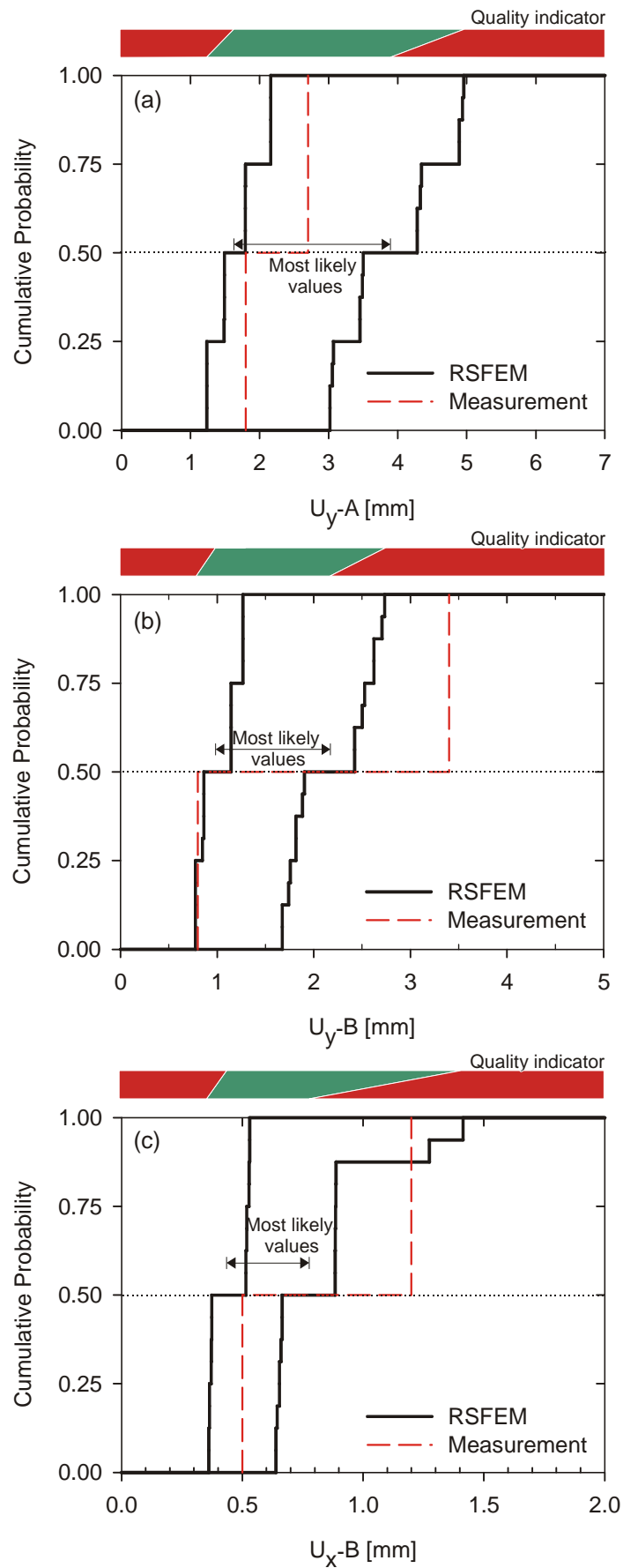


**Fig. 37:** RSFEM prediction from alternative 1, a) vertical displacement at point A, b & c) vertical and horizontal displacement at point B

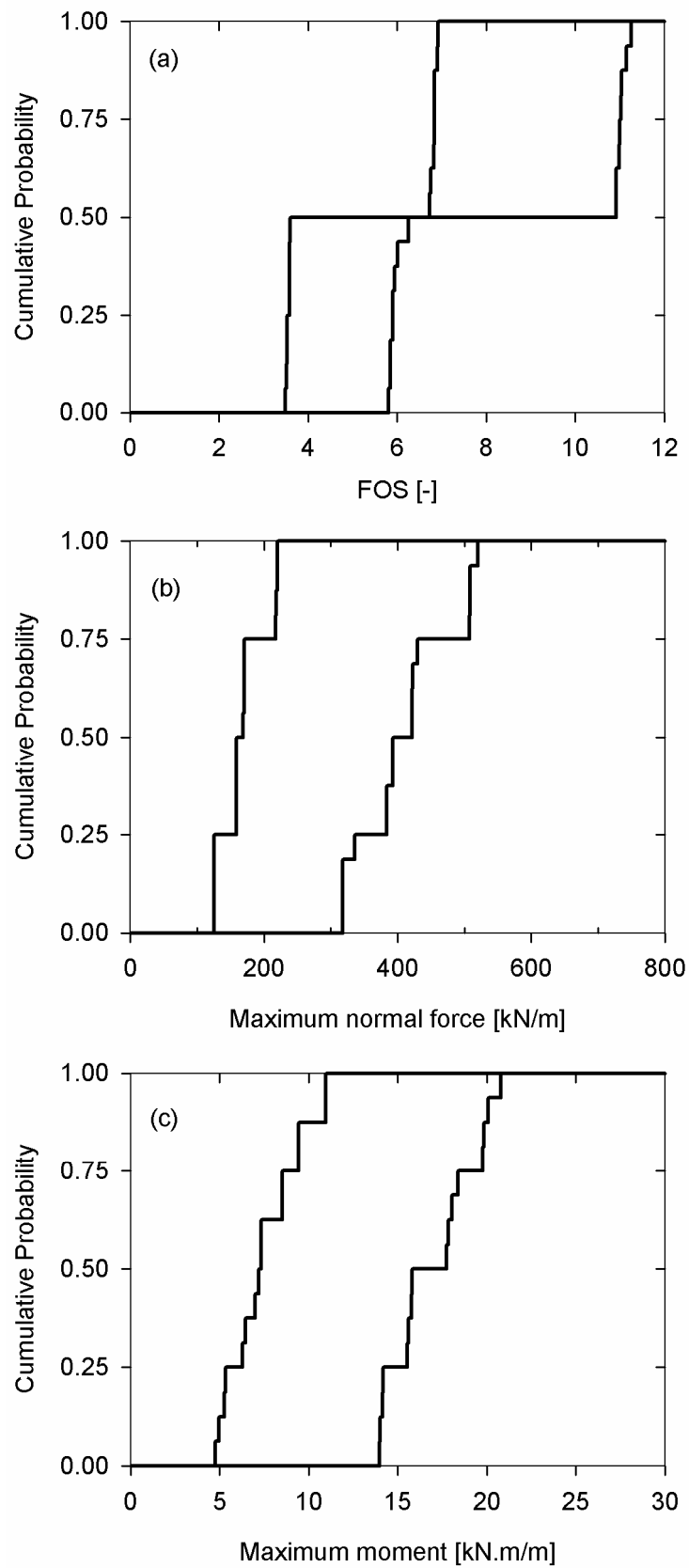


**Fig. 38:** RSFEM results from alternative 1, a) factor of safety after top-heading excavation, b) maximum normal force c) maximum moment in the lining

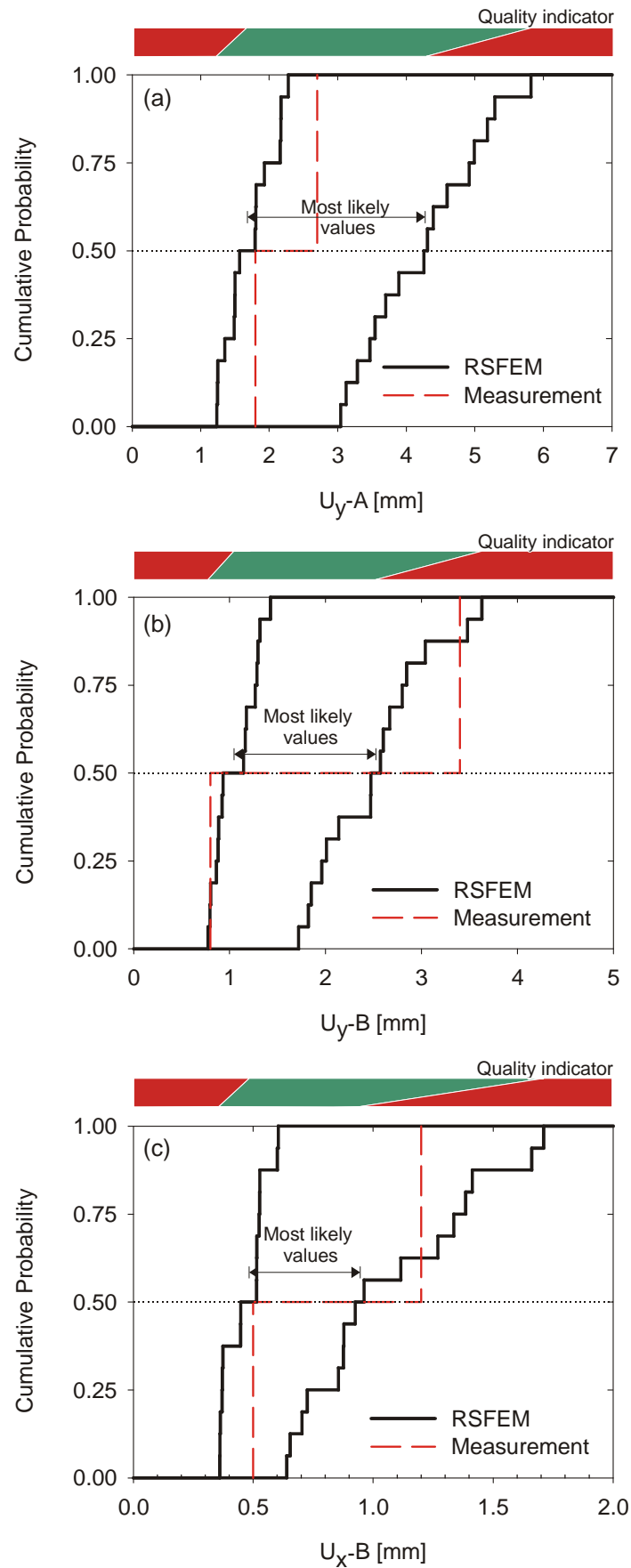


**Fig. 39:** RSFEM prediction from alternative 2, a) vertical displacement at point A, b & c) vertical and horizontal displacement at point B

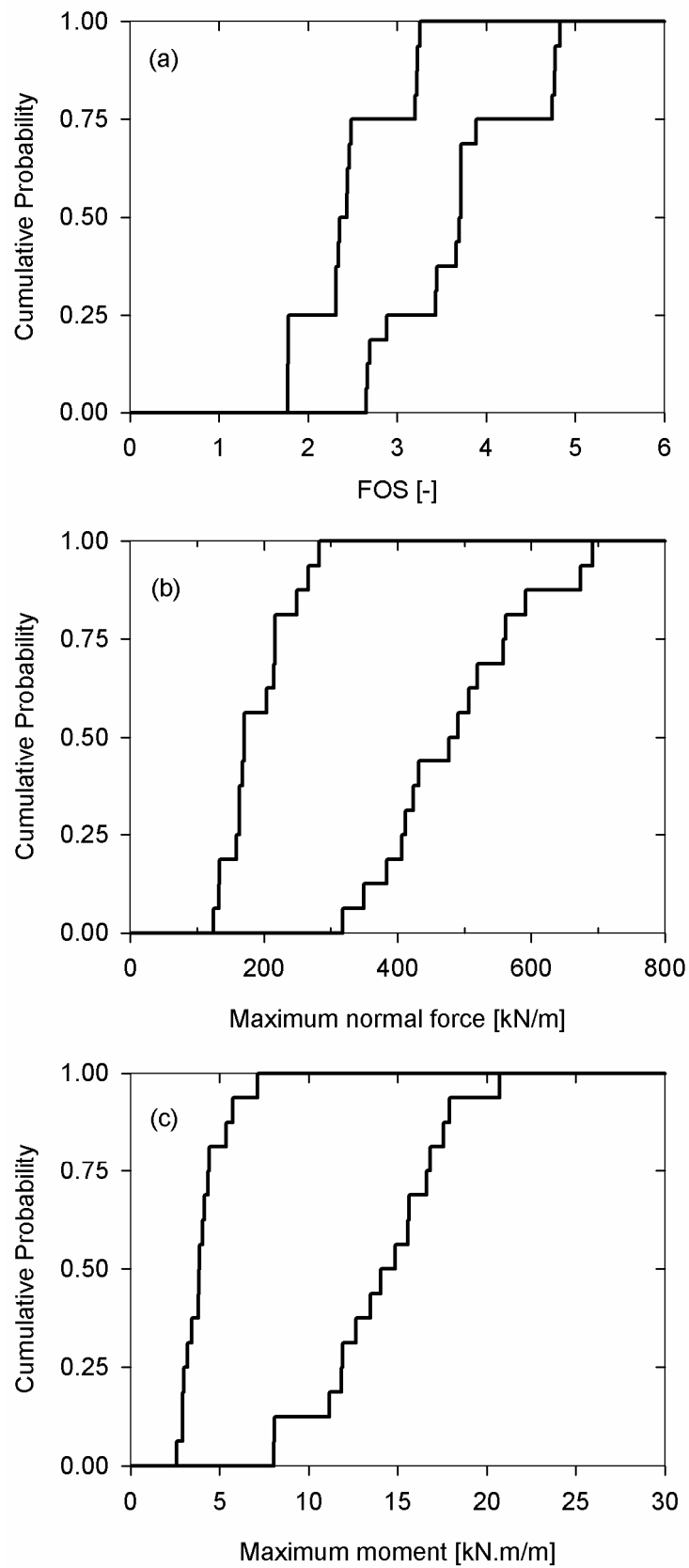


**Fig. 40:** RSFEM results from alternative 2, a) factor of safety after top-heading excavation, b) maximum normal force c) maximum moment in the lining



### 4.2.5 Evaluation of lining performance function

Having the random set results of the internal forces of the shotcrete lining, it is possible to assess the satisfactory performance of the lining against cracking. To do so, again the relationship given by Equations 23 and 24 is utilised. According to the design value, a thickness of shotcrete depending on the position of the element is varied between 15 to 25 centimetres.

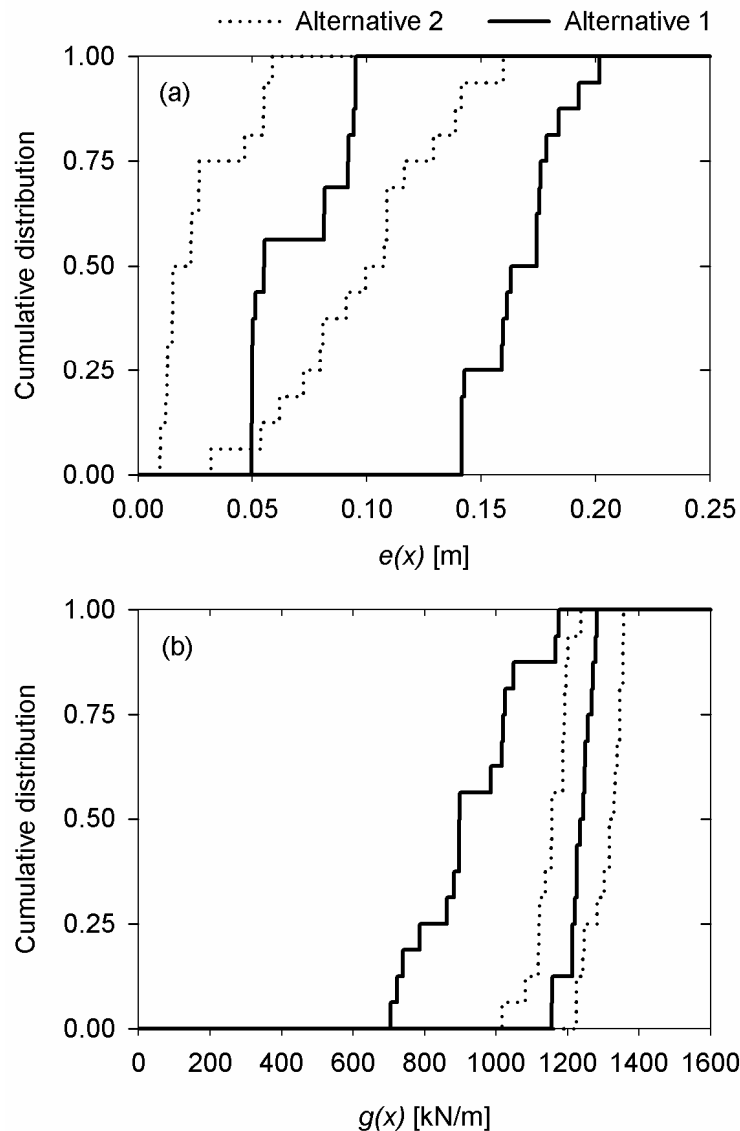


**Fig. 41:** RSFEM results from alternative 1 and 2, a) eccentricity in the lining cross section, b) serviceability performance function of the shotcrete

For the shotcrete a C20/25 with a uniaxial strength of 17.5 MPa is used. To cover imperfections an eccentricity of  $e_a = 2$  cm and safety factor of  $F_s = 2.1$  to consider the serviceability condition are taken. Here, serviceability limit state function,  $g(x)$ , is evaluated directly from the results of each FE calculations as described in Chapter 3. The p-box of the  $g(x)$  in terms of cumulative probability

for both alternatives 1 and 2 at the end of construction are presented in Figure 41. The most probable values of the performance function resulting from alternative 1 ranges from 900 up to 1200 approximately. This range is slightly increased for alternative 2 from 1150 to 1350. The lower and upper probability distribution functions indicate that the probability of exceeding admissible normal force in the lining,  $N_{lim} < N$ , where cracking takes place, is negligible. Hence, the revision of the input random sets maintains a high performance level of the lining and major cracks are not anticipated.

### **4.3 Scenario 2: Change of construction sequence and reconsidering the tunnel design**

At the beginning of the chapter it was shown that random set analysis regarding the tunnel section in the faulted zone exhibited unsuccessful results including large tunnel displacements and a wide range of uncertainty in the system response as well as difficulties in numerical convergences. In section 4.1.2 two scenarios were discussed for treatment. In this section the results of the second scenario are presented and discussed. The objective is to demonstrate that if scenario one is rejected, by changing the construction sequences and a new tunnel design, satisfactory RS results can be obtained. The tunnel geometry and design specifications have been shown in Figure 42 and the corresponding 2D finite element mesh has been depicted in Figure 43.

To control the large displacements predicted by primary random set analysis, a possible solution may be the closure of the tunnel right after the top heading excavation. The temporary bench lining will prevent the lateral displacements and consequently leads to a smaller amount of total displacement. In accordance with the actual construction sequence 5 calculation phases have been modelled:

1. Initial stresses
2. Pre-relaxation phase of top heading excavation (Fig. 44a)
3. Installation of anchors and primary lining in top heading, temporary invert (Fig. 44b)
4. Pre-relaxation phase of bench and invert excavation (Fig. 44c)
5. Destruction of the temporary invert and the excavation of the bench and invert along with the completion of the primary lining and anchors (Fig. 44d)

**Tab. 18:** The range of MC-model parameters extracted from the geotechnical report for zone III and the representative values used in design K6-4A

Parameters	$E_{ref}$	$c$	$\varphi$	$K_0^{nc}$	$\nu$	$R_f$	
Units	[MN/m <sup>2</sup> ]	[kPa]	[°]	[-]	[-]	T.H.	B & I
Geotechnical report	100-200	60-90	21-23	0.4-0.6	0.35	-	-
Design-K6-4A	75	50	20	0.55	0.35	0.5	0.25

**Tab. 19:** Parameters for structural elements used in design K6-4A

Support element	Location	Type	$E$ -modulus		Plastic Limit Force	Thickness /Diameter
			young	old		
			[MPa]		[kN]	[cm]
Shotcrete	Top-heading	Elastic	5000	15000	-	30
Shotcrete	Temp. Bench	Elastic	5000	15000	-	20
Shotcrete	Invert	Elastic	5000	15000	-	30
Anchor	T.H., B., I.	Elasto-plastic	210000		200	2.2

**Tab. 20:** The random sets used in design K6-4A for section BQ3 considering spatial autocorrelation

Set No.	Probability assignment	$E_s$	$c$	$\varphi$	$R_f$	
		[MN/m <sup>2</sup> ]	[kPa]	[°]	T.H.	B & I
1	0.5	79-157	52-82	20-22	0.4-0.6	0.2-0.4
2	0.5	96-192	58-88	21-23	0.3-0.5	0.1-0.3

The material parameters for the rock mass considered in the new design (K6-4A) along with the ranges of the basic variables given by the geotechnical report for zone III have been summarized in Table 18. In the random set model, four basic variables with two sets each are involved, which are given in Table 20. For the deformability of the rock mass,  $E_{rm}$ , and cohesion the random sets are taken similar to the primary random set given in Table 12. Instead of the earth pressure coefficient at rest, the friction angle of the rock mass is taken as a third basic variable. The chosen random set for these parameters are based on the range given by the site investigation report and a small variation suggested by expert opinion. The 3D effects of the tunnel face are treated by introducing the



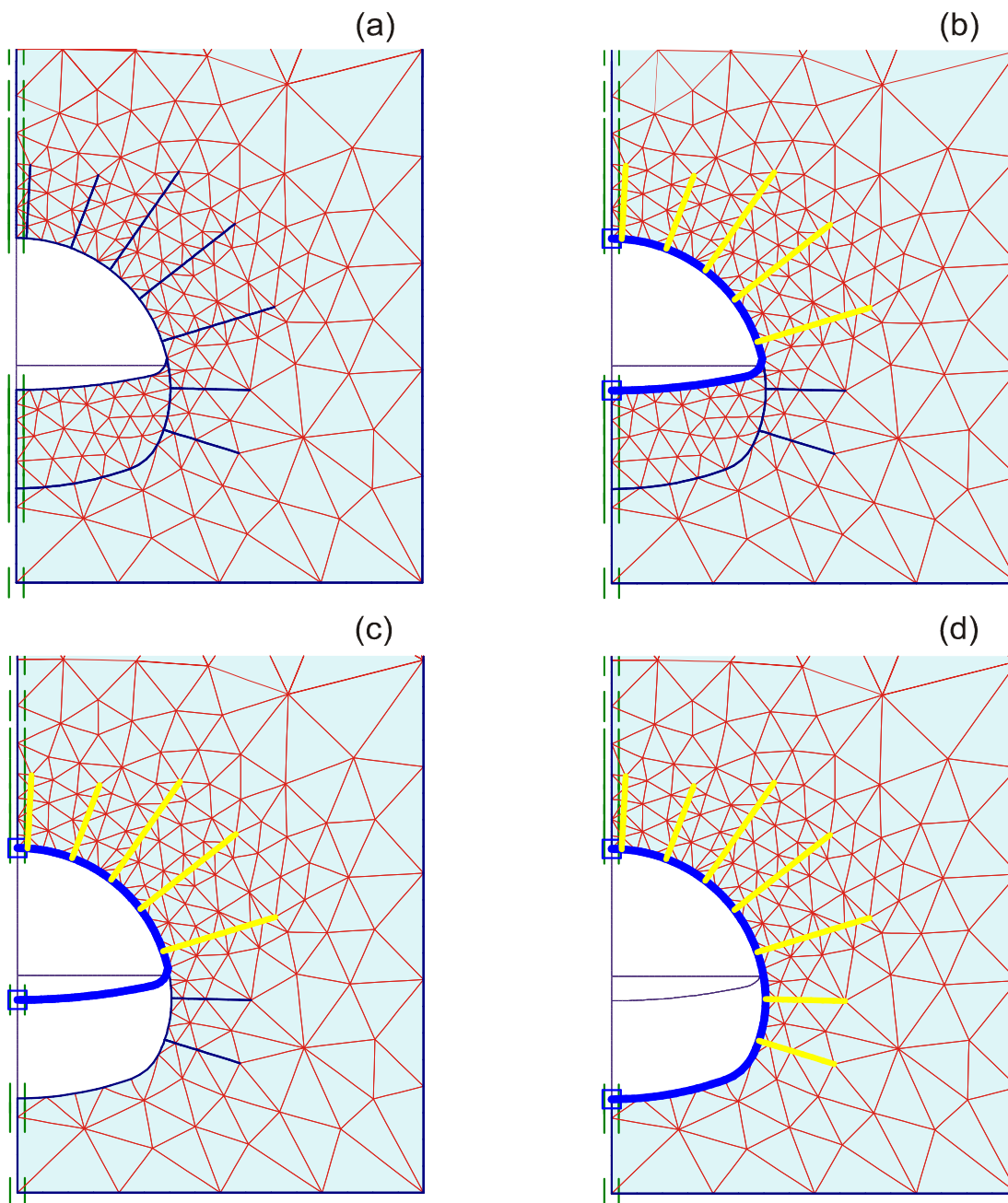


**Fig. 44:** Stage constructions of the new tunnel design (K6-4A) for section BQ3, a) pre-relaxation of the top heading, b) top heading excavation, temporary invert and anchors, c) pre-relaxation of the bench and invert, d) excavation of the bench and invert, completion of shotcrete and anchors

### 4.3.1 Calculation results

The lower and upper bounds on the desirable system responses such as tunnel displacements, internal forces and the evaluated performance function of the shotcrete lining are depicted in Figures 45 and 46. A comparison made with the primary random set results shows a significant decrease in tunnel displacements in the range of few centimetres instead of a few meters.

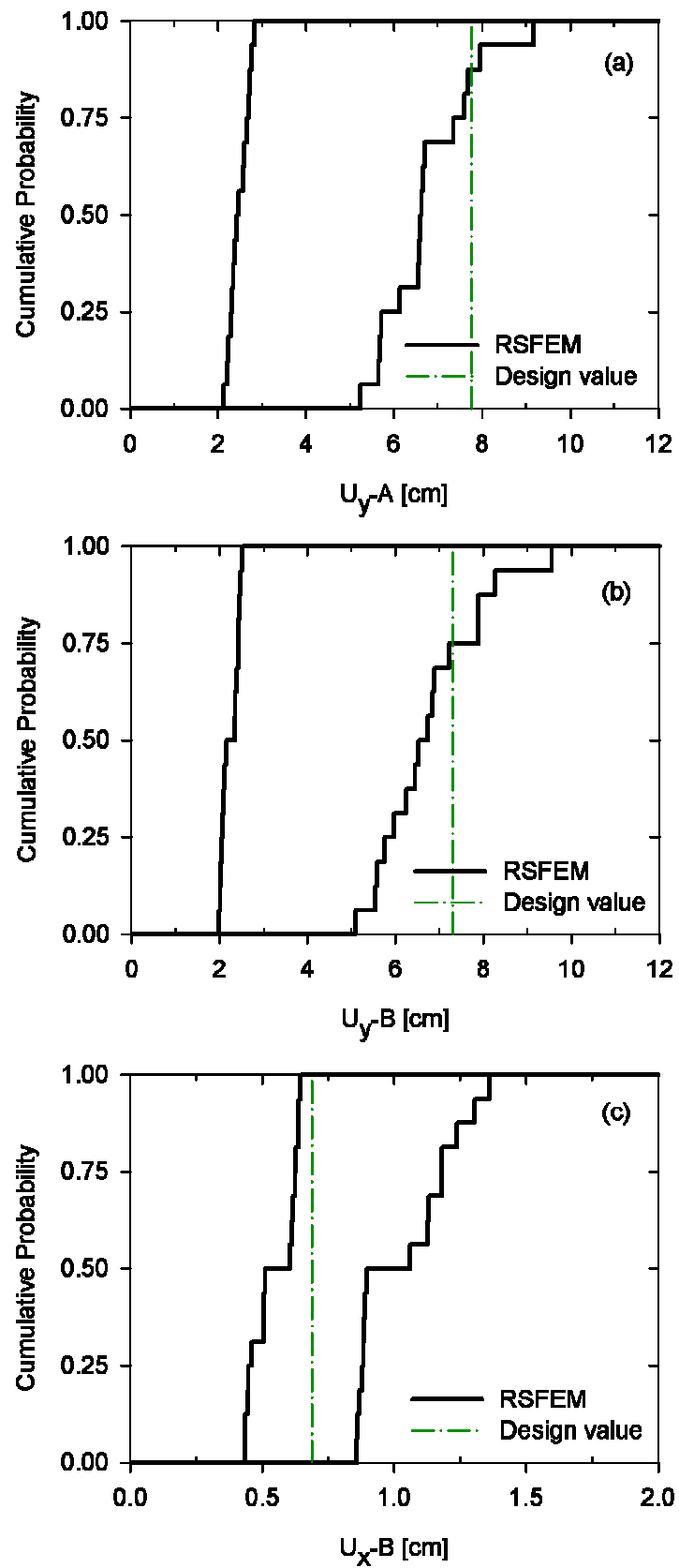


**Fig. 45:** RSFEM results from new design (scenario #2), a) vertical displacement at point A, b & c) vertical and horizontal displacement at point B

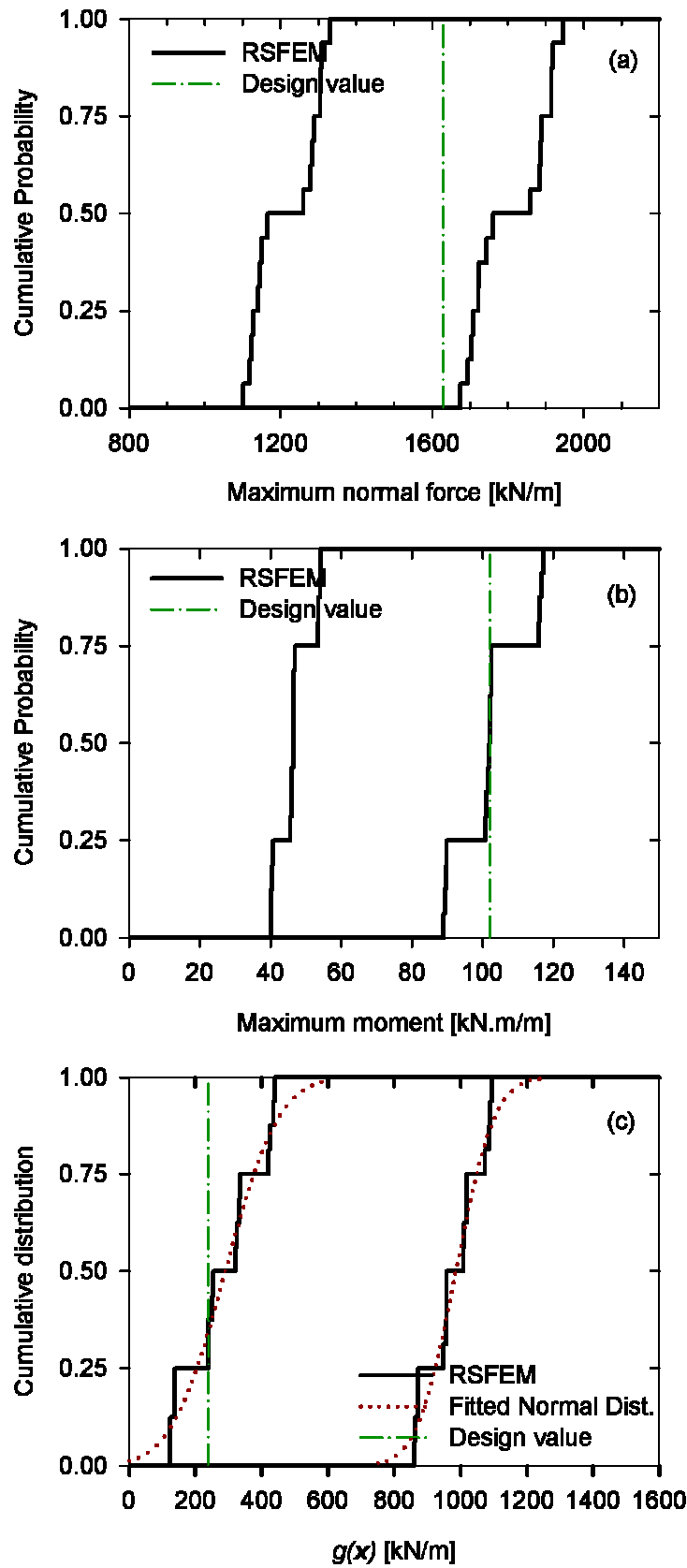


**Fig. 46:** RSFEM results from new design (scenario #2), a) maximum normal force, b) maximum moment in the lining, c) serviceability of the shotcrete performance function

In Figures 45 and 46 besides the random set bounds, result of a deterministic FE calculation based on characteristic values (design value) given in Table 18 has been illustrated. As it is expected, the design values fall within the random set bounds.

Likewise Scenario 1 concerning the shotcrete performance function,  $g(x)$ , the probability of unsatisfactory performance (i.e. probability of failure) should be assessed. Three different well-known distribution functions namely Normal, general Beta and shifted Weibull have been fitted to the discrete cumulative probability function obtained in random set analysis. Probability of failure of  $g(x)$  for respective distributions has been summarized in Table 21. The  $p_f$  obtained directly from random set results is zero because the line of  $g(x) = 0$  does not intercept the discrete CDF. It follows that the probability of failure ranges from almost zero to the maximum value of  $1.48 \times 10^{-2}$ . Thus, in reference to Table 9 the level of expected performance is described as below to above average.

**Tab. 21:** Probability of failure obtained from different distributions fitted to the lower and upper bounds of  $g(x)$

Reliability parameters	Distributions			
	Normal	Beta	Weibull	Discrete CDF
$P_{f\text{-max}}$	$1.15 \times 10^{-2}$	$1.8 \times 10^{-4}$	$1.48 \times 10^{-2}$	0.0
$P_{f\text{-min}}$	$\approx 0.0$	$\approx 0.0$	$\approx 0.0$	0.0

It follows from scenario 2 that in cases where a proportion of the FE calculations show failure, random set results can be improved to a reasonable range by a modification of the tunnel design. This can be considered as an advantage of RS-FEM, which is capable of demonstrating the inefficiency of the design (considering the current state of knowledge of input parameters), while a deterministic calculation with characteristic input values at first sight shows an adequacy of tunnel supports and a successful design.

## 4.4 Summary and conclusion

As can be seen, the tunnel displacement predicted by RSFEM based on the new design and primary random set input parameters are in the range of several centimetres. However, this design was not executed in practice and the measurement showed a good agreement with the range predicted by the revised random set. Therefore, it is concluded that the first scenario has been correct and the primary source of information has given too conservative parameters. Moreover, random set analysis contributed to identifying the most influential input parameters. In addition it was demonstrated that in cases where a



proportion of the FE calculations show failure and consequently the random set bounds cannot not been constructed or result in too wide ranges which are not acceptable from a practical point of view, random set results imply the inefficiency of the tunnel design. By revising the tunnel design, a reasonable range for results can be obtained. Therefore, also in the mentioned cases RS-FEM shows the ability to evaluate a tunnel design considering uncertainties available in input parameters.

## **5 On the effects of constitutive model change**

### **5.1 Problem statement**

Besides the uncertainties in input parameters, loading and geometry, employing different material constitutive models causes different system responses in a numerical model. The objective of the chapter is to assess the uncertainty reflected in the results of a tunnel problem due to the change of the rock model used in the numerical analysis within a probabilistic framework of the Random Set Finite Element Method.

At the beginning of a numerical analysis, a decision has to be made regarding the constitutive material model employed. In a tunnel project when a reliability analysis is to be accomplished, the system response variations caused by this issue become more important and might significantly affect the probability of unsatisfactory performance of the tunnel. There are many factors that are involved in model selection. For instance, some practitioners choose a model like Mohr-Coulomb (MC) for simplicity because it requires fewer input parameters in comparison to an advanced soil model. It may also be difficult to derive the parameters for an advanced soil model due to time limitations, unreliable sources of information, or absence of proper test results. In this chapter, the RS-FEM is employed as a framework to allow for a model variation in a numerical analysis and investigating the consequences of a model change on the results of a reliability analysis. To demonstrate the applicability of the random set model in considering model uncertainty in a reliability analysis, two simple rock/soil models, namely the Hoek-Brown (HB) model and the Mohr-Coulomb (MC) criterion are used.

### **5.2 A tunnel example in rock with 25m overburden**

To illustrate the differences in the outcomes of a numerical analysis resulting from selecting the two above mentioned material models, the master model of the tunnel example given in Section 4.1 was chosen maintaining the layout of the tunnel geometry, support specifications, excavation sequences, and the relevant finite element mesh (using approximately 900 15-noded triangle elements) which have been shown in Figures 30 and 31. No water table is present and consequently all calculations have been performed under drained conditions.

### 5.2.1 Random set input parameters

Similar to Section 4.2 four basic variables are considered for the MC-model including two strength parameters of the rock mass namely cohesion and friction angle, elasticity modulus of the rock mass,  $E_{rm}$ , and the relaxation factor, which are presented in Table 22 and 23. The random sets with respect to  $E_{rm}$  and the relaxation factor are common between the HB-model and the MC-model. Figures 47 and 48 illustrate the random set strength parameters in terms of p-box corresponding to MC and HB model respectively.

**Tab. 22:** Input random set of both MC and HB strength parameters

		HB Parameters				MC Parameters	
Var.	$m(A)$	$m_i$	$\sigma_{ci}$	$D$	GSI	$\varphi$	$c$
Units	-	-	[MPa]	-	-	[°]	[kPa]
Set 1	0.5	15	10	0-0.5	30-40	37-47	80-130
Set 2	0.5	25	50	0-0.5	30-40	53-60	160-280

**Tab. 23:** Common input random set for MC and HB model

Var.	$m(A)$	$E_{rm}$ (rock mass modulus)	Relaxation Factor		
Units	-	[MPa]	T.H.	Bench	Invert
Set 1	0.5	1300-2300	0.4-0.6	0.3-0.5	0.2-0.4
Set 2	0.5	1900-3400	0.3-0.5	0.2-0.4	0.1-0.3

Recalling Section 4.2.1.2 in which the procedure of obtaining the equivalent MC strength parameters from the HB-model parameters has been described, alternative 2 is adopted for the MC strength parameters used in this section. The main reason is that alternative 2 considers a range of minor principal stresses (Equ. 29) in its fitting procedure, which corresponds approximately to the stress state in the vicinity of the tunnel elevation. Consequently the system responses obtained by both HB and MC-models are expected to be close and comparable to each other.

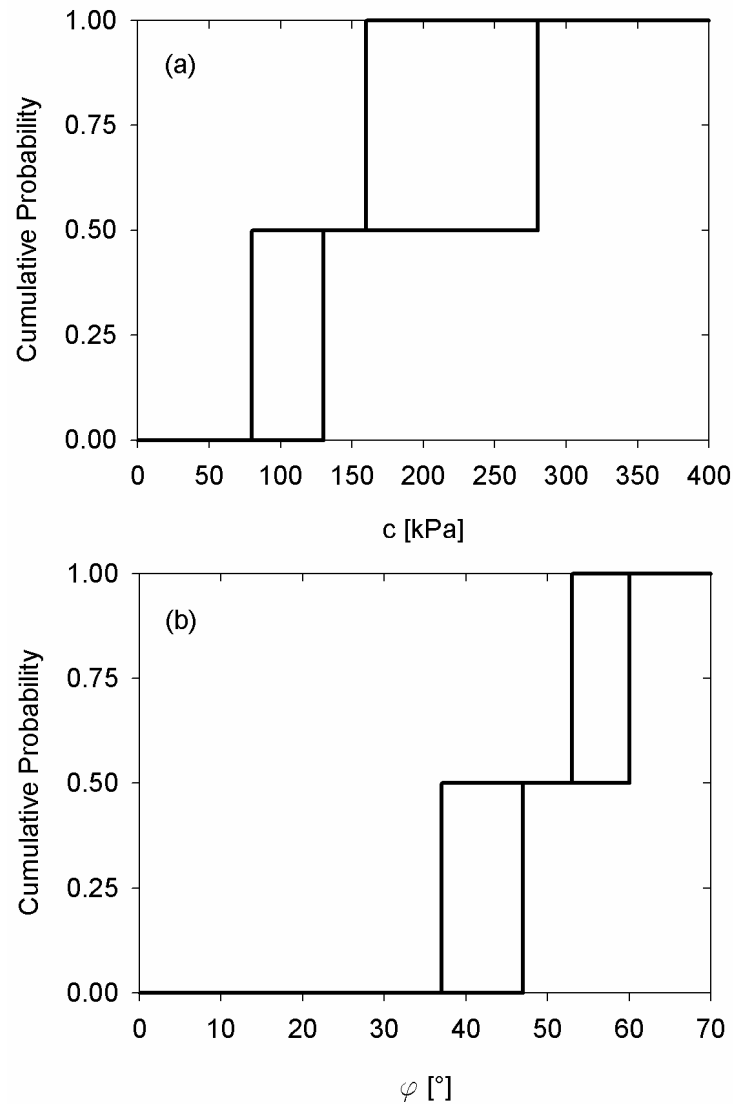


**Fig. 47:** Set-based input random variables of MC-model, a) cohesion b) friction angle

In fact in the HB-model there is only one interval for GSI and  $D$  but by combining it with two constant values of  $m_i$  and  $\sigma_{ci}$  two sets are made in the respective random set model. The strength parameters of the HB model are given in Table 22. It should be noted that the GSI and  $D$  are dependent parameter sets such that the lower limit of  $D$  is used with the upper value of GSI in the calculations and vice versa to represent the best and the worst geological conditions respectively. The input for individual deterministic FE calculations resulted from the random set model for the case of the HB-model is summarized in Table 24.

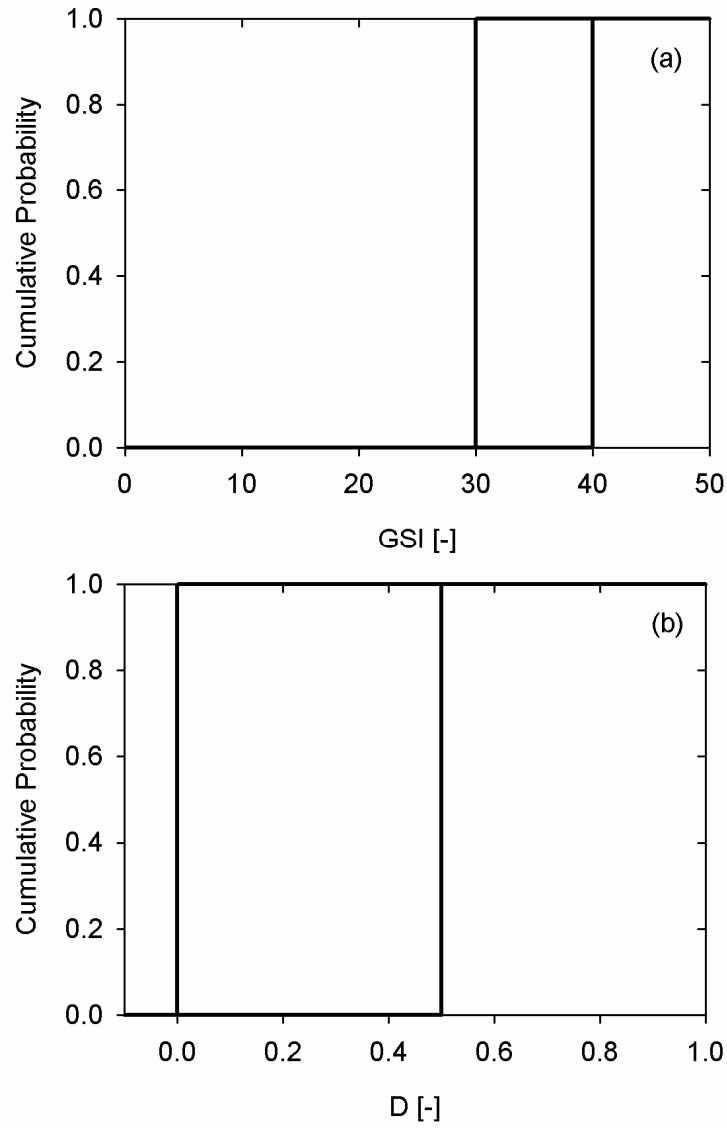


**Fig. 48:** Set-based input random variables of HB-model, a) geological strength index b) Damage factor

**Tab. 24:** Input parameters of 64 FE deterministic calculations used for the HB-model

Run No.	m(A)	Basic Variables		Set No.	Combination of extremes of the sets							
					LLL	LUL	LLU	ULL	UUL	LUU	ULU	UUU
1-8	0.50	HB_Properties	GSI	1	30	30	30	40	40	30	40	40
			D		0.5	0.5	0.5	0	0	0.5	0	0
			m <sub>i</sub>		15	15	15	15	15	15	15	15
			σ <sub>ci</sub>		10	10	10	10	10	10	10	10
0.50	R <sub>f</sub>	Top_Heading	1	0.4	0.6	0.4	0.4	0.6	0.6	0.4	0.6	
0.50	E <sub>rm</sub>		1	1300	1300	2300	1300	1300	2300	2300	2300	
9-16	0.50	HB_Properties	GSI	1	30	30	30	40	40	30	40	40
			D		0.5	0.5	0.5	0	0	0.5	0	0
			m <sub>i</sub>		15	15	15	15	15	15	15	15
			σ <sub>ci</sub>		10	10	10	10	10	10	10	10
0.50	R <sub>f</sub>	Top_Heading	2	0.3	0.5	0.3	0.3	0.5	0.5	0.3	0.5	
0.50	E <sub>rm</sub>		1	1300	1300	2300	1300	1300	2300	2300	2300	
17-24	0.50	HB_Properties	GSI	1	30	30	30	40	40	30	40	40
			D		0.5	0.5	0.5	0	0	0.5	0	0
			m <sub>i</sub>		15	15	15	15	15	15	15	15
			σ <sub>ci</sub>		10	10	10	10	10	10	10	10
0.50	R <sub>f</sub>	Top_Heading	2	0.3	0.5	0.3	0.3	0.5	0.5	0.3	0.5	
0.50	E <sub>rm</sub>		2	1900	1900	3400	1900	1900	3400	3400	3400	
25-32	0.50	HB_Properties	GSI	1	30	30	30	40	40	30	40	40
			D		0.5	0.5	0.5	0	0	0.5	0	0
			m <sub>i</sub>		15	15	15	15	15	15	15	15
			σ <sub>ci</sub>		10	10	10	10	10	10	10	10
0.50	R <sub>f</sub>	Top_Heading	1	0.4	0.6	0.4	0.4	0.6	0.6	0.4	0.6	
0.50	E <sub>rm</sub>		2	1900	1900	3400	1900	1900	3400	3400	3400	
33-40	0.50	HB_Properties	GSI	2	30	30	30	40	40	30	40	40
			D		0.5	0.5	0.5	0	0	0.5	0	0
			m <sub>i</sub>		25	25	25	25	25	25	25	25
			σ <sub>ci</sub>		50	50	50	50	50	50	50	50
0.50	R <sub>f</sub>	Top_Heading	1	0.4	0.6	0.4	0.4	0.6	0.6	0.4	0.6	
0.50	E <sub>rm</sub>		2	1900	1900	3400	1900	1900	3400	3400	3400	
41-48	0.50	HB_Properties	GSI	2	30	30	30	40	40	30	40	40
			D		0.5	0.5	0.5	0	0	0.5	0	0
			m <sub>i</sub>		25	25	25	25	25	25	25	25
			σ <sub>ci</sub>		50	50	50	50	50	50	50	50
0.50	R <sub>f</sub>	Top_Heading	1	0.4	0.6	0.4	0.4	0.6	0.6	0.4	0.6	
0.50	E <sub>rm</sub>		1	1300	1300	2300	1300	1300	2300	2300	2300	
49-56	0.50	HB_Properties	GSI	2	30	30	30	40	40	30	40	40
			D		0.5	0.5	0.5	0	0	0.5	0	0
			m <sub>i</sub>		25	25	25	25	25	25	25	25
			σ <sub>ci</sub>		50	50	50	50	50	50	50	50
0.50	R <sub>f</sub>	Top_Heading	2	0.3	0.5	0.3	0.3	0.5	0.5	0.3	0.5	
0.50	E <sub>rm</sub>		1	1300	1300	2300	1300	1300	2300	2300	2300	
57-64	0.50	HB_Properties	GSI	2	30	30	30	40	40	30	40	40
			D		0.5	0.5	0.5	0	0	0.5	0	0
			m <sub>i</sub>		25	25	25	25	25	25	25	25
			σ <sub>ci</sub>		50	50	50	50	50	50	50	50
0.50	R <sub>f</sub>	Top_Heading	2	0.3	0.5	0.3	0.3	0.5	0.5	0.3	0.5	
0.50	E <sub>rm</sub>		2	1900	1900	3400	1900	1900	3400	3400	3400	

U = Upper Bound      L = Lower Bound

The RS-FEM procedure is applied separately for each constitutive model. The number of realisations required to accomplish the RS-FEM in which the HB and the MC model have been used, based on Equation 11 are 64 and 256 FE calculations respectively.

## 5.2.2 Calculation results

Displacements and internal forces in structural elements obtained from both MC and HB constitutive models are plotted in Figures 49 and 50 along with the in-situ measurements in terms of the lower and upper discrete cumulative probability distribution bounds. It should be noted that the random variables have been assumed stochastically independent, which is generally not correct; but for the sake of simplicity and from a practical point of view it is admissible. Since the measurements of only two sections of the tunnel with similar conditions to the model were available, the measurement values are illustrated in the plot with two steps in form of a discrete cumulative distribution.

The cumulative distributions of the bound of results given by the HB-model are generally more inclined than the MC bounds; consequently, the HB-model indicates more uncertainty in the system response. As a result, HB results could encompass the measurements within its most likely predicted values. For instance, from Figure 49b it can be seen that the upper limit of the measured value lies at the end of the upper bound of the MC-model, whereas in the HB-model it is situated within the most likely values. Nevertheless, it follows that the results of the calculated bounds from both models are in good agreement with the measurements. It maintains the capability of the RS-FEM in capturing the uncertainties involved in the basic random variables, although the displacements are small in the sense of absolute values. Despite the fact there was not a possibility to measure the internal forces of the lining, it is anticipated that like the crown displacement, actual moments and normal forces in the lining fall inside the range shown in Figure 50. Table 25 presents the most likely values of obtained system responses based on the definition given in Chapter 3.

**Tab. 25:** The range of most likely values obtained from HB and MC random set model

<i>Results</i>		$U_{y-A}$	$U_{y-B}$	$U_{x-B}$	<i>FOS</i> <i>T.H.</i>	<i>Max</i> <i>Moment</i>	<i>Max</i> <i>Normal</i> <i>Force</i>
		[mm]	[mm]	[mm]	[-]	[kN.m/m]	[kN/m]
<i>HB-model</i>	<i>lower</i>	1.8	1.2	0.5	2.07	6.7	262
	<i>upper</i>	5.3	3.4	1.3	3.50	16.3	574
<i>MC-model</i>	<i>lower</i>	1.7	1.0	0.5	2.39	3.9	170
	<i>upper</i>	4.3	2.5	0.9	3.70	14.5	477

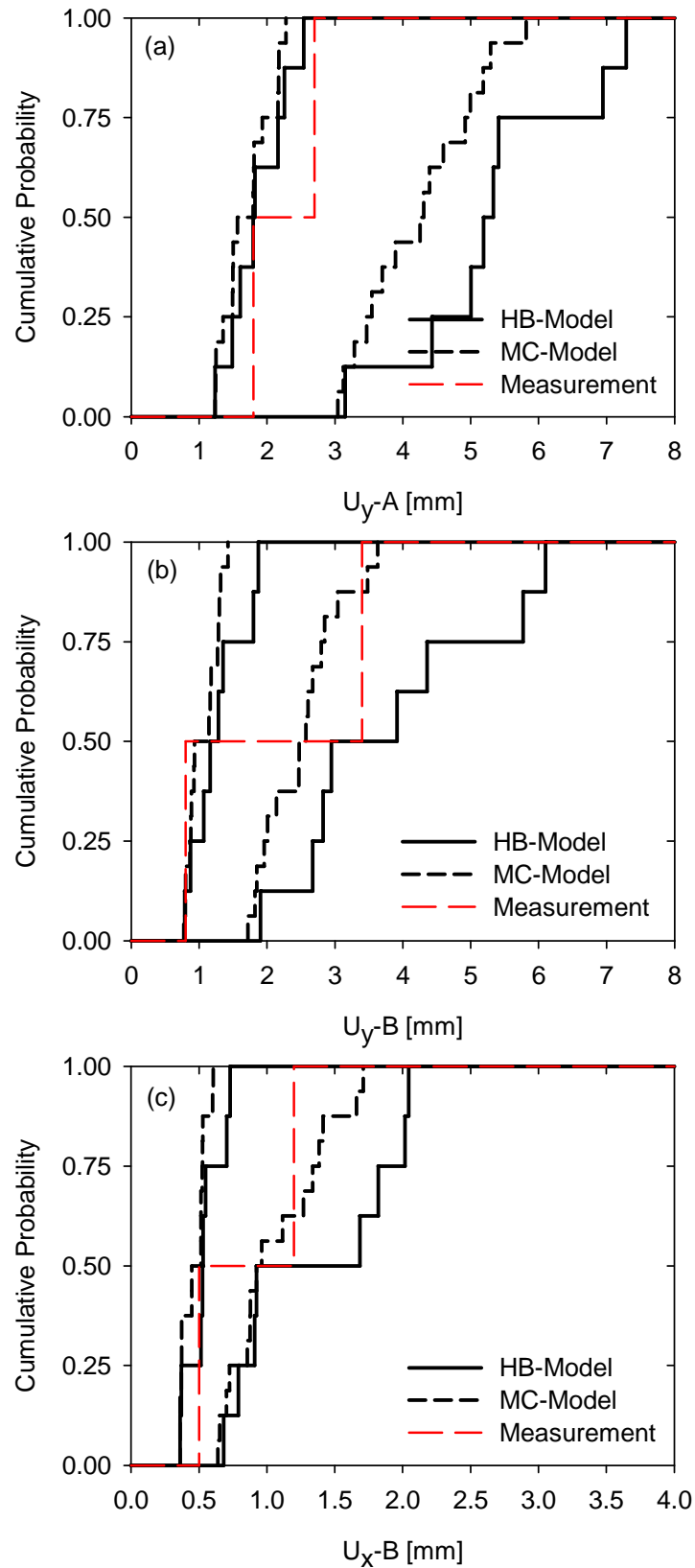


**Fig. 49:** Comparison between RS-FEM predictions obtained from HB and MC models and the measurement a) vertical displacement at the tunnel crown, b & c) vertical and horizontal displacement at point B, respectively



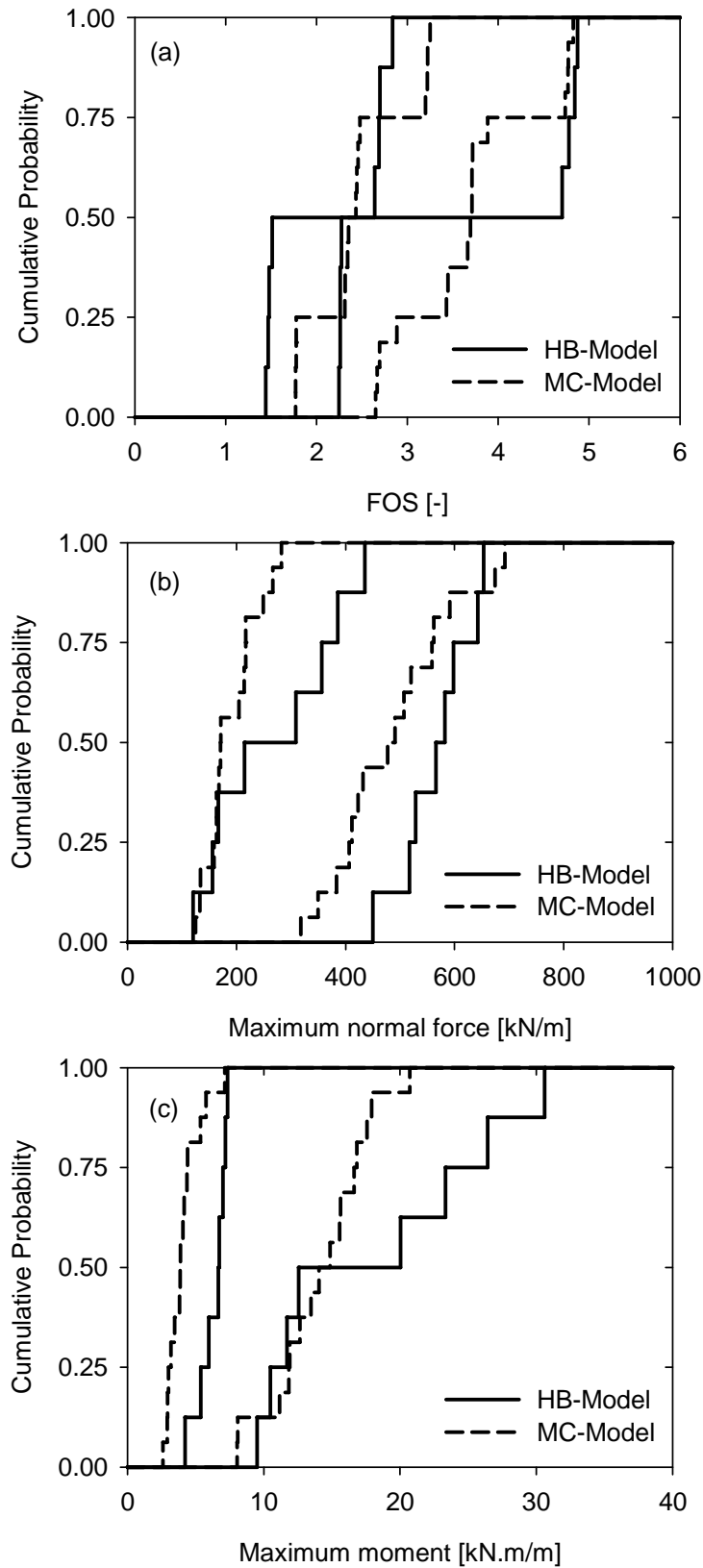


**Fig. 50:** RS-FEM results for both HB and MC constitutive models, a) factor of safety after top-heading excavation, b) maximum normal force, and c) maximum moment in the lining at the end of construction

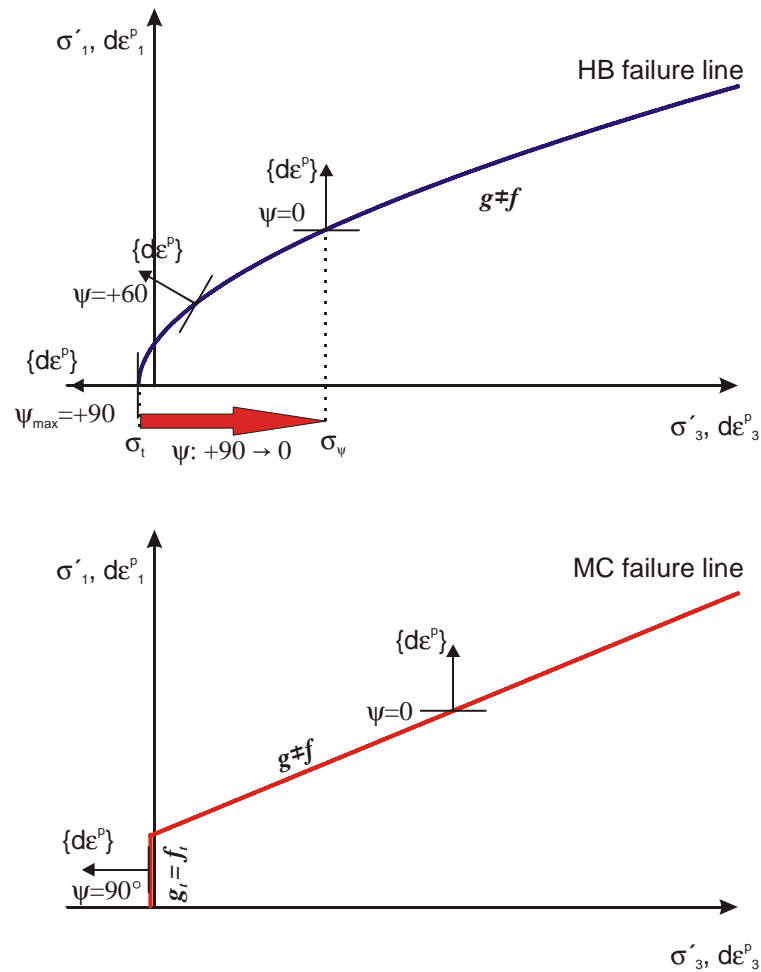


**Fig. 51:** Yield curve and direction of plastic flow in both MC and HB-model

From a modelling point of view, the observed differences between the two models might have originated from minor differences existing in the constitutive models that are discussed next.

In the theory of plasticity, the yield function is defined as being a scalar function of stress. In MC and HB models their respective failure line acts as a yield function (denoted by  $f$  in Fig. 51), which is regarded as a criterion for the onset of plastic straining (Potts and Zdravkovic, 1999). Another issue is to determine the direction of plastic straining at every stress state. This is carried out by means of a flow rule using a potential function (denoted by  $g$  in Fig. 51) that can be the same as the yield function and is then called an associated flow rule. For MC type yield functions, the theory of associated plasticity overestimates dilatancy and results in unrealistic volume changes. Commonly the potential functions contain the dilatancy angle  $\psi$ , which controls plastic volumetric strains. Thus, in a non-associated flow rule, at every stress state an angle exists between the yield function and the plastic potential function, which is a function of the dilatancy angle.

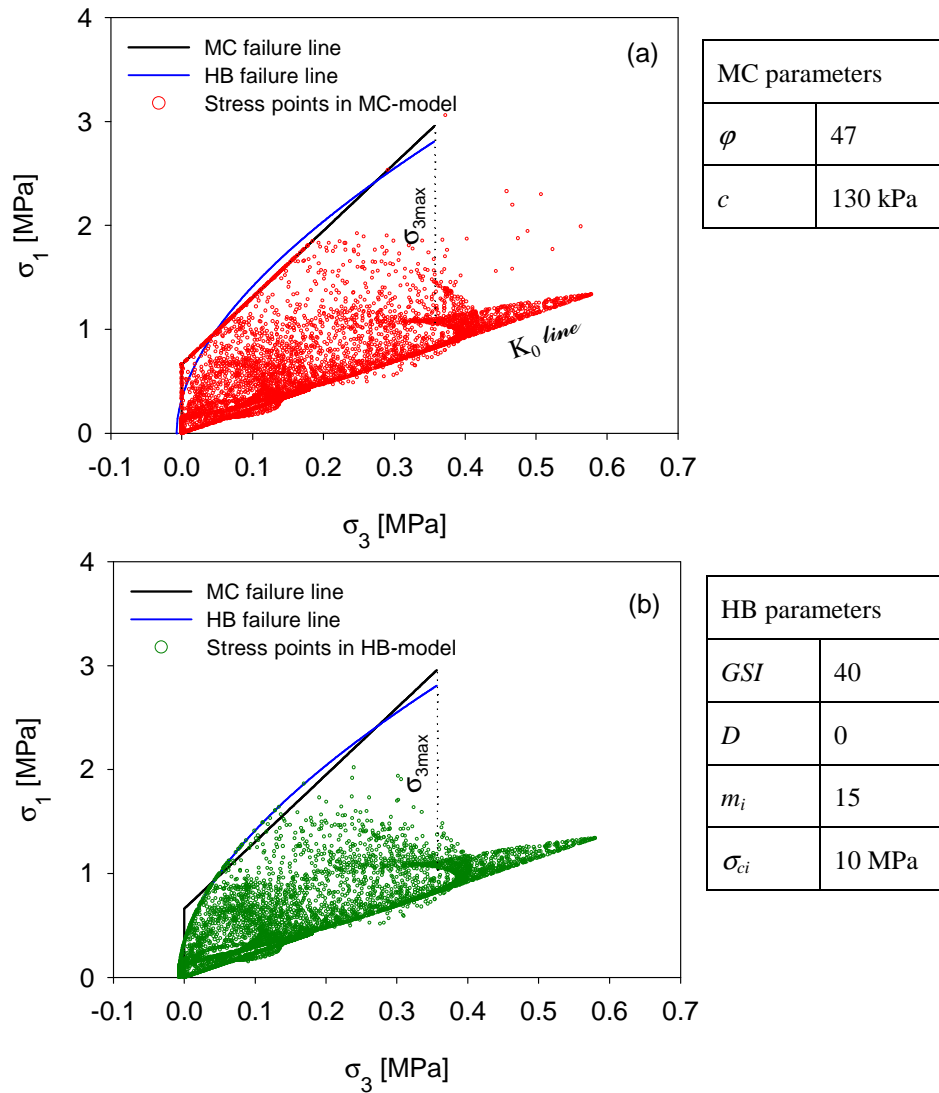


**Fig. 52:** Illustration of stress points of FE calculations in principal stress space for the given equivalent HB and MC strength parameters

The difference in the potential functions used in the MC and HB models is the most influential factor for the differences of the results between the two models. For the MC model two potential functions have been chosen: a non-associated flow rule in the deviatoric part and an associated one on the tension cut-off line. As a limiting case the dilatancy angle is selected equal to  $+90$  at the tension cut-off line (the plastic strain vector has no component in the vertical direction) and  $0$  for the deviatoric line as depicted in Figure 51 (the plastic strain vector has no component in the horizontal direction).

At the apex point of the HB failure line the dilatancy angle is equal to  $\psi_{\max}$ . As depicted in Figure 51,  $\psi$  decreases linearly from  $\psi_{\max}$  to  $0$  within the range of minor principal stresses between uniaxial tensile strength ( $\sigma_t$ ) and  $\sigma_\psi$ . The value of  $\sigma_\psi$  is equal to zero which is a default value for rock material.

After the tunnel excavation, stress points around the tunnel follow stress paths that are deviating from the initial stress state (on the  $K_0$ -line). It can be seen from Figure 52 that most of the stress points that are not affected by the excavation are concentrated near the  $K_0$ -line. Figure 52 shows the stress state in the whole model after the final construction stage. Furthermore, two observations can be made: firstly, the range of  $\sigma_3$  over which HB and MC failure lines are fitted together (Equ. 29) encompasses all the stress points that are close to the failure line. It implies that Equation 29 gives a reasonable estimation for  $\sigma_{3\max}$  (see Figure 52 showing the position of  $\sigma_{3\max}$ ). The second observation is that the majority of the stress points hit the failure line in a range of minor principal stress between  $\sigma_t$  and  $\sigma_{3\max}/2$ . They are especially concentrated around the apex and the tension cut-off line. It follows that the discrepancy depicted in Figures 49 and 50 between the two constitutive models is most likely due to the natural consequences of the difference between the corresponding yield and potential functions in the range of low minor principal stresses.

### 5.2.3 Serviceability limit state

Finally, the serviceability limit state of the shotcrete lining at the final stage will be assessed based on the primary results taken directly from the random set model FE calculations. On the basis of the results obtained from the original design calculation a shotcrete thickness of about 30 cm is required for the top-heading and bench. This amount is decreased to 20 cm for the invert. The limit state function following Equation 23 given by Schikora and Ostermeier (1988) is considered. The serviceability limit state of the shotcrete lining is defined by exceeding the admissible stress, which is based on the potential for damage of the lining due to cracking when the tensile capacity of the material is exceeded. The following assumptions were made regarding other variables involved in the Equation, i.e. for the shotcrete a uniaxial strength of about 17.5MPa is assumed, and to cover the imperfections an eccentricity of  $e_a = 2.0\text{cm}$ , and for the serviceability limit state a safety factor of  $F_s = 2.1$  is considered. Figure 53 depicts the range of the evaluated limit state function using RS-FEM results in terms of CDF. For fitting a density and cumulative distribution function over the discrete data, @RISK<sup>®</sup> (Palisade, 2008) employs only the Root-Mean Squared Error method. This is the same quantity that @RISK minimized to determine the distribution parameters during its fitting process. It is a measure of the “average” squared error between the input and fitted curve. This statistic measures how well the distribution fits the input data and how confident one can be that the data was produced by the distribution function. It turned out that Beta distribution ranks first among the others and has been fitted to all the discrete CDF of  $g(x)$ . The lower and upper values of the probability of exceeding the admissible normal force in the lining,  $N > N_{lim}$ , where cracking takes place, corresponding to lower and upper fitted distributions over  $g(x)$  for both HB and MC models are zero and

$3.19 \times 10^{-5}$  respectively. The values of the probability of failure indicate that the shotcrete satisfies the serviceability criterion and major cracking is not expected to occur in the lining.

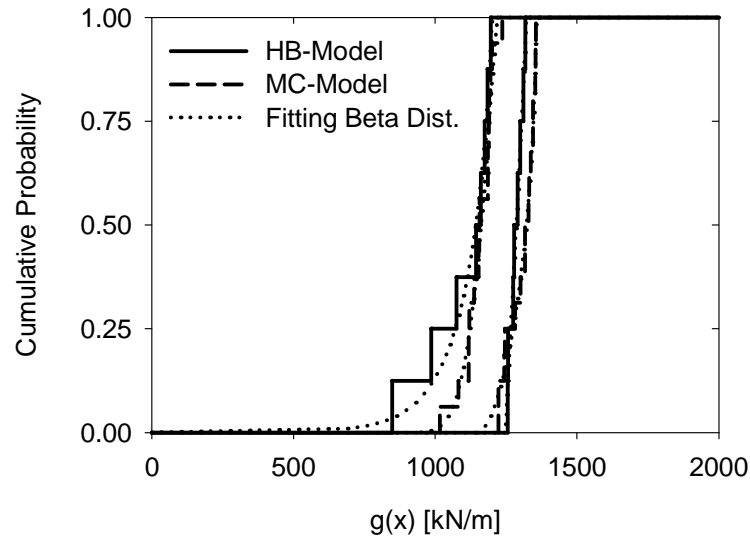


**Fig. 53:** Bounds of the random set results of shotcrete serviceability limit state function

### 5.3 Merging of RS-FEM results obtained from different constitutive models

Model uncertainty is distinguished from parametric uncertainty, which is the uncertainty of the value(s) of a particular variable. In fact, the system response of any mechanical system is affected by both parameter values and the relationships that tie the parameters together. These relationships are expressed in models. This means that model uncertainty could be just as crucial as parametric uncertainty. In general, this source of uncertainty is neglected. Model uncertainty is also referred to uncertainties concerning statistical parameters used in an uncertainty model e.g. uncertainty relating to the distribution family (Oberuggenberger and Fellin, 2008), and dependencies among basic variables (Berleant and Zhang, 2004) for which distribution envelope approaches have been developed, but these are not discussed herein.

To perform a comprehensive reliability analysis and risk assessment it is recommended to examine various scenarios, different theories and constitutive models in the context of the numerical method. Afterwards, an approach is needed to merge all the results for a rational decision-making. The objective of the aggregation of the two model results is to reasonably simplify and unify the

information obtained on the system response for subsequent reliability analysis. In this regard, many operations have been developed recently to combine different sources of information that basically fall in three main categories: conjunctive (based on set intersection), disjunctive (based on set union), and trade-off (an integration of foregoing operations) operations (Sentz and Ferson, 2002). A conjunctive operation is appropriate when the sources are considered reliable, and in situations where only one of the sources is probably reliable a disjunctive operator is recommended.

An extensive review has been carried out by Ferson et al. (2003) regarding the aggregation methods and their respective advantages and disadvantages, discussing how different evidence or sources of information can be combined together in order to consider the model uncertainty. Although they use these methods to combine different sources for the input parameters of a model, the same notion is adopted here to combine the RS-FEM outcomes obtained from two different constitutive models in order to come up with one solution for the system response. The most commonly and widely used aggregation methods consist of: Intersection, Envelope, Dempster's rule, Zhang's rule, Bayes' rule, Mixing, and Convolutional averaging. In the following sections, Envelope, Mixing, and Convolutional averaging, which are more appropriate for the objective mentioned before, are going to be discussed. For instance, Dempster's rule ignores and excludes the conflicting focal elements in the aggregation process, which is not favourable when it is applied for the aggregation of results of various constitutive models.

### 5.3.1 Intersection

The intersection operator is acted over a collection of focal elements of various random set structures. For computational purposes, random set results in the form of p-boxes are discretised into e.g. 100 redundant focal elements, each with a mass of 0.01. The aggregation outcome is simply obtained by intersecting the respective focal elements from the discretisation of the random set results (e.g. of both the MC-model and the HB-model), and then the masses of new focal elements are accumulated to construct the merged random set structure.

From the mathematical point of view, the intersection result holds the true response only when the RS results of each individual model contain the true response. This type of aggregation is only reasonable as long as the mentioned condition regarding the involved models is assured. Since each constitutive model has its own shortcomings and merits, one cannot generally claim that the actual behaviour is thoroughly captured by all of the models. Therefore in the current case, an envelope of the results would be a more logical solution and more conservative.

### 5.3.2 Envelope

Similar to the Intersection method, the random set structures in the form of p-boxes are discretised, but instead of the intersection operation, the union is used. Contrary to the intersection method, enveloping is commonly employed in the situation where the reliability of individual system responses is uncertain. In other words, since each constitutive model can usually characterise only specific aspects of the material behaviour, the true response might fall either within or outside the range predicted by each model. Therefore, choosing the Envelope method would be a reasonable and cautious strategy.

### 5.3.3 Mixing

The general form of the Mixing method takes different weights for each estimate (i.e. source of information) into account, as follows. Suppose that there are  $n$  p-boxes  $[F_1^*, F_{*1}]$ ,  $[F_2^*, F_{*2}]$ , ...,  $[F_n^*, F_{*n}]$ , with their associated weights  $w_1, w_2, \dots, w_n$ , and the resulting p-box from the Mixing process gives  $[F^*, F_*]$  where,

$$F^*(x) = (w_1 F_1^*(x) + w_2 F_2^*(x) + \dots + w_n F_n^*(x)) / \sum w_i \quad (33)$$

$$F_*(x) = (w_1 F_{*1}(x) + w_2 F_{*2}(x) + \dots + w_n F_{*n}(x)) / \sum w_i \quad (34)$$

If the estimates are in terms of  $n$  finite random set structures with masses  $m_1, m_2, \dots, m_n$  the resulting weighted mixture has the basic probability assignment  $m^*(A)$ :

$$m^*(A) = \frac{1}{\sum_i w_i} \sum_i w_i m_i(A) \quad (35)$$

For example, the unweighted mixture of two random set structures:  $F_1 = \{([2, 6], 0.4), ([3, 7], 0.6)\}$ , and  $F_2 = \{([1, 4], 0.5), ([2, 8], 0.5)\}$  results in  $F = \{([2, 6], 0.2), ([3, 7], 0.3), ([1, 4], 0.25), ([2, 8], 0.25)\}$ .

Unlike Convolutional averaging, the Mixing method maintains the disagreement between the estimates or rather summarizes it into a single distribution. In addition, according to Sentz and Ferson (2002) it is reasonable to use the Mixing method when the disagreement between the various estimates represents actual variability.

### 5.3.4 Convolute averaging

Convolute averaging of  $n$  given random set structures  $(\mathfrak{R}_1, m_1), \dots, (\mathfrak{R}_n, m_n)$  with their respective focal elements  $A_1, \dots, A_n$  results in the random set  $(\mathfrak{R}^*, m^*)$  whose focal elements ( $A$ ) are obtained on the Cartesian product of  $A_1 \times \dots \times A_n$ . Assuming the respective random set structures are independent, then the associated masses are defined by:

$$m^*(A) = \sum_{A=w_1A_1+\dots+w_nA_n} \prod_{i=1}^n m_i(A_i) \quad (36)$$

where  $w_i$  is the weight concerned with  $i^{\text{th}}$  random set structure such that  $\sum w_i = 1$  and  $w_i > 0$ .

From Equation 36 it follows that all of the focal elements of one random set structure are convolved with those of the other (that is, all possible pairs are considered). In fact, the relationship mentioned above is nothing but a random set analysis with a simple arithmetic averaging as its mapping function. For the purpose of illustration, a numerical example is given in Table 26.

As an advantage, the Convolute averaging is applicable to those random set structures between which conflicting and disjoint focal elements exist. Both the Mixing and Convolute averaging operations possess the property of commutativity but not associativity; therefore, special care should be taken when these operators are acting on multi-arguments. In addition, it can readily be shown that the Mixing operation is idempotent; however, Convolute averaging does not possess this algebraic property.

**Tab. 26:** Combination of the random set variable A and B using the Convolute averaging

		Set ( $A_1$ ), $m(A_1)$	Set ( $A_2$ ), $m(A_2)$
		[3, 5], 0.4	[4, 6], 0.6
Set ( $B_1$ ), $m(B_1)$	[1, 3], 0.5	[2, 4], 0.2	[2.5, 4.5], 0.3
Set ( $B_2$ ), $m(B_2)$	[2, 4], 0.5	[2.5, 4.5], 0.2	[3, 5], 0.3



## 5.4 Calculation and results

In section 5.2.2, the difference in the results obtained from two constitutive models in the framework of random sets has been shown. Here an attempt will be made to aggregate the results of the two separate random set analyses (i.e. one with the HB and the other with the MC model) to come up with the final bounds enclosing the uncertainty in the material model selection. The random set result of each material model is considered as one source. The bounds created by the above mentioned methods have been shown in Figures 54 and 55 for the results of the crown displacement and the maximum moment of the tunnel lining. As it can be seen, the envelope of the bounds results in a conservative solution, whereas the Convolutional averaging and the Mixing method yield almost a compromise between the bounds obtained by both constitutive models. The measured values of the tunnel crown displacement (Fig. 54) lie within the most likely values region of both the HB and MC random set results and still remain in the corresponding most likely value regions when applying various aggregation methods. The Intersection method makes the resulting bandwidth of the aggregation narrower and it contains the drawback mentioned in the previous section.

Ferson et al. (2003) argue that when the estimates to be aggregated represent variability (aleatory uncertainty) the Mixing method is more justifiable to be applied, and if it is appropriate to ignore the variability (i.e. the estimates represent an epistemic type of uncertainty) as well as the dependency between the estimates, employing the Convolutional averaging method would be more suitable. The constitutive model uncertainty basically lies in the epistemic category and it cannot be considered as a real variability in the model selection. Therefore, the latter aggregation method would be more reasonable to be adopted for the current case.

On the other hand, the Envelope ensues more conservative values, albeit the Convolutional results in some locations are outside of the envelope bounds (Fig. 54 and 55). Ferson et al. (2003) have also pointed out that if many independent p-boxes having similar scatter are combined by means of the Convolutional averaging, the results tend to become an interval whose band reflects the overall incertitude. This phenomenon can be seen in the presented results because the scatter of the resulting bounds has been considerably reduced although only two p-boxes have been involved. On the contrary, the Mixing method has resulted in a larger scatter even with respect to each input p-box.

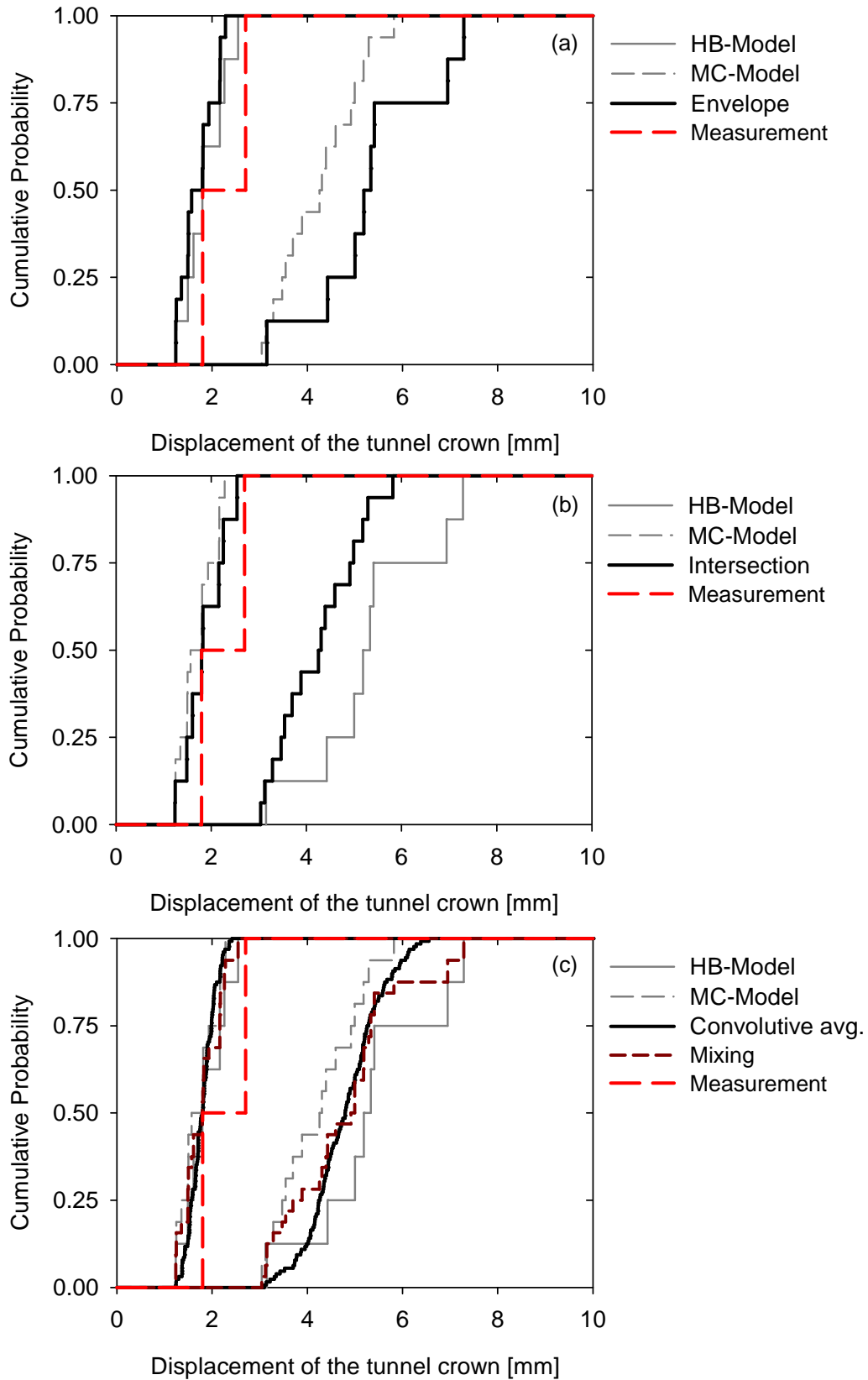


**Fig. 54:** Illustration of different aggregation methods applied on the random set results of the vertical tunnel crown displacement, a) Envelope, b) Intersection, c) Convolutional averaging and Mixing

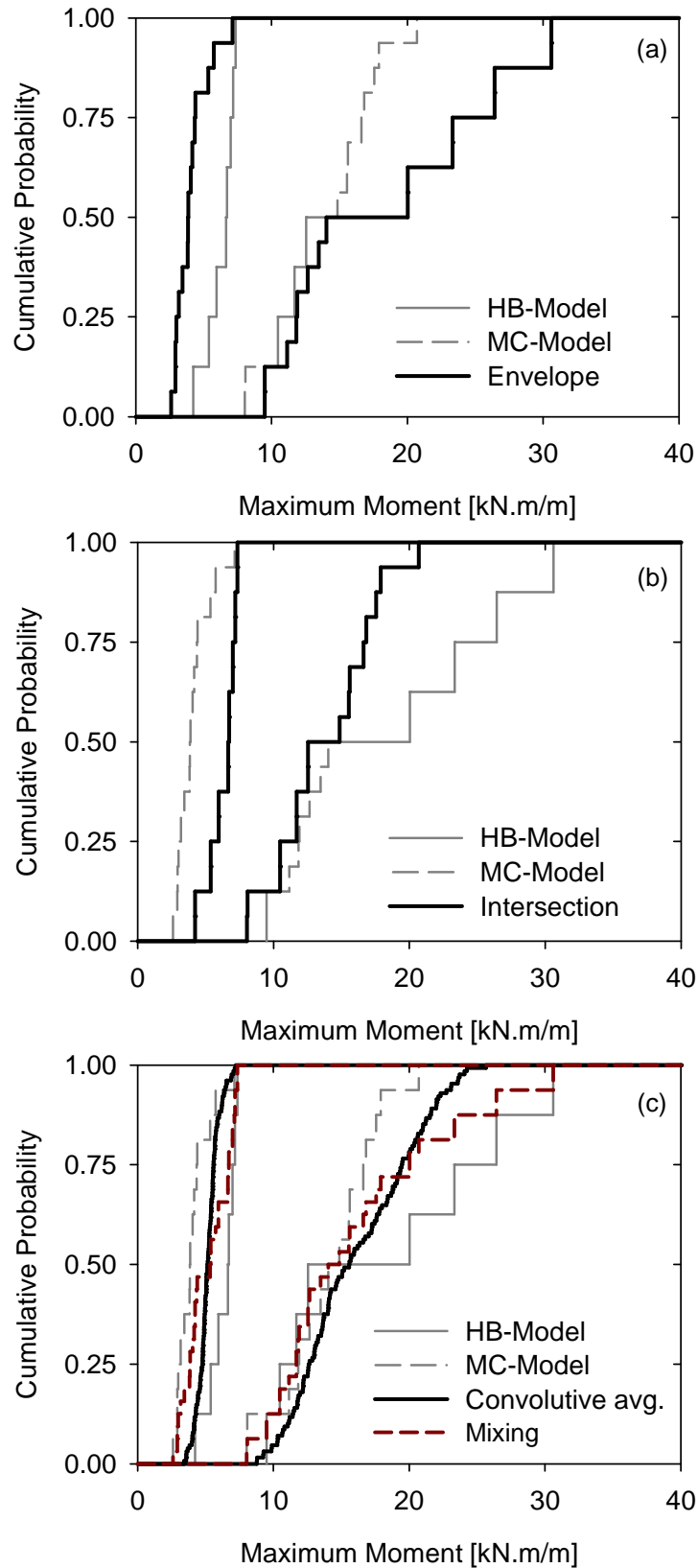


**Fig. 55:** Illustration of different aggregation methods applied on the random set results of the maximum lining moment, a) Envelope, b) Intersection, c) Convolutional averaging and Mixing

### Evaluation of serviceability limit state function

To show the effects of different aggregation methods on reliability analysis of a tunnel system, a performance function relating to the tunnel crown deformation is considered. The simplest form of such performance function is assumed below:

$$g(\mathbf{U}_{yA}) = 6 - U_{yA} \quad (37)$$

where  $U_{yA}$  is the vertical displacement of the tunnel crown downwards, and 6 mm is the criterion adopted in this example.

CDF of the upper bound of  $U_{yA}$  results illustrated in Figure 54 are used to obtain the probability of failure (or probability of unsatisfactory performance) using the following Equation:

$$p_f = p(g(\mathbf{u}) \leq 0) = \int_{g(\mathbf{u}) \leq 0} f_u(\mathbf{u}) d\mathbf{u} \quad (38)$$

The upper values of the probability of ‘failure’ (meaning in this context that the limiting value for crown displacement is exceeded) have been summarized in Table 27 regarding various aggregation methods. It follows that for a certain performance function, the adoption of an aggregation method could result in a considerable discrepancy in the calculated probability of unsatisfactory performance. As expected, the Envelope has produced a conservative value in contrary to the Intersection method.

**Tab. 27:** Maximum probability of unsatisfactory performance of Equation 37 considering various aggregation methods

Aggregation method	Envelope	Intersection	Convolute avg.	Mixing
Probability of failure	0.25	0.0	0.0599	0.125

## 5.5 Conclusion and summary

In this chapter an extension of the RS-FEM was presented that enables the Random Set model to consider the uncertainty of the constitutive model used in numerical analysis by using evidence aggregation methods. By using the existing method of combining different sources of information the results of two separate RS-FEM analyses are merged to come up with the bounds that take the uncertainty in model selection into account. Among the four applied merging methods, namely Intersection, Mixing, Envelope and Convolutional averaging only the later two are suitable for the aggregation of the two models' results. The Mixing method is appropriate when the differences between results come from actual variability. However, in model uncertainty there is no inherent variability and in fact the differences between results are a type of epistemic uncertainty. The Envelope method yields conservative bounds of results.

Two separate Random Set Finite Element Analyses were performed in which common constitutive models, namely the Hoek-Brown and the Mohr-Coulomb model were employed. The range of the predicted results of the tunnel displacements extracted from both models was compared to the measurements available in the project and good agreement was observed. The HB-model requires less finite element realisations as compared to the MC model maintaining the quality of the random set model, which can be seen as an advantage from a practical point of view.

The differences between HB and MC results originate from two main reasons. First, despite the suitable fitting procedure, there is a difference between the two failure criteria, which results in different numbers of failure points in each model, leading to different plastic strains and consequently internal forces in the lining. Secondly, different flow rules are adopted for the two models, which has some influence on element results in particular at low stress levels and tensile stresses.

## 6 Comparison of RS-FEM and Point Estimate Method

This chapter aims to compare the results of two uncertainty models, namely the Point Estimate Method (PEM), and the Random Set Method having different theoretical backgrounds, against the measurements of the tunnel problem presented earlier. The Point Estimate Method is supported by probability theory, while the Random Set Method is categorized in the imprecise probability group and is backed by random set theory. PEM has been first introduced by Rosenblueth (1975). In simple words, PEM as uncertainty model defines each random variable by two numbers. The mean value of these two numbers gives the magnitude of the variable, and the difference is a measure of the uncertainty. In the original form of PEM the calculations were made for all combinations of input data. For instance, for  $n$  numbers of variables this will lead to  $2^n$  numbers of calculations. RSM and PEM are similar from the two following aspects:

- PEM does not care about the mapping function of a mechanical system that maps the input variables from a domain into the space of the system response. Therefore it is applicable to a probabilistic evaluation of a mechanical system whose solution is given by a number of empirical graphs or the required calculation is carried out by a non-accessible computer code, or in other words, there are no explicit equations characterizing the problem. However, only the statistical moments of target values are yielded by PEM, and no information about the type or the shape of the distribution can be obtained.
- Reliability analysis of a mechanical system in connection with numerical models can be broken down into a limited number of deterministic finite element calculations based on the number of predetermined points given by the method. In this sense Point Estimate Method is similar to the Random Set Finite Element Method.

The accuracy and precision of the two methods are not comparable but it is anticipated that random set results encompass the distribution of the system response obtained from PEM. By comparing the measurements both methods can be evaluated against each other and their limitations are pointed out.

Schweiger et al. (2001) demonstrated the applicability of PEM to determine the low-order statistical moments of the considered limit state function (LSF) in geotechnical problems. PEM would be rather used in the reliability analysis of complex problems, since commonly used reliability methods such as FORM (First Order Reliability Method) or SORM (Second Order Reliability Method)

require an extra code coupled with a Finite Element tool to numerically calculate the partial derivatives of the implicit LSF (Schweckendiek, 2006). For each LSF a modification should be performed to the code due to the existing partial derivatives. Furthermore, it seems that PEM is still appealing and has been satisfactorily applied in some civil engineering applications (e.g. Tsai and Franceschini, 2005).

## 6.1 Point estimation method

In reliability analysis it is favourable to estimate the actual distribution of the system response or the desired limit state function and subsequently the corresponding failure probability of the system. However, for most geotechnical problems this is a very difficult task and normally impractical. Thus an assortment of approaches have been proposed to simplify the issue and among others the most commonly used method in engineering practice is the first order reliability method (FORM) using the notion of reliability index ( $\beta$ ), (according to Ang, 2009) first suggested by Cornell (1969) and subsequently improved by Hasofer and Lind (1974). To compute the reliability index it is only essential to obtain the low order moments of the limit state function  $G(\mathbf{X})$ . The exact  $k$ -th moment of  $G(\mathbf{X})$ ,  $E[G^k(\mathbf{X})]$ , is obtained by the solution of the multiple integral given in the following:

$$E[G^k(\mathbf{X})] = \int_{-\infty}^{+\infty} \cdots \int_{-\infty}^{+\infty} f_{\mathbf{X}}(x_1, \dots, x_n) G^k(x_1, \dots, x_n) dx_1 \dots dx_n \quad (39)$$

where  $f_{\mathbf{X}}(\mathbf{X})$  is the joint PDF of the random vector  $\mathbf{X} = (X_1, X_2, \dots, X_n)$ . When a closed-form solution for such a limit state function  $G(x)$  is not available, approximate solutions are used. A common approach to solving this problem is to expand the limit state function in a Taylor series (Harr, 1996), in which only the linear terms are considered. In terms of the solution process, the method is very similar to PEM but should not be confused with each other. The accuracy of their results, depending on the form of the limit state function is however less than that of the point-estimation method (Thurner, 2000).

In the Point Estimate Method (PEM), the continuous joint distribution density function  $f_{\mathbf{X}}(x)$  is replaced by specially defined discrete probabilities which are supposed to model the same low-order moments of  $f_{\mathbf{X}}(x)$ . The determination of these moments is done by adding up the weighted discrete realisations. In Figure 57 this relationship is simplified by the two realisations at  $x_+$  and  $x_-$  represented with the corresponding weights  $w_+$  and  $w_-$ . This method implicitly allows input random variables to have any distribution, provided the mean, variance and skewness (at least first two moments) are known.

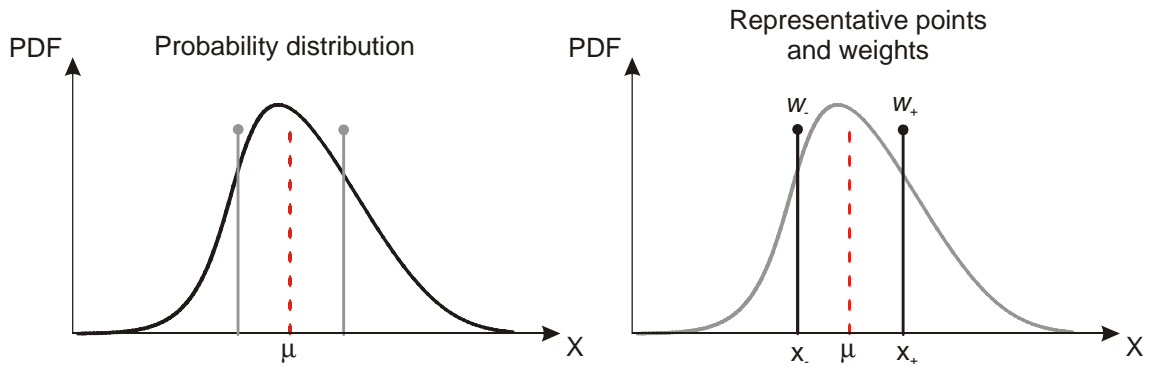


**Fig. 56:** Notion of PEM in representing a random variable (after Thurner, 2000)

There are two main distinguishable approaches for the point estimate method: first, Rosenblueth's approach for the point estimate method (for the first time introduced by Rosenblueth, 1975) and its modified method given by his followers (e.g. Lind 1983, Harr 1989, Hong 1998) that attempted to save computational cost by reducing the number of prefixed sampling points; however in the case of large numbers of variables some pre-determined sampling points lie outside the range of PDF of the respective variable or give negative values which have non-physical meaning for some specific variables. This issue has been addressed by Christian and Baecher (2002). Second, the approach proposed by Zhou and Nowak (1988) including three different integration rules, namely  $n+1$ ,  $2n$ ,  $2n^2+1$  ( $n$  is the number of basic variables involved in the analysis) and the latter is used in this chapter since from the investigation accomplished by Thurner (2000), it turned out that the  $2n^2+1$  integration rule results in an optimum compromise between accuracy and computational effort. Theory, procedure and the accuracy of this method are going to be briefly presented and discussed in the next sections.

## 6.2 Approach proposed by Zhou & Nowak (1988)

Zhou and Nowak (1988) have presented a general procedure to numerically approximate Equ. 40, considering various possibilities (e.g. with and without a known joint distribution function, a correlation between variables, any type of distribution) using the Gauss-Hermite quadrature formula. Basically this method has been established for a multivariate case in standard normal space, which gives the approximation of the Equ. 40 as follows:

$$E[G^k(\mathbf{Z})] \cong \sum_{j=1}^m w_j G^k(z_{1j}, \dots, z_{nj}) \quad (40)$$

where  $n$  is the number of variables,  $m$  is the number of considered points,  $z_j$  are typical predetermined points and  $w_j$  are the respective weights given in Table 28.



Therefore the required number of realisations is presented in the first column, the formulas for the calculation of the required points in the second column, and the corresponding weights in the third column. The sum of the weights is always 1.0 and the number of required calculations thus depends on the integration rule. In their original paper formulas for three rules known as  $n+1$ ,  $2n$ , and  $2n^2+1$  have been presented and only the two latter are given in Table 28 and hereafter they are designated as ZN-II and ZN-III respectively. The effects of different integration rules on the accuracy of the results have been discussed by Turner (2000). The case of a single, normally distributed variable  $Z$  and a non-linear limit state function  $G(\mathbf{Z})$  is graphically illustrated in Figure 57.

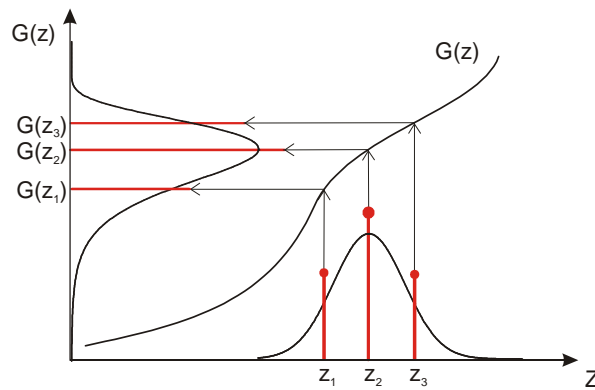


**Fig. 57:** Illustration of Gauss-Hermite quadrature Integration using 3 points

For a non-normally distributed variable  $\mathbf{X}$  the same principle applies, only a transformation from the standard normal space to the  $x$ -space is necessary:

$$E[G^k(\mathbf{X})] \cong \sum_{j=1}^m w_j G^k(x_j) = \sum_{j=1}^m w_j G^k(F_x^{-1}(\Phi(z_j))) \tag{41}$$

where  $\Phi(z)$  is the cumulative distribution function of standard normal variable  $Z$ .

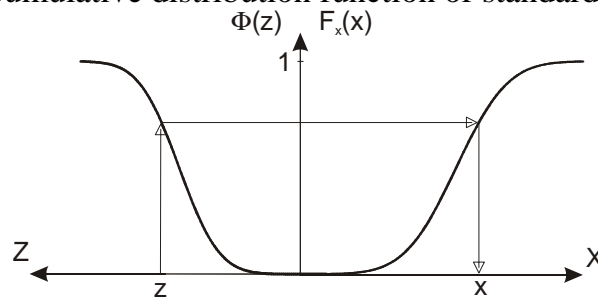


**Fig. 58:** Transformation of a random variable from normal to non-normal space

Figure 58 depicts how the transformation is carried out by setting the value of the cumulative distribution function  $F_x(x)$  at the point  $x_j$  equal to the value  $\Phi(z_j)$ .

**Tab. 28:** Evaluation points and respective weights in PEM after Zhou and Nowak (1988)

Formulas $m$	Points $(z_{1j}, \dots, z_{ij}, \dots, z_{nj})$	Weights factors $w_j$
$2n$ or ZN-II	$Z_1 = -Z_{n+1} = (\sqrt{n}, 0, \dots, 0)$	$w_1 = w_{n+1} = \frac{1}{2n}$
	$Z_2 = -Z_{n+2} = (0, \sqrt{n}, 0, \dots, 0)$	$w_2 = w_{n+2} = \frac{1}{2n}$
	...	...
	$Z_n = -Z_{n+n} = (0, 0, \dots, \sqrt{n})$	$w_n = w_{n+n} = \frac{1}{2n}$
$2n^2+1$ or ZN-III	$Z = (0, 0, \dots, 0)$	$w_j = \frac{2}{n+2}$
	$Z = (\pm\sqrt{n+2}, 0, \dots, 0)^a$	$w_j = \frac{4-n}{2(n+2)^2}$
	$Z = (\pm\sqrt{\frac{n+2}{2}}, \pm\sqrt{\frac{n+2}{2}}, \dots, 0)^a$	$w_j = \frac{1}{(n+2)^2}$

<sup>a</sup> Points include all possible permutations of coordinates.

The difficulties that may arise in numerical operations and respective approximations are not discussed here, and interested readers are referred to the original paper of Zhou and Nowak for more details; but in summary, in the general case of correlated, non-normally distributed variables, the following process determines the required input data for the individual realisations in the original space (Thurner, 2000):

- Step 1: Setting up the correlation matrix  $\rightarrow \mathbf{C}$
- Step 2: Transforming the correlation coefficients  $(\rho_{ij})$  from the original space to the correlated normal space  $\mathbf{Y}$  using a Nataf-transformation  $\rightarrow \mathbf{C}_0$
- Step 3: Determining the lower triangular matrix using the Cholesky-decomposition of  $\mathbf{C}_0 \rightarrow \mathbf{L}_0$
- Step 4: The predefined uncorrelated integration points  $\mathbf{Z}$  (given in Tab. 28) are correlated to each other based on the correlation matrix  $\mathbf{L}_0$  and are accordingly transformed into the correlated normal space  $\rightarrow \mathbf{Y} = \mathbf{L}_0\mathbf{Z}$  and in matrix form:

$$\begin{pmatrix} y_{1j} \\ \cdot \\ \cdot \\ \cdot \\ y_{nj} \end{pmatrix} = \begin{pmatrix} L_{11} & 0 & \dots & \cdot & 0 \\ \cdot & \cdot & \cdot & \cdot & \cdot \\ \cdot & \cdot & L_{ii} & \cdot & \cdot \\ \cdot & \cdot & \cdot & \cdot & 0 \\ L_{n1} & \cdot & \dots & \cdot & L_{nn} \end{pmatrix} \begin{pmatrix} z_{1j} \\ \cdot \\ \cdot \\ \cdot \\ z_{nj} \end{pmatrix} \quad (42)$$

Step 5: Mapping the variables from the correlated normal space to the original space with "arbitrary" marginal distributions  
 $\rightarrow \mathbf{X} = F_{\mathbf{x}}^{-1}(\Phi(\mathbf{Y}))$  and in matrix form:

$$\begin{pmatrix} x_{1j} \\ \cdot \\ \cdot \\ \cdot \\ x_{nj} \end{pmatrix} = \begin{pmatrix} F_{x_1}^{-1}[\Phi(y_{1j})] \\ \cdot \\ \cdot \\ \cdot \\ F_{x_n}^{-1}[\Phi(y_{nj})] \end{pmatrix} \quad (43)$$

Step 6: Computing the low-order moments of G using Equ. (41) as follows:

$$\mu_G = E[G(\mathbf{X})] = \sum_{j=1}^m w_j G(x_{1j}, \dots, x_{nj}) \quad (44)$$

$$E[G^2(\mathbf{X})] = \sum_{j=1}^m w_j G^2(x_{1j}, \dots, x_{nj}) \quad (45)$$

$$\text{Var}[G(\mathbf{X})] = E[G^2(\mathbf{X})] - (\mu_G)^2 \quad (46)$$

The formula expressing the skewness in terms of the non-central moment  $E[X^3]$  can be expressed by expanding the definition formula as follows:

$$\gamma_G = \text{Skew}[G(\mathbf{X})] = \frac{E[G^3(\mathbf{X})] - 3\mu_G\sigma_G^2 - \mu_G^3}{\sigma_G^3} \quad (47)$$

where  $\mu_G$  and  $\sigma_G$  are the mean and variance of  $G(\mathbf{X})$  respectively.

### 6.3 Accuracy of the PEM

The accuracy of the PEM generally varies from exact to approximate statistical parameters of a target value depending on the complexity of the mapping function and the number of points included in the calculations. The result of Rosenblueth's PEM is precise for sums of uncorrelated or correlated variables (Alén, 1998) while in the case of more complex functions the degree of accuracy

drops. However, it can be sufficiently accurate in many practical situations (Harr, 1996; Baecher and Christian, 2003). According to Alén (1998) the more linear the function is, the more accurate the method probably is, also the error given by the PEM-approximation is on the safe side. Then again, the latter comment is not true for all types of limit state function (especially in association with Rosenblueth methods; see work of Eamon et al. (2005)). Yet Baecher and Christian (2003) state “The method is reasonably robust and is satisfactorily accurate for a range of practical problems, though computational requirements increase rapidly with the number of uncertain quantities of interest”.

In the case of Zhou and Nowak (1988), the error due to the nonlinearity of a function can be reduced by using integration rules with more points (e.g. integration rule with  $2n^2+1$  instead of  $n+1$  points). Thurner (2000) has found the  $2n^2+1$  integration rule given by Zhou and Nowak (1988) to be an optimum compromise between accuracy and computational effort.

Zhou and Nowak (1988) provide no evaluation as to the expected effectiveness or limitations of the method; however, their assumptions in deriving the method are clear. They made an attempt to approximate the integral required for the reliability analysis. Such an approach has been basically developed concerning polynomial functions using the Gauss-Hermite integration method. An  $m$ -point Gaussian quadrature integration method is exact for polynomials of a degree up to  $2m-1$ . It should be noticed that by definition, a polynomial is an expression of finite length constructed from variables and constants, using only the operations of addition, subtraction, multiplication, and non-negative whole-number exponents. That means PEM might result in a biased response, especially when the considered LSF is related to a specific input variable with a non-polynomial expression along with a significant sensitivity to the variation of that particular input random variable. On the other hand, Thurner (2000) demonstrated the applicability of PEM in the reliability analysis of a classical bearing capacity problem with sufficient accuracy.

Assessment of the reliability index of numerous commonly used limit state functions in the context of structural engineering have been investigated by Eamon et al. (2005) comparing the accuracy and efficiency of the number of simulations and sampling methods including e.g. ZN-I and II, Latin Hypercube (LH) and Importance Sampling (IS). Unfortunately the ZN-III method, which is expected to have higher precision with respect to the other Zhou-Nowak methods, has not been considered in their survey scheme. It turned out that in estimating the reliability index PEMs should be utilized with care in the context of structural reliability calculations, since its results vary significantly in terms of accuracy and precision. The accuracy limits of PEMs applied on various types of limit state functions in terms of linearity, number of random variables, distribution type and variance of input variables have been quantified.

Considering all major influential factors affecting the reliability analysis, the mean value of the error ratio (calculated  $\beta$ / exact  $\beta$ ) using the ZN-I method is 0.8 with a COV of 15%, and using ZN-II is 0.88 with a COV of 15%. It implies that in an extreme case, assuming that the error is normally distributed the ratio amounts to 0.35 in ZN-I. Thus, a nearly high COV of the error indicates that the precision of the PEMs in calculating the reliability index is low. PEMs are ideal methods and give perfect answers for functions that have normally distributed random variables, are linear and/or have low variance. Also according to this study PEM shows unsatisfactory results in comparison with Monte-Carlo based sampling methods in computing the failure probability than the reliability index. Recently Russelli (2008) modified Rosenblueth's PEM and called it the Advanced Point Estimate Method (APEM) in order to cope with the shortcoming of the Point Estimate method in assessing small values of the failure probability. Also according to her findings, the bearing capacity of strip footings as an LSF can be characterised well enough with a shifted lognormal distribution function provided one may be able to evaluate the skewness of the target function or the considered LSF reasonably accurate.

Next, the accuracy of ZN-III in estimating low-order statistical moments is investigated over several basic functions of  $X$  that typically arise in geotechnical reliability analyses and are similar to those carried out by Baecher and Christian (2003) which is a reference to compare Rosenblueth's Point Estimate Method; furthermore, their exact statistical moments are not difficult to obtain. The functions are namely,  $\tan(X)$ ,  $\exp(X)$ ,  $1/X$ ,  $\ln(X)$ ,  $X^3$ , and a polynomial function with two variables  $Y=X_1^3+X_2$ . To evaluate the accuracy of PEM with regard to the distribution type of the variable, Normal and Uniform distribution have been considered. The effects on the number of random variables have been examined in the case of polynomial functions. In addition, the influence of the absolute mean value on the accuracy has been assessed in the case of  $\tan(X)$ . The results of the investigation are illustrated in Figures 59 to 61 in terms of the error produced by PEM and given by the following Equation:

$$Error\% = \frac{y^k(exact) - y^k(PEM)}{y^k(exact)} \times 100 \quad (48)$$

where  $y^k(exact)$  is the exact value of  $k$ -th statistical moment of function  $Y$ . More details about statistical specifications of each function have been given on each individual graph. The following observations can be inferred from Figures 59 to 61:

- In all cases, the error in the estimate of the standard deviation is almost half of the variance. In addition the mean values are always accurate or very close to the exact value. In general ZN-III has given more satisfactory results in the case of polynomials.

- Normally it is expected that the larger the COV, the higher the error in the estimate of the moments; for instance, see the results of the first two moments in Figure 59a and all of the moments calculated in Figure 61. Surprisingly however, it is not always the case, for example, in the reverse function (Fig. 59b) ZN-III yields the exact mean and variance at  $COV = 0.27$  (probably by coincidence) while for higher and lower COV values the method respectively overestimates and underestimates the low-order moments. For the function  $\ln(X)$ , the corresponding COV value by which the method would yield the exact mean and variance, is about 0.5, which is a relatively high value for the coefficient of variation.
- From Figure 60 it follows that the absolute mean value of a random variable slightly affects the trend of the error although  $\tan(X)$  with the specifications given in Figure 60b is the only function that does not exhibit error variation with the change of COV.
- In the ZN-III method  $2n^2+1$  integration rule is used which means in a single variable function like  $X^3$  as mentioned before, the results of PEM will be exact for polynomials of order 5 or less. Thus, the mean of  $Y$  of order 3 is computed exactly, while in estimating its variance and skewness that are of order 6 and 9 respectively, some error is anticipated.
- From Figure 61 it can be seen that the error is slightly reduced when the number of variables increase; it should be noted that the added term ( $X_2$ ) does not dramatically influence the value of the function. The reduction in error takes place because more integration points are used when the random variables increase and consequently the results of the integral tend to be more accurate. Furthermore, in contrast to other types of functions, skewness in the case of polynomials can be evaluated with an admissible accuracy in practical cases and especially in the range of normal COVs in geotechnical engineering since, based on Phoon and Kulhawy (1999), the mean value of COVs of most soil properties are less than 35%.
- A conclusive statement cannot be made as to whether the statistical moments computed by ZN-III are always overestimated or underestimated. The results show the accuracy depends highly on the type of distribution and the range of COV.

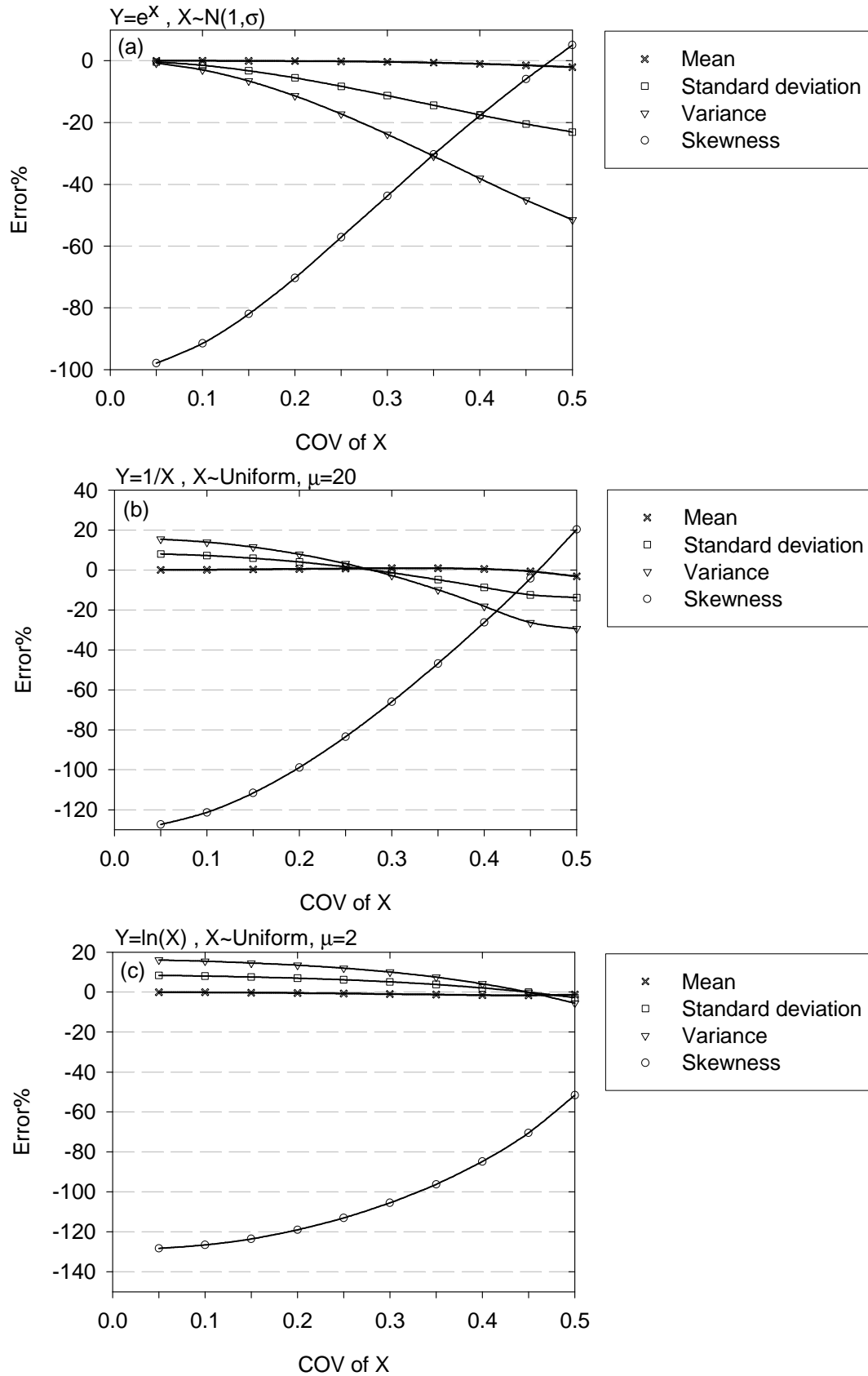


**Fig. 59:** Error in the estimate of the statistical moments for functions: a)  $e^x$  b)  $1/x$  c)  $\ln(x)$ , using the ZN-III method

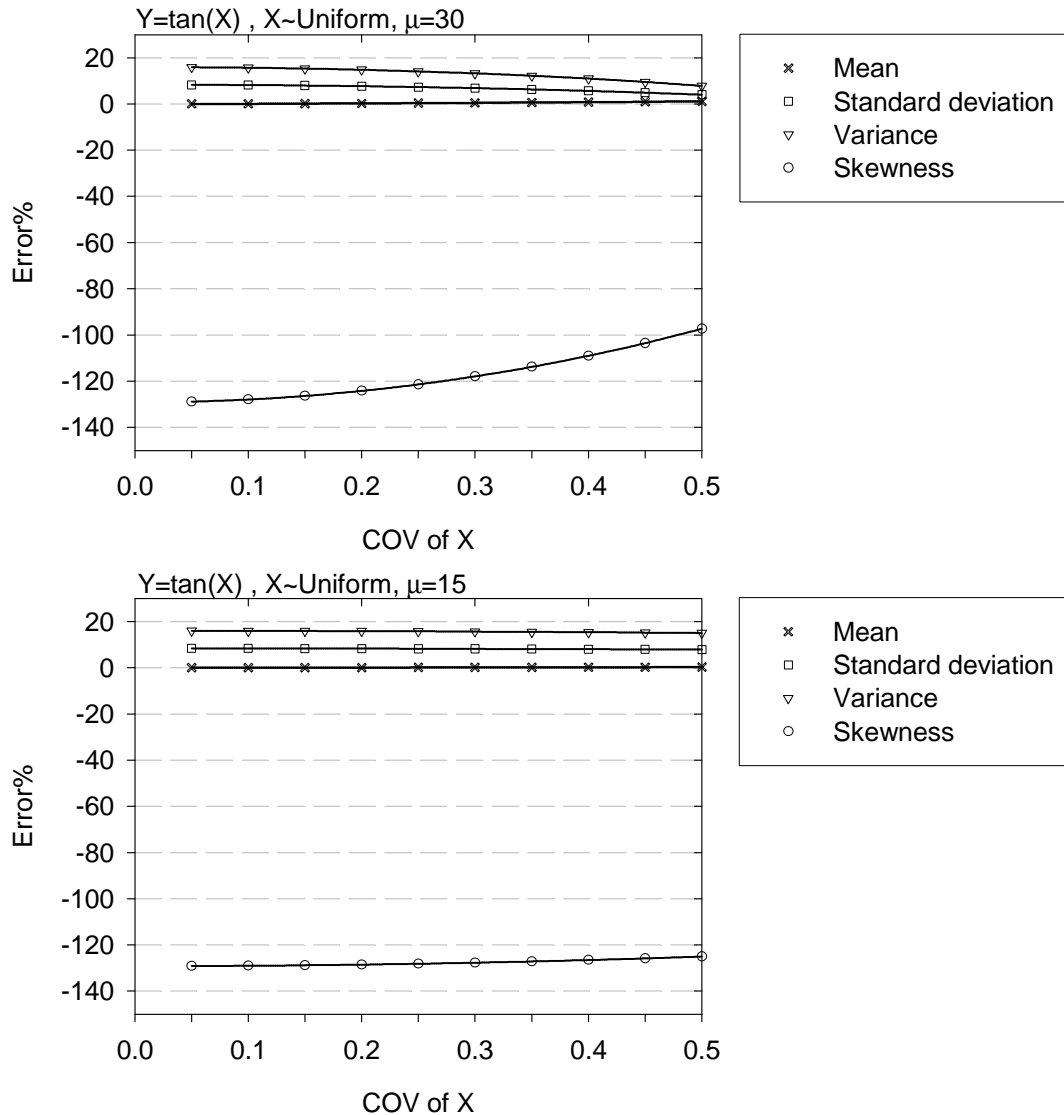


**Fig. 60:** Error in the estimate of the statistical moments for function  $\tan(x)$  with different mean values, using the ZN-III method

All above evaluations consider only explicit LSFs, and no particular PEM accuracy assessment in complex geotechnical boundary value problems with implicit LSFs has been found in the literature. A practical example of the above functions would be a specific LSF in which soil stiffness is an uncertain random variable and the displacement of a tunnel is evaluated by knowing the fact that there is an inverse relationship between these variables. The accuracy of the method strongly depends on the type of LSF, and before applying such an approach it should be verified against a reference method such as the MC simulation approach. It should be noted that the objective of the present study is to compare the range of system responses obtained by the two selected methods (PEM and RSFEM) with each other rather than calculating a precise failure probability.



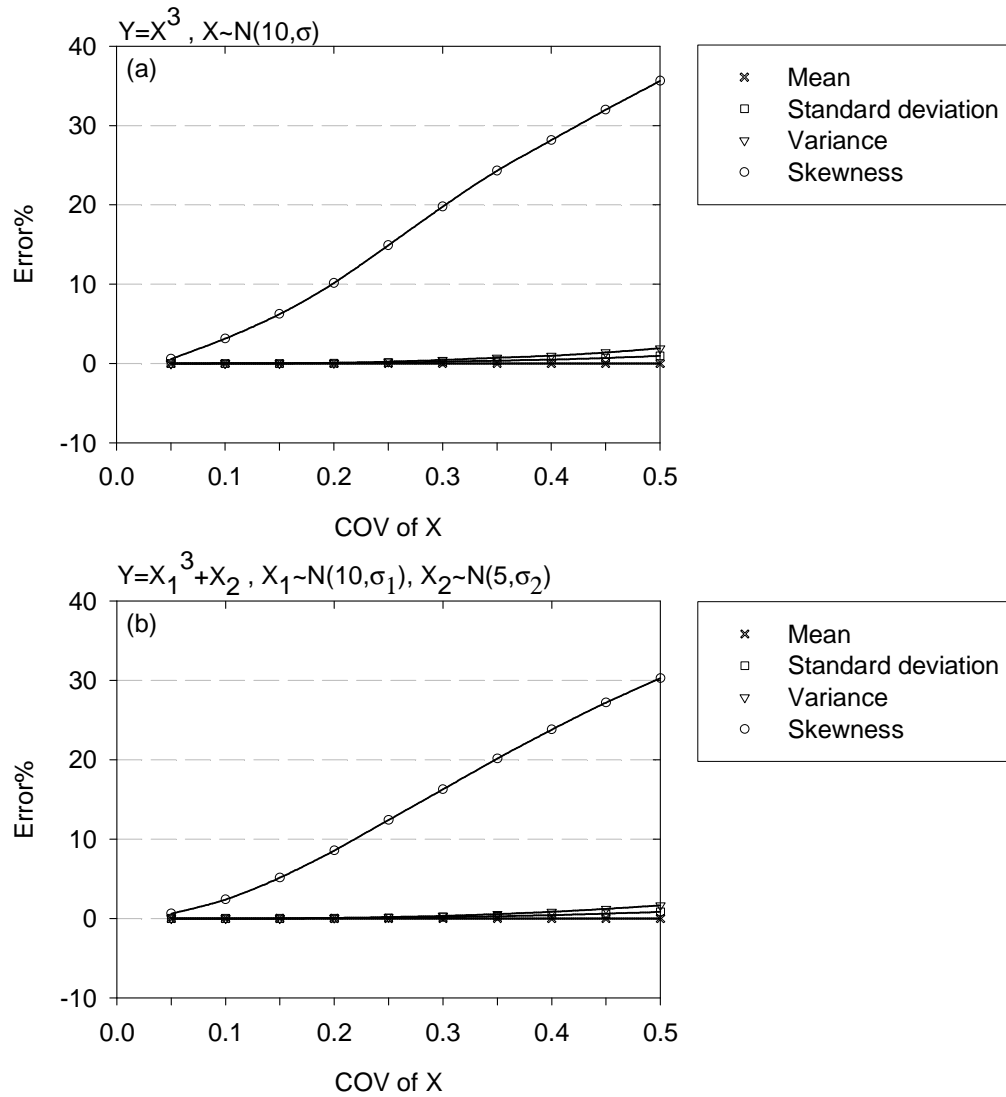


**Fig. 61:** Error in the estimate of the statistical moments for two polynomial functions: a)  $x^3$  b)  $x_1^3+x_2$ , using the ZN-III method

## 6.4 Limitations and advantages

Regarding the Point Estimate Method, particularly ZN-III, the following advantages are pointed out:

1. The simplicity of the method, which allows engineers to benefit from it with limited knowledge of probability.
2. Correlations between random variables can be considered.
3. It gives reasonable accuracy in the estimate of the mean (the most accurate result) and variance of polynomials and most complex functions.

4. It is a favourable method in terms of the number of FE calculations comparing to the Random Set Finite Element Method. Random set analysis with the total number of calculations ( $4^n$ ) –given 2 sources of information for each basic variable– leads to a significantly larger computational effort in comparison with that of ZN-III ( $2n^2+1$ ) in cases where the number of basic variables is more than 3 (see Fig. 62).

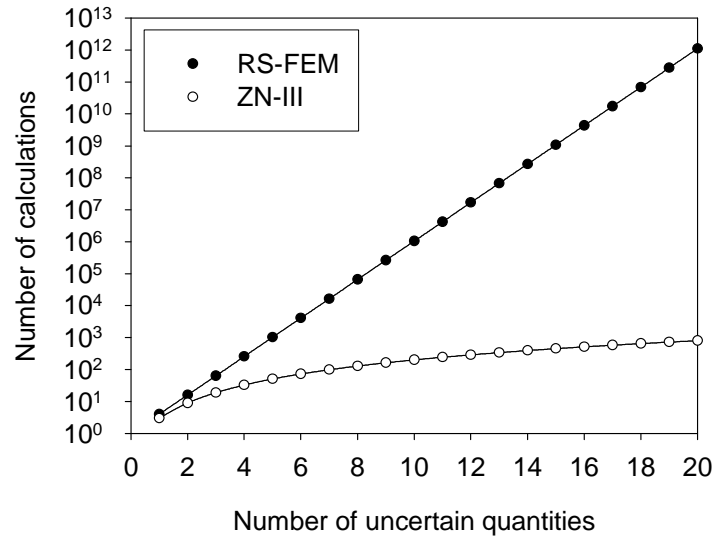


**Fig. 62:** Comparison of RS-FEM with ZN-III in terms of the number of realisations

Despite many appealing points regarding PEM, based on the above discussion there are some disadvantages as follows:

1. PEM yields only the statistical parameters of the system response but no information concerning the shape of the response distribution. Therefore a subjective assumption is needed in this regard, which may affect the amount of  $P_f$  obtained by this method.
2. The method has severe limitations in handling large numbers of variables because if the case, difficulties may arise in the determination of meaningful points in the x-space.
3. According to Baecher and Christian (2003), approximating statistical moments higher than second have less accuracy in the Rosenblueth method (for instance, the computed skewness is less reliable). However, based on the investigation above, ZN-III may result in a reasonably accurate skewness in the case of polynomial functions.
4. Low accuracy will be achieved when the functions of the variable  $X$  to be integrated, are largely disparate from a polynomial form.

## 6.5 Evaluating PEM against RS-FEM for tunnel example

In this section, an uncertainty analysis of a tunnel structure whose random set results are already in hand, is performed by means of PEM using ZN-III and are compared with each other. For this purpose, a section with an overburden of 25 m described in Chapter 4 was selected. The tunnel geometry and its relevant 2D finite element model mesh including the model specifications are depicted in Figures 30 and 31 respectively. The material properties are those adopted for alternative 1 in section 4.2.3 and given in Table 16 and are not repeated here.

### 6.5.1 Providing distribution functions equivalent to random sets

In order to apply PEM, it is necessary to have a probability distribution function for each random variable. To determine the distribution function for a particular soil property, more than 40 data points are needed (Carter et al., 2000). In fact due to the lack of test results and limited sampling, it was not feasible to build an exact PDF of the considered random variables. In addition, in order to be able to compare PEM results with those of RS-FEM, the uncertainty of the input should be matched with each other; although it cannot be yielded perfectly, it is achievable to some extent. The following three alternatives are discussed to properly match the random set input variable given in the Table 16 with a corresponding PDF used in the prospective PEM calculations. At the end, one alternative is selected for this purpose.

#### Alternative 1, averaging random set bounds

The objective is gaining a distribution, which supposedly represents the true PDF of a random variable as well as covering the whole extent of the random set. One possible approach might be to average the probability distributions fitted to the lower and upper bounds of the random set input variable. Figure 63 illustrates an example of this alternative applied to the random set of the friction angle. Fitting a curve to the discrete cumulative random set bounds can be accomplished by the best fitting procedure or just assuming various typical well-known distributions as it has been carried out in the example. For the purpose of illustration, the Pareto distribution (@Risk<sup>®</sup>, 2008) has been fitted to the left bound and a Lognormal type was fitted to the right bound. Multiple combinations of various distribution types have been tried out and the respective PDF and CDF of the resulting averaging have been illustrated in Figure 63. Irrespective of what distribution type one chooses for lower and upper bounds, the mean distribution

does not properly cover the whole range of the random variable. Therefore, this approach is ruled out since it is not able to appropriately fulfil the purpose.

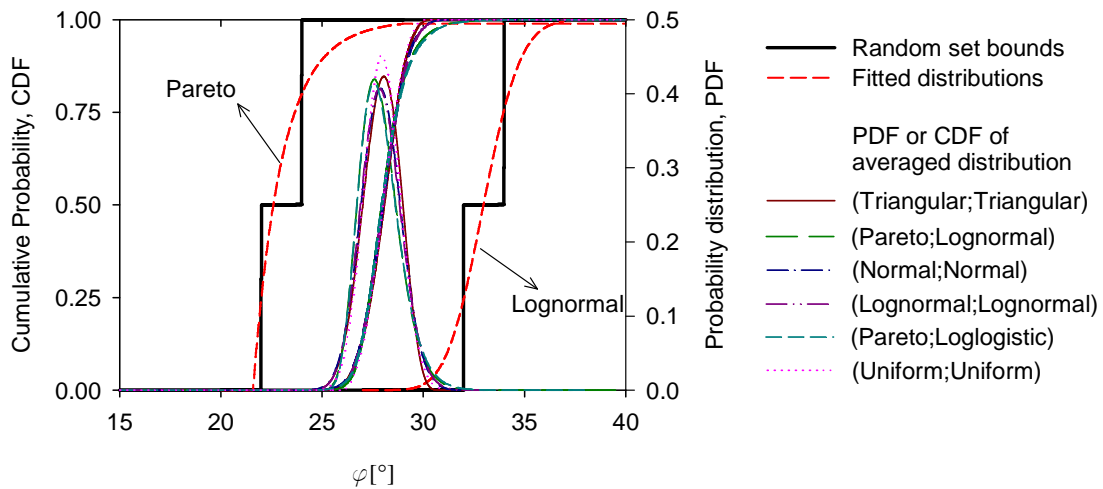


**Fig. 63:** Input PDF of the friction angle obtained by alternative 1 (averaging) assuming various PDFs fitted to the lower and upper bounds of the random set of  $\varphi$

### Alternative 2, the “three-sigma” rule

In probability theory Tchebysheff's inequality asserts that in any data sample or probability distribution, no more than  $1/k^2$  of the distribution's values can be more than  $k$  standard deviations away from the mean, which can be expressed in terms of the following mathematical equation:

$$P(|X - \mu| \geq k\sigma) \leq \frac{1}{k^2} \quad (49)$$

where  $X$  is a random variable with the expected value  $\mu$  and finite variance  $\sigma^2$  and  $k$  is any positive real number. In fact,  $(1-1/k^2) \times 100$  indicates the level of confidence that the random variable is within the abovementioned interval. This confidence level for the case of  $X$  being an  $N(\mu, \sigma^2)$  normally distributed variable increases to about 99.7% since for any real number  $k > 0$ ,  $P(|X - \mu| < k\sigma) = 2\Phi(k) - 1$ , where  $\Phi(\cdot)$  is the standard normal cumulative distribution function. In a particular case  $k = 3$ , it follows that  $P(\mu - 3\sigma < X < \mu + 3\sigma) = 0.9973$ . Based on the relationship held for a normally distributed variable, as a rule of thumb, an event is considered to be “practically impossible” if it falls away from its mean by more than 3 times the standard deviation. This is known as the “three-sigma” rule. For non-normal distributions the 3-sigma rule possesses 95% confidence level, provided the distribution  $X$  is uni-modal in the sense that having a mode  $\nu$ , its density function  $f(X)$  is non-decreasing on  $(-\infty, \nu)$  and non-increasing on  $(\nu, +\infty)$  (Pukelsheim, 1994). Duncan (2000) has applied the ‘3- $\sigma$

rule' to estimate COVs of most commonly used soil parameters and extended the method to a graphical procedure in geotechnical engineering. In addition, Schneider (1999) proposed the relationships given below implicitly using the 3-sigma rule to determine the true mean and standard deviation of soil parameters when no test values are in hand:

$$\mu \cong \frac{x_l + 4\nu + x_r}{6} \quad \text{and} \quad COV = \frac{\sigma}{\mu} \cong \frac{x_r - x_l}{x_l + 4\nu + x_r} \quad (50)$$

where  $x_l$  is the estimated minimum value,  $x_r$  the estimated maximum value, and  $\nu$  is the most likely value or mode.

As an example, Figure 64 shows an application of 3- $\sigma$  rule to a random set of the friction angle using the relationship given by Schneider. The most probable value is obtained by averaging all random set extreme values. The estimated extreme values ( $x_l, x_r$ ) would be the most outer values of the random set bounds as depicted in the Figure with red dashed lines. This method can be used but it could pose a drawback that the probability measure of the values around the random set bounds is very low. Therefore, this approach may underestimate some values around the edge of the random set. It might be more reasonable to use an approach that can allow for a more appropriate probability share for extreme values in the random set to provide a better match between the RS and PEM input variable.

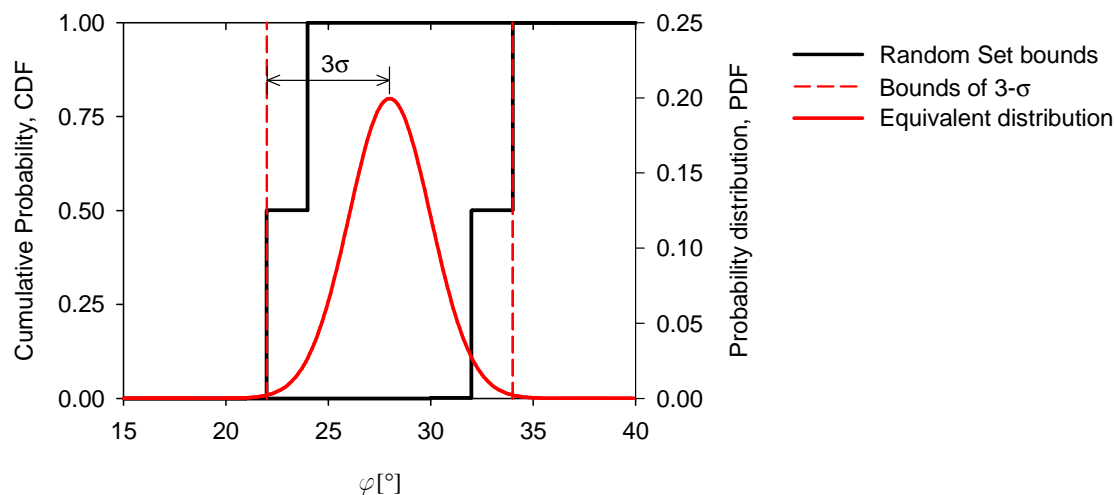


**Fig. 64:** Distribution of the friction angle equivalent to the random set using the 'three-sigma' rule

### Alternative 3, the selection of a best fit to a uniform distribution

In this alternative, first a uniform distribution is constructed whose left and right extreme values are respectively medians of left and right random set bounds (green distribution in Fig. 65). Then, typical and well-known distributions are fitted to the obtained distribution and depending on the shape of the random bounds and the variable itself, one can judge to select an appropriate distribution for further analysis. For instance, the approach was applied again to the friction angle using Triangular, Normal and Lognormal distributions as depicted in Figure 65. In this particular case where the CDF of the variable is very coarse, a considerable discrepancy between the different distribution types occurs and engineering judgment is necessary. Selecting a Normal distribution seems to be very conservative with large dispersion, which there is no need for since the random set is wide enough itself. Although the random set exhibits some kind of symmetry on the right and left bounds, the selection of Lognormal looks more reasonable since it covers the whole range of random set values and it is also a commonly used distribution for the friction angle in the literature because it always gives positive values. When there is abundant information and the random set bounds are smoother, the appropriateness of this alternative emerges. Thus, this alternative is chosen for providing the equivalent probability distribution for further point estimate analysis.

The approach has been applied to other random variables of the problem whose results are illustrated in Figure 66.

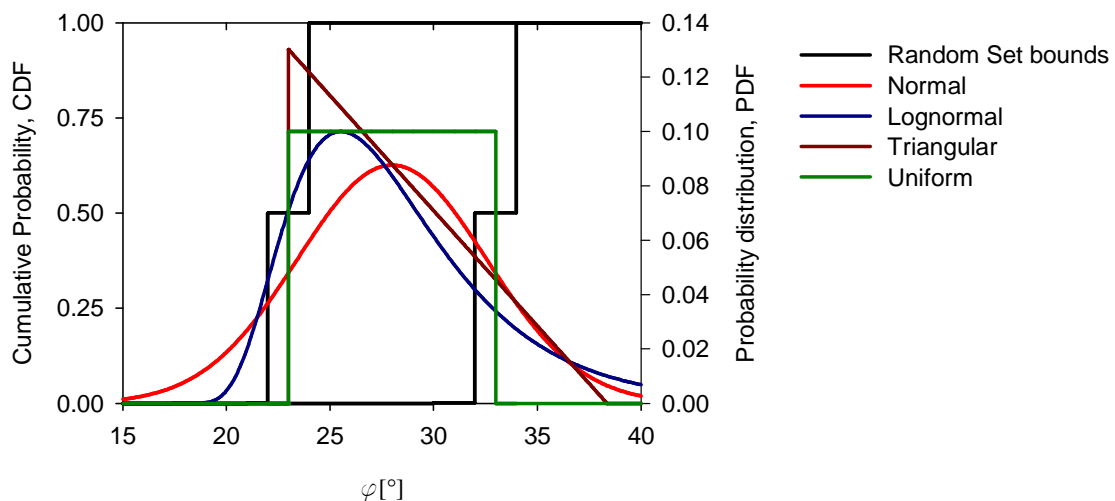


**Fig. 65:** Distribution of friction angle equivalent to the random set using alternative 3

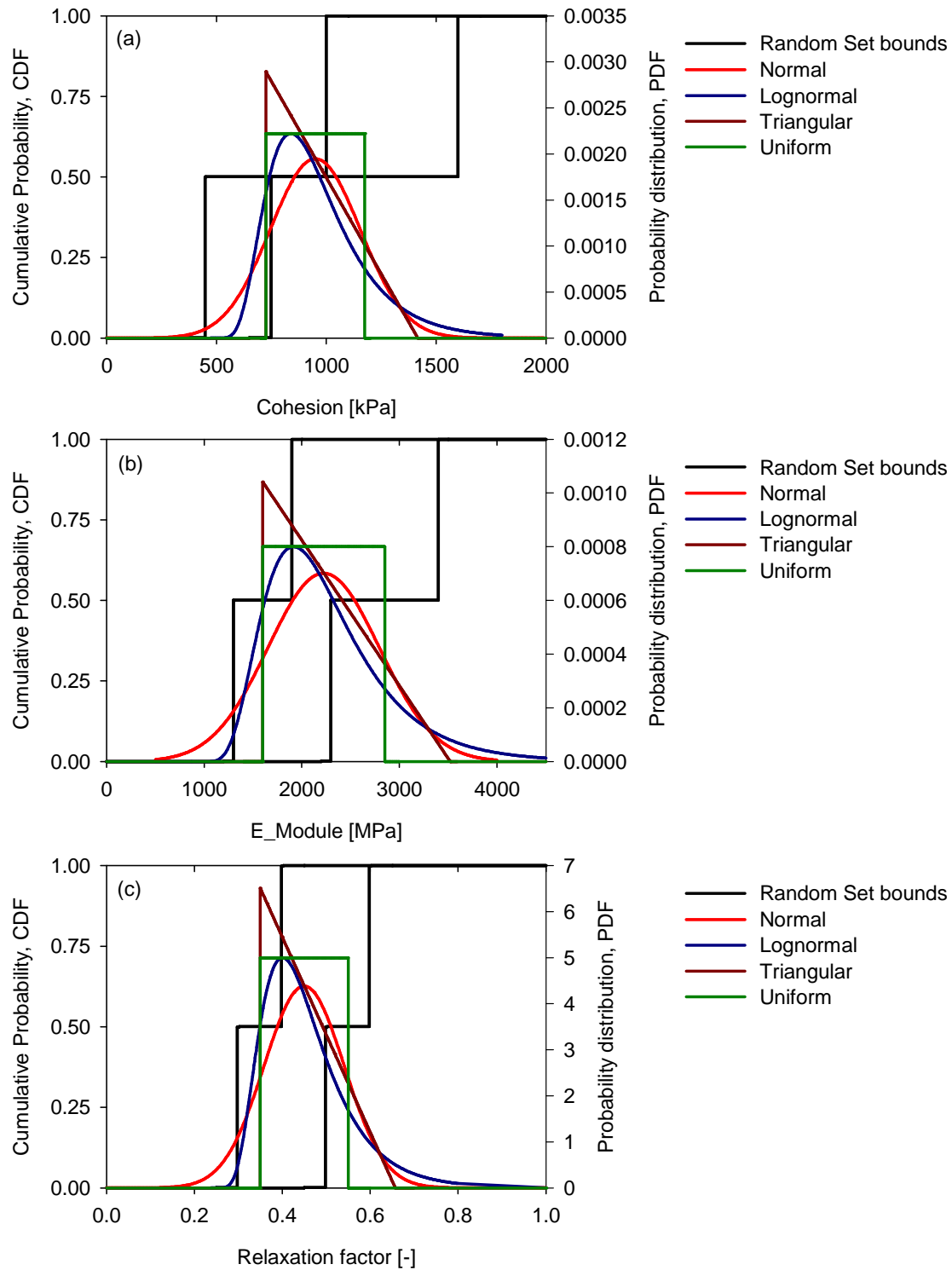


**Fig. 66:** Equivalent distribution to the random set using alternative 3 for variables, a) cohesion b) elastic modulus c) relaxation factor

For each random parameter some judgment has been carried out as follows:

**Elasticity modulus:** Lognormal distribution shows skewness to the left inspired by the random set; it also covers the entire range of the random set rather well. Triangular and Uniform distributions do not entirely cover the random set.

**Cohesion:** Normal distribution is chosen since it has a better coverage on the whole random set than the others, and also shows no skewness or predisposition to the left or right just like the corresponding random set.

**Relaxation factor:** Normal distribution is adopted since there is no evidence that the relaxation factor has any sort of skewness. On the other hand, Normal distribution covers the range of the random set quite well and takes some values out of the range into account (but with a very small probability value), which places the results on the safe side.

According to the above discussion, detailed information about the probability distribution of the four basic random variables selected for PEM analysis is given in Table 29.

**Tab. 29:** Basic random variables and the respective PDF details

Basic variable	Unit	Distribution type	Mean	Standard dev.	COV %
Friction angle, $\varphi$	degree	Lognormal	28	5	17.8
Elasticity modulus, $E$	MPa	Lognormal	2256	631	28
Cohesion, $c$	kPa	Normal	950	205	21.6
Relaxation factor, $R_f$	-	Normal	0.45	0.09	20

## 6.5.2 Calculation results

The Point Estimate procedure described in section 6.2 using the ZN-III integration rule is applied. The input parameters are given in Table 29. No correlations between basic random variables have been taken into account. According to the integration rule the numerical model of the tunnel based on the sampling points summarised in Table 30 has to be evaluated 33 times. Eight realisations can be left out since the respective weights are zero; therefore, the number of calculations decreases to 25 realisations. The number of calculations in comparison with the random set carried out in Chapter 4 is dramatically lower and can be considered as an advantage of the PEM.



**Tab. 30:** Value of variables of sampling points and respective weights

Analysis No.	Input variables				Weights
	$\varphi$	$E$	$R_f$	$C$	
1	27.8	2172.9	0.45	949.6	0.33333
2	42.9	2172.9	0.45	949.6	0
3	18.0	2172.9	0.45	949.6	0
4	27.8	4256.8	0.45	949.6	0
5	27.8	1109.1	0.45	949.6	0
6	27.8	2172.9	0.67	949.6	0
7	27.8	2172.9	0.23	949.6	0
8	27.8	2172.9	0.45	1451.4	0
9	27.8	2172.9	0.45	447.8	0
10	37.8	3495.8	0.45	949.6	0.02778
11	37.8	1350.6	0.45	949.6	0.02778
12	20.5	3495.8	0.45	949.6	0.02778
13	20.5	1350.6	0.45	949.6	0.02778
14	37.8	2172.9	0.61	949.6	0.02778
15	37.8	2172.9	0.29	949.6	0.02778
16	20.5	2172.9	0.61	949.6	0.02778
17	20.5	2172.9	0.29	949.6	0.02778
18	37.8	2172.9	0.45	1304.4	0.02778
19	37.8	2172.9	0.45	594.8	0.02778
20	20.5	2172.9	0.45	1304.4	0.02778
21	20.5	2172.9	0.45	594.8	0.02778
22	27.8	3495.8	0.61	949.6	0.02778
23	27.8	3495.8	0.29	949.6	0.02778
24	27.8	1350.6	0.61	949.6	0.02778
25	27.8	1350.6	0.29	949.6	0.02778
26	27.8	3495.8	0.45	1304.4	0.02778
27	27.8	3495.8	0.45	594.8	0.02778
28	27.8	1350.6	0.45	1304.4	0.02778
29	27.8	1350.6	0.45	594.8	0.02778
30	27.8	2172.9	0.61	1304.4	0.02778
31	27.8	2172.9	0.61	594.8	0.02778
32	27.8	2172.9	0.29	1304.4	0.02778
33	27.8	2172.9	0.29	594.8	0.02778

The following results similar to those considered in Chapter 3 have been selected for comparison:

1. Vertical displacement of the tunnel crown (Point A in Fig. 16)
2. Vertical and horizontal displacement of the side wall (Point B in Fig 16)
3. Maximum normal force and moment in the lining
4. Safety factor after the top-heading excavation
5. The serviceability limit state of the shotcrete lining based on Equation 24
6. The eccentricity of the normal force acting on the cross section of the shotcrete lining,  $e(x)$ , which is a function of both normal force and moment of the lining (see Equ. 23)

The first three statistical moments of the results have been tabulated below (Tab. 31) and graphically illustrated in Figures 67 to 70 with the overlaid corresponding RS-FEM p-boxes. For each result, two commonly used distributions, namely Normal and Lognormal have been assumed corresponding to the estimated statistical moments given in Table 31 and if possible, a shifted lognormal distribution recommended for some geotechnical application by Russelli (2008) has also been considered. It should be noted that shifted lognormal can be used only when the skewness of the distribution is known and positive. Therefore, it was impossible to use shifted lognormal for displacement results with negative skewness. In addition, it turned out that in the cases in which skewness  $\gamma < 1$  the difference between Lognormal and shifted Lognormal is negligible. For instance, as Figure 68a depicts the maximum normal force having a skewness of 0.7, the modal values of both distributions are close to each other and have been captured by the range of the most likely values given by RS-FEM.

**Tab. 31:** Statistical moments of some results and the range of the most likely values given by RS-FEM

	Response	U <sub>y</sub> -A	U <sub>x</sub> -B	U <sub>y</sub> -B	FOS	Normal Force	Moment	e(X)	g(X)
	Unit	mm	mm	mm	-	kN.m/m	kN/m	m	kN/m
PEM results	Average ( $\mu$ )	2.5	0.58	1.5	6.7	264	12.2	0.158	966
	Stan. dev. ( $\sigma$ )	0.8	0.14	0.4	1.3	78	2.6	0.047	307
	Skewness ( $\gamma$ )	-0.79	-0.58	-0.78	0.10	0.71	0.56	1.10	-1.61
	$\mu+1.8\sigma$	3.9	0.83	2.2	9.0	405	16.9	0.243	1519
	$\mu-1.8\sigma$	1.2	0.33	0.7	4.5	124	7.5	0.073	412
RS-FEM	Upper limit	3.9	0.77	2.2	8.6	407	16.8	0.174	1239
most likely values	lower limit	1.6	0.44	1.0	5.2	164	7.3	0.068	897

Based on the mean ( $\mu$ ) and standard variation ( $\sigma$ ) of the results, Table 31 gives the extremes of the 86% confidence interval ( $\mu \pm 1.8\sigma$ ), regardless of distribution type (Pukelsheim, 1994). They show a good conformity with the range of the most likely values (see section 3.3.4 for the definition) given by RS-FEM except for target variables  $e(x)$  and  $g(x)$ . The range,  $\pm 1.8\sigma$ , has been identified for the PEM results because it can have the same functionality as the range of the most likely values given by RS-FEM for the quality indicator, which is discussed later. As it can be seen in Figures 67 and 68 primary responses such as displacements and internal forces show a good conformity with the RS-FEM results in the sense that PEM's results are supposed to present the 'true' distribution of the system response and should not exceed the random set bounds. However, the secondary responses, which are obtained from the primary answers show a larger scatter than random set bounds (Fig. 69) which is inadmissible because RSs are supposed to give the boundaries of the real response and the answers outside these bounds are theoretically not allowable. In the case of  $g(x)$  a large

proportion of the distribution given by PEM falls outside the random set answers. The inadequate accuracy of PEM in estimating the variance of the limit state functions that are not the direct FE results, should be proven by further investigation.

Recalling from Chapter 3 a quality indicator was employed in order to evaluate the probabilistic results obtained by RS-FEM against the measurement, and assess the validity of the calculation method. A quality indicator analogous to that used for the RSFEM is established for interpreting the results of PEM providing more or less the same validity concepts and zone. The concept of the quality indicator is explained by illustrating the cumulative distribution of tunnel displacements calculated by PEM along with the in-situ measurement in Figure 70. The quality indicator consists of three zones: a) most likely zone (in green) b) warning zone (green and red) and c) unlikely zone (red), which are quantified by the intervals:  $\{-1.8\sigma < x < +1.8\sigma\}$ ,  $\{\pm 1.8\sigma < x < \pm 3.0\sigma\}$ , and  $\{+3.0\sigma < x \text{ \& } x < -3.0\sigma\}$ , respectively. From probability theory (Pukelsheim, 1994) it is known that the interval,  $\pm 1.8\sigma$ , represents the 86% confidence interval irrespective of what distribution the target variable has, on condition that the distribution is unimodal. As it was shown before in Figures 67 and 68 this interval either conforms to the most likely zone given by RSFEM or presents a larger range than that. Therefore, this range is chosen for the PEM results to represent the most likely range (green zone) for the expected measurement values. Outside the most likely values zone, the green colour zone in the quality indicator starts to fade and convert into the red one. This transition zone can be called an alarm zone because it indicates that the measured value is gradually moving away from the expectation value calculated by the PEM analysis and the validity of the results is gradually decreasing. If it goes beyond  $3\sigma$ , a very small probability of the occurrence of such an event is expected, or in other words, it should be practically 'unlikely' since the interval  $\pm 3.0\sigma$  theoretically encompasses at least 95% of the expected results. Finally, Figure 70 shows a relatively good conformity between the RS-FEM quality indicator and that proposed for PEM from a practical point of view.

In a tunnel, as soon as the reflectors are installed on the shotcrete lining, the measurable displacements are recorded and they develop further as the tunnel face progresses. In practice if a designer provides such results (i.e. Fig. 70) the measurements can be easily checked against the calculation. In any case, the measured value lies within one of above mentioned zones and probably changes with the progress of the tunnel. So the inspector can make an appropriate decision if the measured value in a special section deviates significantly away from the expected results. Thus accommodating such results may be helpful in the context of the 'Observational Method'.

Furthermore, the concept of the quality indicator can be also utilised in setting the warning and alarm values required for monitoring the tunnel deformations.

For instance, it is suggested that  $\pm 1.8\sigma$  be considered as the warning values and  $\pm 3.0\sigma$  as the alarm values.

The two-step discrete cumulative probability distribution of the measurements implies that only the measurements of two tunnel cross sections were available. As it can be seen from Figure 70a, both measured values of the tunnel crown could be captured by the interval  $\pm 1.8\sigma$ . However, concerning the side wall displacement, the measurement of one of the cross sections falls outside of  $\pm 3\sigma$ . Since the absolute values are small, this deviation from the predicted result may be neglected in practice.

As depicted in Figure 70c, one of the measured values falls outside the  $3\sigma$ -range, while the RS-FEM results covers that in its warning zone. Obviously the two discrete cumulative steps on the right side of the measured value indicate that the two combinations involved in the random set analysis result in higher values. Although the discrepancy between random set analysis and PEM results in terms of absolute displacement value is not of importance, it shows that these two extreme values have distinctly higher values relative to other upper bound values of RS-FEM. The reason is that a certain combination of RS input parameters result in a larger plastic zone around the tunnel in comparison to the rest of the combinations. Higher deformations are the consequence. On the other hand, the predetermined point estimate samples have a certain distance from the mean value, depending on the number of basic variables involved. Also it is known that the more basic variables are involved, the farther the sampling points get from the respective mean value. In the current example, by reviewing the sampling points in Table 30, one can realise that the sampling points of the cohesion (which is one of the most influential rock parameters on displacement, see Chapter 3 sensitivity analysis) are inside the respective random set input p-box. Therefore, all the FE calculations of the prefixed combination of the sampling points result in relatively limited plastic zones, and accordingly lower horizontal displacement at point (B). Actually, this issue does not lead to significantly different results between both the methods, but it might happen in a higher nonlinear problem that the discrepancy between PEM and RS-FEM becomes considerably larger. In addition, this finding affirms that alternative 2 (three-sigma rule) is not a good choice for matching the random set input p-boxes with the PEM input distributions.

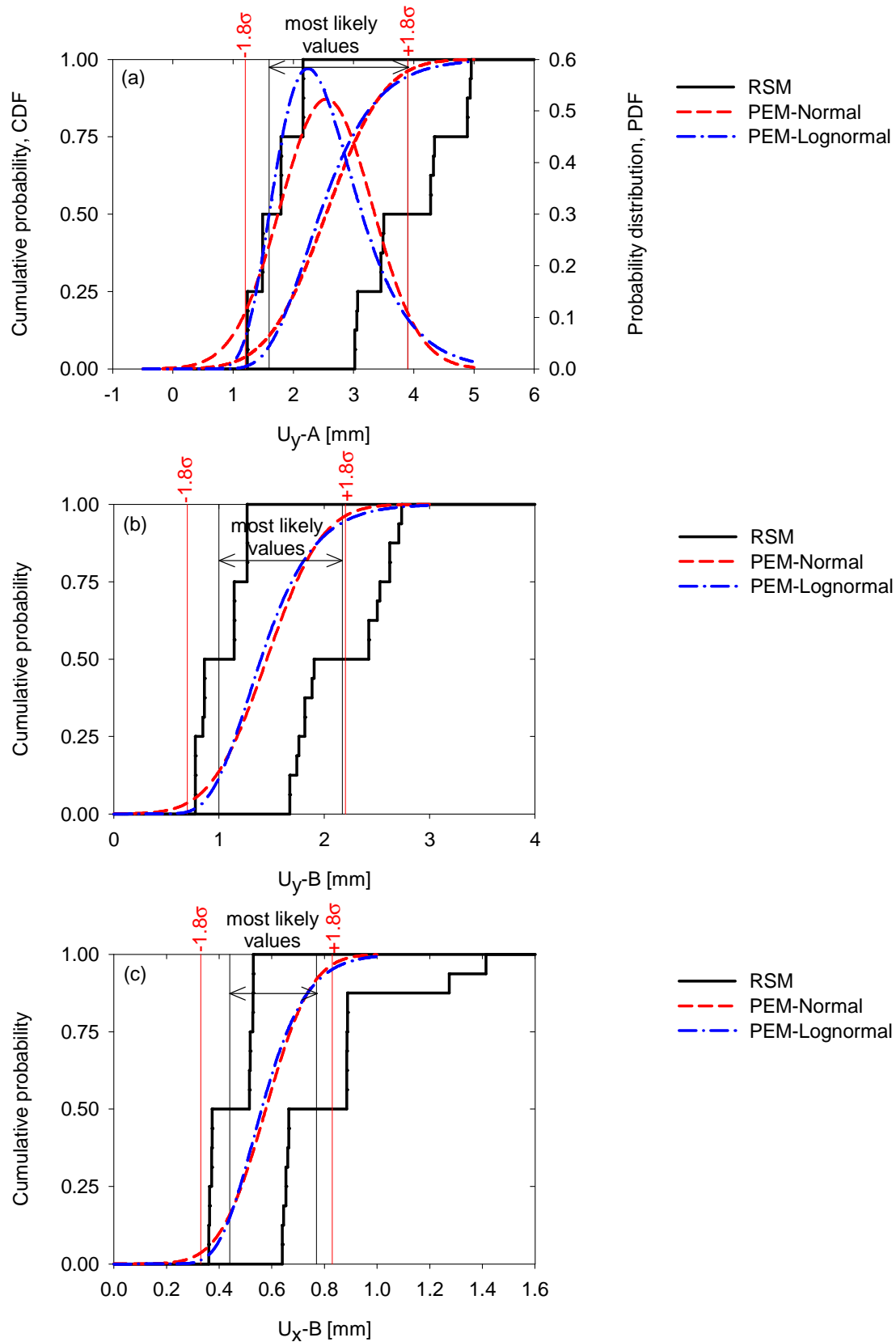


**Fig. 67:** Comparison of PEM with RS-FEM results in terms of displacement at, a) tunnel crown b) point B-horizontal direction c) point B-vertical direction

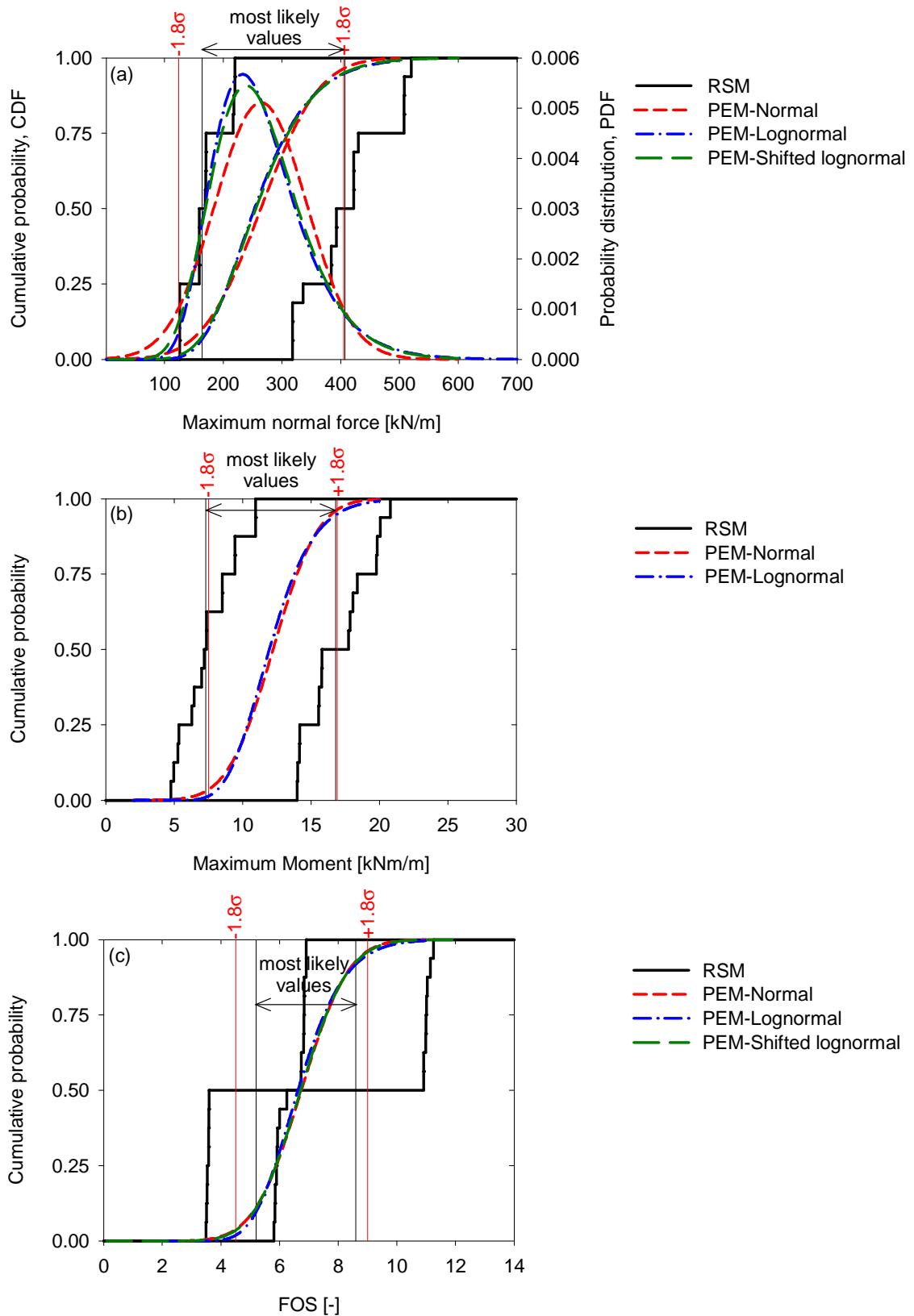


**Fig. 68:** Comparison of PEM with RS-FEM results in terms of tunnel internal forces, a) maximum normal force b) maximum moment, and c) safety factor of top-heading excavation

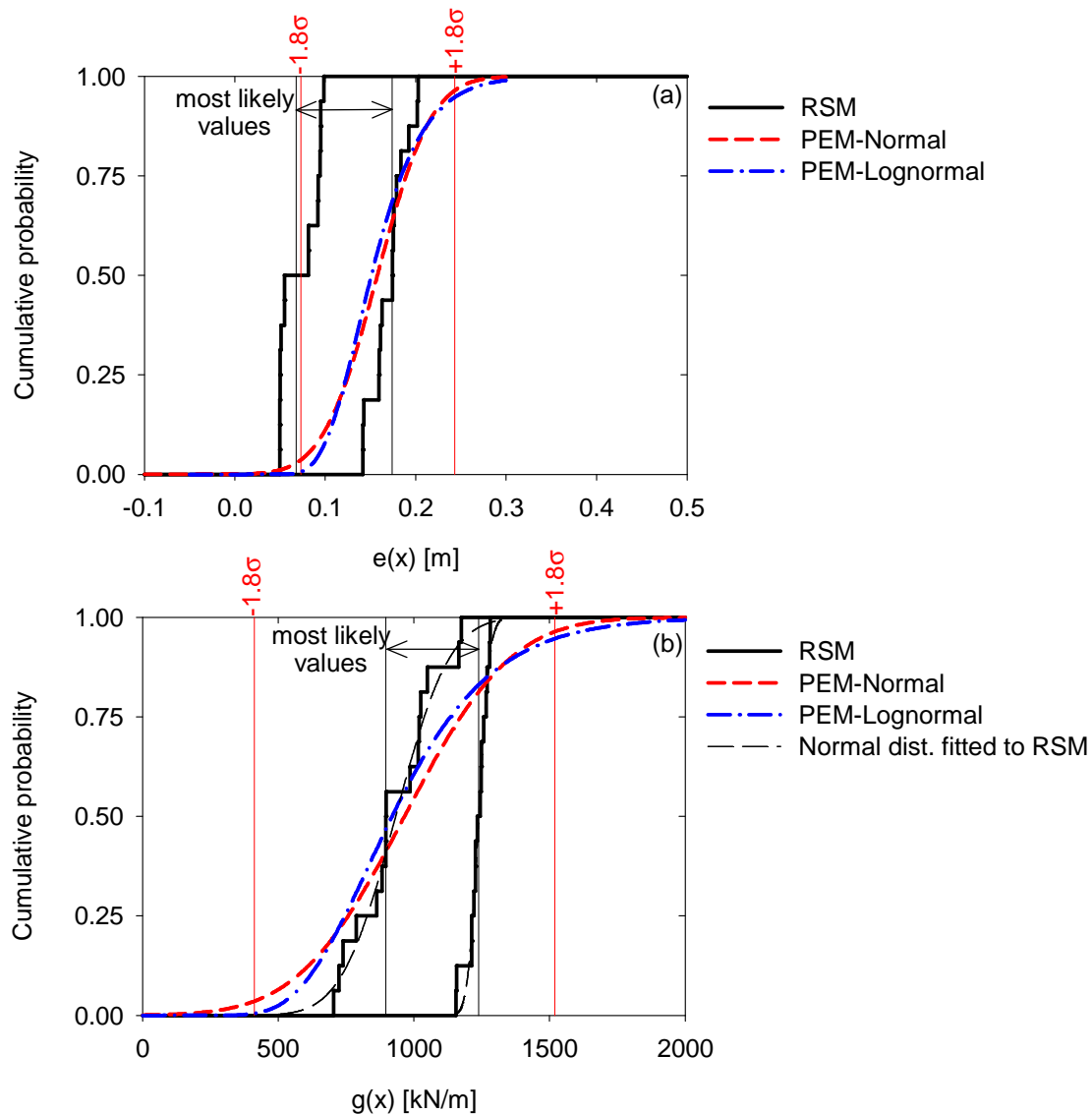


**Fig. 69:** Comparison of PEM with RS-FEM results, a) eccentricity of normal force in the lining b) shotcrete limit state function  $g(x)$

In the context of reliability analysis it is of interest to compare the probability of unsatisfactory performance of the shotcrete lining (i.e. using the limit state function,  $g(x)$ ) obtained from the two methods. The upper bound probability of failure, calculated based on the RS-FEM results is  $1.0E-9$ , which is considerably less than  $8.5E-4$  obtained by PEM assuming a Normal distribution for the function  $g(x)$ . As discussed above, this is due to the high standard deviation calculated by PEM. Nevertheless, PEM yields a conservative answer on the safe side. Basically, a level three method of reliability analysis is required to calculate the value of  $P_f$  accurately enough, such as Monte-Carlo based simulation methods that need many FE realisations and have not been considered in this work.

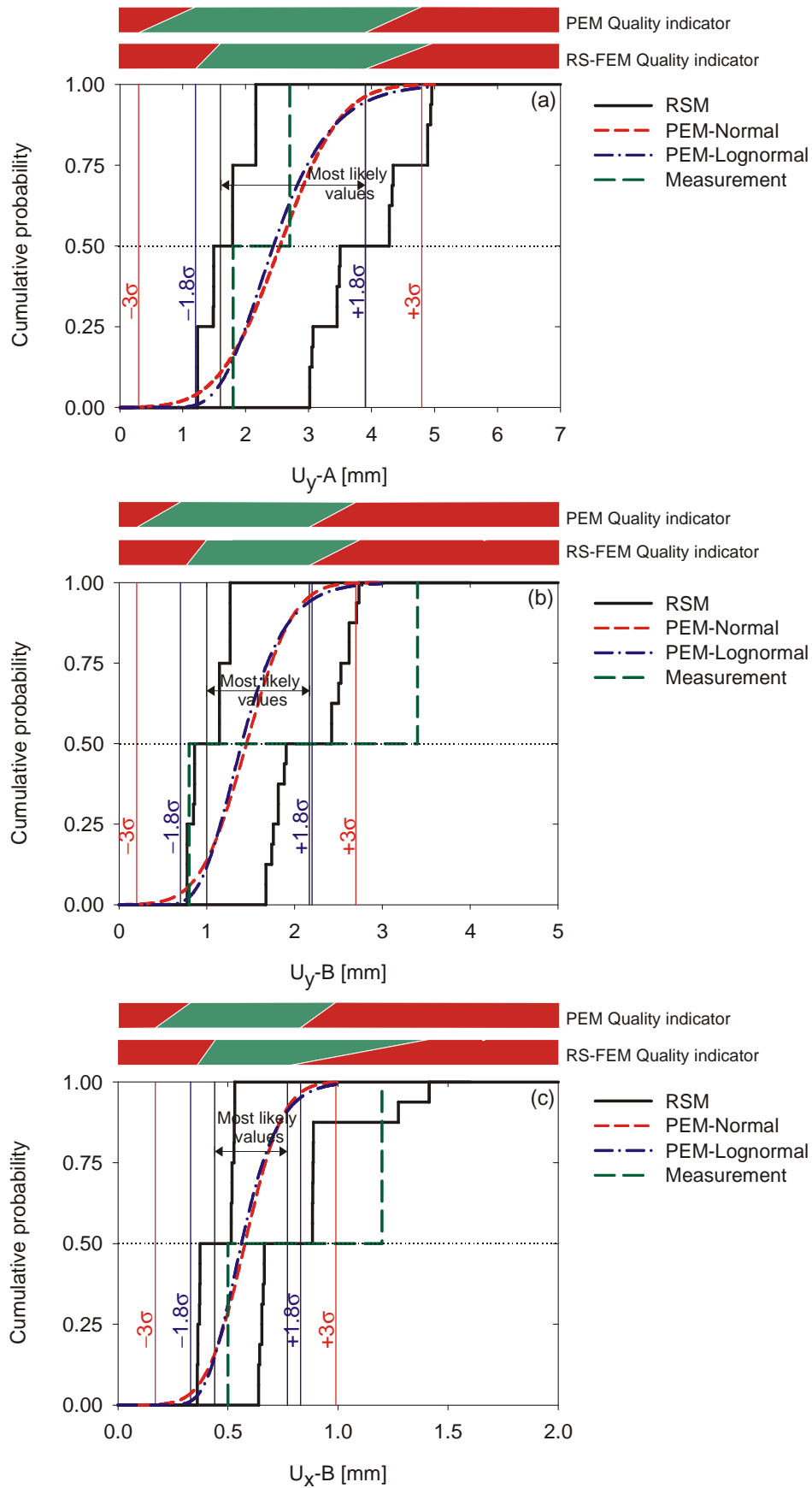


**Fig. 70:** Comparison of tunnel displacements obtained by PEM and RS-FEM with measurement at a) tunnel crown b) point B-horizontal direction c) point B-vertical direction



## 6.6 Summary and conclusion

The limitations and advantages of PEM were discussed. In particular, the accuracy of PEM in estimating the statistical moments of some basic functions (section 6.3) using the ZN-III integration rule was investigated. It was shown that the first two moments of functions can be estimated with reasonable accuracy while the skewness may be accompanied by a large error except in the case of polynomial type functions. The PEM was applied to a real case tunnel problem. A process of obtaining a probability distribution consistent with the corresponding random set p-box was proposed. The results of PEM in comparison with RS-FEM were satisfactorily consistent, in particular, in the case of the primary FE results.

The standard deviation of the secondary target variables (e.g. Limit State Functions) -calculated based on the primary FE results- is overestimated by PEM. Consequently, the estimated probability distribution of the LSF considerably exceeded random set bounds. Although this overestimated scatter is on the safe side, it might be too large from a practical point of view. Thus, it can be considered as a shortcoming of the PEM. On the other hand, the number of FE calculations required by PEM is significantly lower than those in the random set method especially when the number of basic random variables increases. Furthermore, it was found that in all results the range of  $\pm 1.8\sigma$  with respect to the mean value encompasses the range of most likely values estimated by RS-FEM. This range theoretically represents an interval at least with 86% confidence. A range in terms of the standard deviation of the results obtained by PEM was established as a quality indicator similar to those discussed in Chapter 3 for the RS-FEM by which the validity of the probabilistic FE results can be checked against the measurement. When the “observational method” is used, setting up warning values is beneficial for decision-making.

It should be noted that the main objective of the chapter was to estimate the most likely range of system responses resulted from the uncertainty available in the current state of knowledge, rather than calculating a precise probability of failure ( $P_f$ ). A practical aspect of providing a most probable range is that the inspecting engineer, design team, and client would be more capable of making a timely and rational decision when the measurements exceed the anticipated values. Measurements are commonly carried out in tunnel projects, but what is more crucial is to interpret them and make the engineering decisions in the appropriate time. The essential decision making tool is proper calculations, which enables one to determine the nonconformity between the designing engineer’s understanding of the tunnel environment and the reality. This research work illustrated that from a practical point of view, PEM succeeds to provide such information with reasonable calculation effort.

RS and PEM methods both produce a common range of results, although their input and assumptions are clearly different, and thus difference in results have to be expected. Depending on each case, the quantity and quality of the required input data of a system could determine which method is favoured. When the soil/rock data parameters are abundantly available, their probability distributions are definable with sufficient accuracy, thus applying PEM is advantageous in this case. However, in practice the results of geotechnical investigations are set valued rather than being precise and point valued. Often the value of the required parameters exists in form of ranges with no probability assignment across the interval from various independent sources e.g. based on engineering judgement, expert opinion or experience from neighbouring projects. In this case it is advisable to combine the sources of information according to the RS method.

## 7 Conclusions and further research

### 7.1 Summary and achievements

In uncertainty and reliability analysis of tunnel problems involved in this work two methods from two different underlying mathematical backgrounds were selected, namely, the random set approach and the point estimate method. The Random set approach is categorised as a non-probabilistic method and PEM originates from probabilistic approaches.

The main focus was on the RS-FEM method, since at the beginning of the tunnel projects usually there is a lack of sufficient information and thus a probability distribution for input parameters is not available. The required data are derived from different independent sources which are to be combined. This data also suffers from ambiguity and imprecision. According to these conditions, previous researchers had already recognized RS-FEM as an appropriate mathematical framework to deal with such kind of information. When a large number of uncertain variables exists and each are estimated from several sources (numerous focal elements), the computational effort of the random set approach increases exponentially, which is not favourable. However, it is fortunately not the case in the majority of tunnel projects and insignificant input variables are identified in order to reduce the number of the underlying uncertain variables by performing a sensitivity analysis scheme.

This work demonstrates the merits of applying the Random Set approach as a beneficial tool in the context of engineering judgment and decision making. For instance: 1) the wide range of uncertainty in the system response may lead to different classes of tunnel section design, 2) RS-FEM results simplify the interpretation of the numerical results against measurements, and 3) the RS-FEM framework can be placed within the observational method design procedure as a supplementary analysing tool.

It was illustrated that the RS-FEM not only takes uncertainty of input parameters into account, but also has the capacity in considering constitutive model uncertainty or combining the numerical results of different soil/rock constitutive models.

From a practical point of view RS-FEM has provided a simple framework to predict the system response within a range. This range is in the form of a p-box which incorporates imprecise probabilities concepts. Working with a range of probabilities seems to be more acceptable for geotechnical engineers in practice. Furthermore, employing the RS-FEM framework helps increasing the credibility

of numerical analysis results since its computational results -shown in a real project- could successfully capture the range of the ground behaviour.

The spatial variability of the soil/rock parameters cannot be allowed for in rigorous manner; although, the two approaches proposed in Chapter 3 are consistent with the RS-FEM procedure.

When only one set (the focal element) is available for each basic random variable, the random set approach converts into an Interval Analysis and results in merely an interval for each system response and consequently no reliability analysis can be carried out. On the other hand, in the case of abundant sources of information (many focal elements) and a large number of uncertain basic variables, a rather high computational effort is indispensable in RS-FEM. In the latter case, an alternative approach (i.e. PEM) can be employed that not only requires considerably less calculations, but also results in a reasonable agreement with the random set approach almost with comparable benefits. However, the secondary results (e.g. the limit state function of the tunnel shotcrete) obtained by PEM tends to show a higher scatter than the corresponding results obtained by the random set approach. This finding needs to be confirmed by further studies.

## 7.2 Further research

Throughout the study it is assumed that the system on which the random set approach is performed has a monotonic behaviour with respect to the considered uncertain parameters. However, it is not a straightforward task to prove the monotonicity condition for a geomechanical boundary value problem. In the examples presented herein, the monotonicity property has been roughly examined by the sensitivity analysis (U.S. EPA: TRIM 1999) which is acceptable from a practical point of view. The monotonicity behaviour should be investigated with an appropriate mathematical framework such as efficient optimization methods in a more rigorous manner. This has been addressed in Chapter 1.

The accuracy of the Point Estimate Method using the Zhou-Nowak  $2n^2+1$  integration rule should be verified and assessed against fully probabilistic methods such as the Crude Monte Carlo simulation method in uncertainty and reliability analysis of tunnel problems, which are missing in geotechnical literature, since most of the validations and studies available in the literature have been conducted in simple geotechnical problems considering mostly linear performance functions. The range of problems can vary from tunnel problems having closed form solutions (e.g. deformation behaviour of circular deep tunnels in an elasto-plastic material) to the numerical analysis of non-circular shaped

tunnels in multi-layered subsurface conditions with advanced constitutive material models.

In the current RS-FEM all the input random variables are assumed to be independent. This assumption is mostly conservative regarding soil/rock parameters and also logical when little knowledge exists concerning the dependency among the parameters. However for future work, the influence of dependency between soil parameters can be investigated on the results of RS-FEM in tunnel problems. In this regard two approaches are available:

1. Computing the envelope on the Random Set bounds assuming no specific dependency. The developments have been lately carried out, for instance one may refer to the computational algorithms given by Berleant and Goodmanstrauss (1998) and Berleant and Zhang (2004).
2. Using the notion of copulas or Pearson correlation coefficients, which quantitatively describe the dependency between the parameters, and obtaining the corresponding joint probability of the basic random variables. In this context Ferson et al. (2004), and Williamson and Downs (1990) provide a good guidance.
3. A comprehensive study can be conducted for a real tunnel project in which the results and the current accomplishments obtained by RS-FEM provide the primary computational steps required for subsequent essential uncertainty analysis associated with the cost and time estimate of the tunnel project up to a risk analysis.

## 8 Bibliography

Alén, C. (1998)

On Probability in Geotechnics. Random Calculation Models Exemplified on Slope Stability Analysis and Ground-Superstructure Interaction. Department of Geotechnical Engineering, Chalmers University of Technology. Dissertation.

Ang, A.H-S. (2009)

On Risk and Reliability – Contributions to Engineering and Future Challenges. Safety, Reliability and Risk of Structures, Infrastructures and Engineering Systems. Furuta, Frangopol & Shinozuka (eds). Taylor & Francis, London, 1-20.

Ang, A.H-S.; Tang, W.H. (1975)

Probability Concepts in Engineering Planning and Design. Volume I-Basic Principles. New York: Wiley & Sons.

Baecher, G.B.; Christian, J.T. (2003)

Reliability and Statistics in Geotechnical Engineering. New York: Wiley & Sons.

Barton, N. (2002)

Some new Q value correlations to assist in site characterisation and tunnel design. *Int. J. Rock. Mech. Min. Sci.*, Vol. 39, 185-216.

Barton, N.; Lien, R.; Lunde, J. (1974)

Engineering classification of rock masses for the design of tunnel support. *Rock Mech.*, Vol. 6, 189-239.

Barton, N.; Loset, F.; Lien, R.; Lunde, J. (1980)

Application of the Q-system in design decisions. *Subsurface Space*, Bergman (ed.), Vol. 2, 553-561.

Ben-Haim, Y. (1994)

A non-probabilistic concept of reliability. *Structural Safety*, Vol. 14, No. 4, 227-245.

Ben-Haim, Y.; Elishakoff, I. (1990)

Convex Models of Uncertainty in Applied Mechanics. Amsterdam: Elsevier.

- Berleant, D.; Goodman-Strauss, C. (1998)  
Bounding the results of arithmetic operations on random variables of unknown dependency using intervals. *Reliable Computing*, Vol. 4, 147-165.
- Berleant, D.; Zhang, J. (2004)  
Representation and problem solving with Distribution Envelope Determination (DEnv). *Reliability Engineering and System Safety*, Vol. 85, No. 1-3, 153-168.
- Bieniawski, Z.T. (1976)  
Rock mass classification in rock engineering. Proc. of the Symp. in Exploration for Rock Engineering, Bieniawski (ed.), Cape Town, Balkema, 97-106.
- Bieniawski, Z.T. (1978)  
Determining rock mass deformability—experience from case histories. *Int. J. Rock Mech. Min. Sci. Geomech Abstr.*, Vol. 15.
- Brinkgreve, R.B.J.; Broere, W. (2008)  
PLAXIS, Finite element code for soil and rock analyses, users manual. Version 9, Rotterdam: Balkema.
- Brown, E.T. (1970)  
Strength of models of rock with intermittent joints. *J. Soil Mech. Found. Div.*, ASCE 96, SM6, 1935-1949.
- Carter, J.P.; Desai, C.S.; Potts, D.M.; Schweiger, H.F.; Sloan, S.W. (2000)  
Computing and computer modeling in geotechnical engineering. Proc. GeoEng 2000, Melbourne, Australia, Vol. 1, 1157-1252.
- Christian, J.T.; Baecher, G.B. (2002)  
The point-estimate method with large numbers of variables. *Int. J. Numer. Anal. Meth. Geomech.*, Vol. 26, 1515-1529.
- Cornell, J.A. (1990)  
How to Apply Response Surface Methodology. *The ASQC Basic References in Quality Control: Statistical Techniques*, Vol. 8, ASQC, Wisconsin.
- Dempster, A.P. (1967)  
Upper and lower probabilities induced by a multivalued mapping. *Annals of Mathematical Statistics*, Vol. 38, 325-339.

- Dodagoudar, G.R.; Venkatachalam, G. (2000)  
Reliability analysis of slopes using fuzzy set theory. *Computers and Geotechnics*, Vol. 27, No. 2, 101-115.
- Dong, W.; Shah, H.C. (1987)  
Vertex method for computing functions of fuzzy variables. *Fuzzy Sets & Systems*, Vol. 24, 65-78.
- Dubois, D.; Prade, H. (1990)  
Consonant approximation of belief functions. *Int. J. of Approximate Reasoning*, Vol. 4, 419-449.
- Dubois, D.; Prade, H. (1991)  
Random sets and fuzzy interval analysis. *Fuzzy Sets and Systems*, Vol. 42, 87-101.
- Duncan, J.M. (2000)  
Factors of Safety and Reliability in Geotechnical Engineering. *Journal of Geotechnical and Geoenvironmental Engineering*, ASCE, Vol. 126, No. 4, 307-316.
- Eamon, C.D.; Thompson, M.; Liu, Z. (2005)  
Evaluation of accuracy and efficiency of some simulation and sampling methods in structural reliability analysis. *Structural Safety*, Vol. 27, No. 4, 356-392.
- Edelbro, C. (2003)  
Rock mass strength—a review, technical report. Department of civil engineering of Luleå University of Technology.
- Elishakoff, I. (2000)  
Possible limitations of probabilistic methods in engineering. *Applied Mechanics Reviews (ASME)*, Vol. 53, No. 2, 19-36.
- Ferson, S.; Kreinovich, V.; Ginzburg, L.; Myers, D.S.; Sentz, K. (2003)  
Constructing probability boxes and Dempster-Shafer structures, Tech. Rep. SAND2004-3072, Sandia National Laboratories.
- Ferson, S.; Nelson, R.B.; Hajagos, J.; Berleant, D.; Zhang, J.; Tucker, W.T.; Ginzburg, L.; Oberkampf, W.L. (2004)  
Dependence in Probabilistic Modeling, Dempster-Shafer Theory, and Probability Bounds Analysis, Tech. Rep. SAND2002-4015, Sandia National Laboratories.



- Fetz, T.; Oberguggenberger, M. (2009)  
Multivariate models for random sets generated by non-parametric methods. Safety, Reliability and Risk of Structures, Infrastructures and Engineering Systems. Furuta, Frangopol & Shinozuka (eds.), Taylor & Francis, London, 1246-1253.
- Gardner, W.S. (1987)  
Design of drilled piers in the Atlantic Piedmont. Foundations and Excavations in Decomposed Rock of the Piedmont Province, GSP, Smith (ed.), ASCE, Vol. 9, 62-86.
- Ghanem, R.G.; Spanos, P.D. (1991)  
Stochastic finite elements: a spectral approach. Springer-Verlag, New York.
- Gokceoglu, C.; Sonmez, H.; Kayabasi, A. (2003)  
Predicting the deformation moduli of rock masses. Int. J. Rock Mech. Min. Sci., Vol. 40, 701-710.
- Goodman, I.R.; Nguyen, H.T. (1985)  
Uncertainty Models for Knowledge-Based Systems; A Unified Approach to the Measurement of Uncertainty. New York, Elsevier Science Inc.
- Goodman, R.E. (1995)  
Block theory and its application. Géotechnique, Vol. 45, No. 3, 383-423.
- Goricki, A. (2007)  
Classification of Rock Mass Behaviour based on a Hierarchical Rock Mass Characterization for the Design of Underground Structures, Institut für Felsmechanik und Tunnelbau, TU-Graz, Dissertation.
- Griffiths, D.V.; Fenton, G.A. (eds.) (2007)  
In Probabilistic Methods in Geotechnical Engineering. CISM courses and lectures No. 491, Springer-Verlag, Wien - New York.
- Haldar, A.; Mahadevan, S. (2000)  
Probability, reliability, and statistical methods in engineering design. New York, Wiley & Sons.
- Harr, M.E. (1989)  
Probabilistic estimates for multivariate analyses. Applied Mathematical Modelling, Vol. 13, No. 5, 313-318.

- Harr, M.E. (1996)  
Reliability-based design in civil engineering. Dover Publications Inc., Mineola, New York.
- Hasofer, A.M.; Lind, N.C. (1974)  
An exact and invariant first order reliability format, *J. Eng. Mech., ASCE*, Vol. 100, No. 12, 111-121.
- Health and Safety Executive (HSE) (1996)  
Safety of New Austrian Tunnelling Method (NATM) Tunnels, A review of sprayed concrete tunnels with particular reference to London Clay, (HSE) Books, Sudbury, 80p.
- Hoek, E.; Brown, E.T. (1980)  
Empirical strength criterion for rock masses. *J. Geotech. Engng Div., ASCE* Vol. 106, (GT9), 1013-1035.
- Hoek, E.; Kaiser, P.K.; Bawden W.F. (1995)  
Support of underground excavations in hard rock. Rotterdam, Balkema.
- Hoek, E.; Brown, E.T. (1997)  
Practical estimates of rock mass strength. *Int. J. Rock. Mech. Min. Sci.*, Vol. 34, No. 8, 1165-1186.
- Hoek, E.; Carranza-Torres, C.; Corkum B. (2002)  
Hoek–Brown failure criterion—2002 edition. Proceedings of the North American Rock. Mechanics Society Meeting, Toronto.
- Hoek, E.; Diederichs, M.S. (2006)  
Empirical estimation of rock mass modulus. *International Journal of Rock Mechanics & Mining Sciences*. Vol. 43, 203-215.
- Hong, H.P. (1998)  
An efficient point estimate method for probabilistic analysis. *Reliability Engineering and System Safety*, Vol. 59, No. 3, 261-267.
- Jasiński, M.; Pownuk, A. (2000)  
Modelling of heat transfer in biological tissue by interval fem. *Compu. Assisted Mech. Engrg. Sci.*, Vol. 7, No. 4, 699-705.
- Karakus, M.; Fowell, R.J. (2004)  
An insight into the New Austrian Tunnelling Method (NATM). VIIth Regional Rock Mechanics Symposium, ROCKMEC'2004, Sivas, Turkey.

- Kaufman, A.; Gupta, M.M. (1991)  
Introduction to fuzzy arithmetic: theory and applications. New York, Van Nostrand Reinhold Company.
- Keese, A. (2003)  
A review of recent developments in the numerical solution of stochastic partial differential equations (stochastic finite elements). Report No. Informatikbericht 2003-6, Technische Universität Braunschweig, Braunschweig.
- Kendall, D.G. (1974)  
Foundations of a theory of random sets. In stochastic Geometry, Harding & Kendall (eds.). New York, Wiley.
- Kielbassa, S.; Duddeck, H. (1991)  
Stress-Strain Fields at the Tunnelling Face – Three dimensional Analysis for Two-dimensional Technical Approach. Rock Mechanics and Rock Engineering, Springer-Verlag, Austria, Vol. 24, 115-132.
- Kulpa, Z.; Pownuk, A.; Skalna, I. (1998)  
Analysis of linear mechanical structures with uncertainties by means of interval methods. *Compu. Assisted Mech. Engrg. Sci.*, Vol. 5, No. 4, 443-477.
- Lacasse, S.; Nadim, F. (1996)  
Uncertainties in Characterizing Soil Properties. Proc. Conference on Uncertainty in the Geologic Environment: From Theory to Practice (Uncertainty '96), Shackelford, Nelson & Roth (eds.), Madison, Wisconsin, 49-75.
- Lacasse, S.; Nadim, F.; Høeg, K.; Gregersen, O. (2004)  
Risk assessment in geotechnical engineering: The importance of engineering judgement. In Proc. Advances in Geotechnical Engineering: The Skempton conference, London, Vol. 2, 856-867,.
- Li, K.S.; White, W. (1987)  
Reliability index of slopes. Proc. 5<sup>th</sup> Int. Conf. on Application of Statistics and Probability in Soil and Structural Engineering, Vol. 2, 755-762.
- Lind, N.C. (1983)  
Modelling uncertainty in discrete dynamical systems. *Applied Mathematical Modelling*; Vol. 7, No. 3, 146-152.

- Matheron, G. (1975)  
Random Sets and Integral Geometry. New York, John Wiley & Sons.
- McWilliam, S. (2000)  
Anti-optimisation of uncertain structures using interval analysis. *Comput. Struct.*, Vol. 79, 421-430.
- Merifield, R.S.; Lyamin, A.V.; Sloan, S.W. (2006)  
Limit analysis solutions for the bearing capacity of rock masses using the generalised Hoek–Brown yield criterion. *Int. J. Rock Mech. Min. Sci.*, Vol. 43, 920-937.
- Mitri, H.S.; Edrissi, R.; Henning, J. (1994)  
Finite element modeling of cable-bolted stopes in hard rock ground mines. Presented at the SME annual meeting, New Mexico, Albuquerque, 94-116.
- Möller, B.; Graf, W.; Beer, M. (2000)  
Fuzzy structural analysis using  $\alpha$ -level optimization. *Comput. Mech.*, Vol. 26, No. 6, 547-565.
- Moens, D.; Vandepitte, D. (2005)  
A survey of non-probabilistic uncertainty treatment in finite element analysis. *Computer Methods in Applied Mechanics and Engineering*, Vol. 194, No. 12-16, 1527-1555.
- Moore, R.E. (1966)  
Interval analysis. Prentice-Hall, Englewood Cliffs, NJ.
- Müller, L. (1978)  
The reasons for unsuccessful applications of the New Austrian Tunnelling Method, *Tunnelling Under Difficult Conditions*, Proc. of the Int. Tunnel Symp., Pergamon Press, Tokyo, 67-72.
- Müller, L. (1990)  
Removing the misconceptions on the New Austrian Tunnelling Method, *Tunnels & Tunnelling*, special issue, Vol. 22, 15-18.
- Muhanna, R.L.; Zhang, H.; Mullen, R.L. (2007)  
Interval Finite Elements as a Basis for Generalized Models of Uncertainty in Engineering Mechanics. *Reliable Computing*, Vol. 13, 173-194.
- Neumaier, A. (1990)  
Interval methods for systems of equations. Cambridge University Press.

- Neumaier, A. ; Pownuk, A. (2007)  
Linear Systems with Large Uncertainties, with Applications to Truss Structures. *Reliable Computing*, Vol. 13, 149-17.
- Nicholson, G.A.; Bieniawski, Z.T. (1990)  
A nonlinear deformation modulus based on rock mass classification. *Int. J. Min. Geol. Eng.*, Vol. 8, 181-202.
- Nicholson, D., Tse, C-M.; Penny, C. (1999)  
The observational method in ground engineering: principles and applications, CIRIA Report 185, London, 214.
- Oberguggenberger, M.; Fellin, W. (2002)  
From probability to fuzzy sets: The struggle for meaning in geotechnical risk assessment. *Proc. of Int. Conf. on Probabilistics in Geotechnics - Technical and Economical Risk Estimation*, Pöttler & Klapperich & Schweiger (eds.), Graz, Austria. Essen: VGE, 29-38.
- Oberguggenberger, M.; Fellin, W. (2008)  
Reliability bounds through random sets: nonparametric methods and geotechnical applications. *Comput. Struct.*, Vol. 86, No. 10, 1093-1101.
- Olsson, L.; Stille, H. (2002)  
Alarm thresholds and their use in design of underground openings. *Proc. of Int. Conf. on Probabilistics in Geotechnics - Technical and Economical Risk Estimation*, Pöttler & Klapperich & Schweiger (eds.), Graz, Austria. Essen: VGE, 215-221.
- Pacher, F. (1964)  
Deformationsmessungen im Versuchsstollen als Mittel zur Erforschung des Gebirgsverhaltens und zur Bemessung des Ausbaues, *Felsmech. und Ing. Geol.*, Suppl. I.
- Palisade Corp. (2008)  
@RISK, Risk Analysis and Simulation, Version 5.0, Manual. Newfield USA: Palisade Corporation.
- Peschl, G.M. (2004)  
Reliability Analyses in Geotechnics with the Random Set Finite Element Method. Graz University of Technology, Dissertation..
- Peschl, G.M.; Schweiger, H.F. (2003)  
Reliability Analysis in Geotechnics with Finite Elements - Comparison of Probabilistic, Stochastic and Fuzzy Set Methods. *Proc. of the Third Int.*

- Symp. on Imprecise Probabilities and Their Applications (ISIPTA '03), Bernard & Seidenfeld & Zaffalon (eds.), Lugano, Switzerland. Canada: Carleton Scientific, 437-451.
- Pine, R.J.; Harrison, J.P. (2003)  
Rock mass properties for engineering design. Q. J. Engrg. Geol. Hydrogeol., Vol. 36, 5-16.
- Phoon, K.-K.; Kulhawy, F.H. (1999)  
Characterization of geotechnical variability. Canadian Geotechnical Journal, Vol. 36, 612-624.
- Phoon, K.-K.; Cheng, Y.-G. (2009)  
Some Observations on Tunneling Simulation in Spatially Random Soil using the Displacement Controlled Method. Proc. of 2nd Int. Conf. on Computational Methods in Tunnelling. (EURO:TUN 2009), Meschke & Beer & Eberhardsteiner & Hartmann & Thewes (eds.), Bochum, Germany, Aedificatio Publishers: Vol. 2, 1061-1078.
- Pöttler, R.; Schweiger, H.F.; Peschl, G. (2007)  
Geohazards – Cost Hazards, A New Method For Evaluation Of Risks In Underground Structures. Available on-line:  
['http://ftp.ilf.com/fileadmin/user\\_upload/publikationen/'](http://ftp.ilf.com/fileadmin/user_upload/publikationen/)
- Popova, E.D. (2002)  
Quality of the Solution Sets of Parameter Dependent Interval Linear Systems, ZAMM, Vol. 82, 723-727.
- Potts, D.M.; Zdravković, L. (1999)  
Finite element analysis in geotechnical engineering, Theory. Thomas Telford, London.
- Pukelsheim, F. (1994)  
The Three Sigma Rule. The American Statistician, Vol. 48, No. 2 , 88-91.
- Qiu, Z.; Elishakoff, I. (1998)  
Antioptimization of structures with large uncertain-but-non-rand parameters via interval analysis. Compt. Meth. Appl. Mech. Engng., Vol. 152, 361-372.
- Rabcewicz, L. (1964)  
The New Austrian Tunnelling Method, Part I, *Water Power*, November 1964, 453-457, Part II, *Water Power*, December 1964, 511-515.

- Rama Rao, M.V.; Mullen, R.L.; Muhanna, R.L. (2010)  
Primary and Derived Variables with the Same Accuracy in Interval Finite Elements . 4<sup>th</sup> International Workshop on Reliable Engineering Computing (REC 2010), Beer & Muhanna & Mullen (eds.), Research Publishing Services, Singapore, 129-148.
- Rama Rao, M.V.; Pownuk, A. (2007)  
Stress Distribution in a Reinforced Concrete Flexural Member with Uncertain Structural Parameters, Part I. The University of Texas at El Paso, Department of Mathematical Sciences Research Reports Series, Texas Research Report No. 2007-05, El Paso, Texas, USA.
- Rao, S.S.; Berke, L. (1997)  
Analysis of uncertain structural systems using interval analysis. AIAA J., Vol. 35, No. 4, 727-735.
- Rosenblueth, E. (1975)  
Point estimates for probability moments. Proc. Nat. Acad. Sci. USA, Vol. 72, No. 10, 3812-3814.
- Russelli, C. (2008)  
Probabilistic Methods applied to the Bearing Capacity Problem. Mitteilung 58 des Instituts für Geotechnik, Vermeer (ed.), Universität Stuttgart, Germany.
- Sentz, K.; Ferson, S. (2002)  
Combination of evidence in Dempster-Shafer theory. Report SAND2002-0835. New Mexico, Albuquerque: Sandia Nat. Laboratories.
- Serafim, J.L; Pereira, J.P. (1983)  
Consideration of the geomechanical classification of Bieniawski. Proc. Int. Symp. Eng. Geol. underground Construction (Lisbon), Vol. 1, No. (II), 33-44.
- Schikora, K.; Ostermeier, B. (1988)  
Temporäre Sicherung von Tunneln mit Spritzbeton - Tragwirkung und Bemessung. Bauingenieur, Vol. 63, 399-403.
- Schneider, HR. (1999)  
Determination of characteristic soil properties. In: Proc. XII Int. Conf. on Soil Mech. and Geot. Eng., Vol. 1, Barends et al. (eds.), 273-281.

- Schubert, W.; Moritz, B.; Sellner, P. (2000)  
Tunneling Methods for Squeezing Ground. Italian Geotechnical Journal, Vol. XXXIV, No. 1, 16-21.
- Schweckendiek, T. (2006)  
Section Structural Reliability Applied To Deep Excavations - Coupling Reliability Methods With Finite Elements - Hydraulic and Geotechnical Engineering Delft University of Technology, Master Thesis.
- Schweiger, H.F.; Thurner, R.; Pöttler, R. (2001)  
Reliability Analysis in Geotechnics with Deterministic Finite Elements - Theoretical Concepts and Practical Application. Int. Journal of Geomechanics, Vol. 1, No. 4, 389-413.
- Schweiger, H.F.; Peschl, G.M. (2005)  
Reliability analysis in geotechnics with the random set finite element method. Computers and Geotechnics; 32, 422-435.
- Schweiger, H.F.; Peschl, G.M.; Pöttler, R. (2007)  
Application of the random set finite element method for analysing tunnel excavation in: Georisk 1, S. 43-56.
- Shafer, G. (1976)  
A Mathematical Theory of Evidence. Princeton: Princeton University Press.
- Shrestha, B.; Duckstein, L. (1998)  
A fuzzy reliability measure for engineering applications. In: Uncertainty Modeling And Analysis in Civil Engineering, Ayyub (ed.), CRC Press LLC, Boca Raton, 121-135.
- Sjöberg, J. (1997)  
Estimating rock mass strength using the Hoek-Brown failure criterion and rock mass classification-a review and application to the Aznalcollar open pit. International report BM 2. Department of civil engineering of Luleå University of Technology.
- Smith, S.A.; Krishnamurthy, T.; Mason, B.H. (2002)  
Optimized Vertex Method and Hybrid Reliability. American Institute of Aeronautics and Astronautics, AIAA-2002-1465.
- Steiner, A. (2005)  
Classification Criteria for the Determination of Ground Behaviour Types, Institut für Felsmechanik und Tunnelbau, TU-Graz, Diploma Thesis.



- Stille, H.; Holmberg, M.; Schubert, W.; Grossauer, K. (2010)  
Observational method and reliability analysis in rock engineering. Tunnelling and Underground Space Technology, in print.
- Suchomel, R.; Mašín D. (2010)  
Comparison of different probabilistic methods for predicting stability of a slope in spatially variable c-phi soil. Computers and Geotechnics. Vol. 37, 132-140.
- Thurner, R. (2000)  
Probabilistische Untersuchungen in der Geotechnik mittels Deterministischer Finite Elemente-Methode, Institut für Bodenmechanik und Grundbau, TU-Graz, Dissertation.
- Tonon, F.; Mammino, A. (1996)  
A random set approach to the uncertainties in rock engineering and tunnel lining design. Proc. ISRM International Symposium on Prediction and Performance in Rock Mechanics and Rock Engineering (EUROCK '96), Vol. 2, Barla (ed.). Torino, Italy, Rotterdam: Balkema, 861-868.
- Tonon, F.; Bernardini, A.; Mammino, A. (2000a)  
Determination of parameters range in rock engineering by means of Random Set Theory. Reliability Engineering & System Safety, Vol. 70, No. 3, 241-261.
- Tonon, F.; Bernardini, A.; Mammino, A. (2000b)  
Reliability analysis of rock mass response by means of Random Set Theory. Reliability Engineering & System Safety, Vol. 70, No. 3, 263-282.
- Tsai, C.W.; Franceschini, S. (2005)  
Evaluation of probabilistic point estimate methods in uncertainty analysis for environmental engineering applications, J. Environ. Eng.-ASCE, Vol. 131, No. 3, 387-395.
- US Army Corps of Engineers (1997)  
Introduction to probability and reliability methods for use in geotechnical engineering. Engineering Technical Letter No. 1110-2-547.
- U.S. EPA: TRIM (1999)  
TRIM, Total Risk Integrated Methodology. TRIM FATE Technical Support Document Volume I: Description of Module. EPA/43/D-99/002A, Office of Air Quality Planning and Standards.

- Vanmarcke, E.H. (1983)  
Random Fields - Analysis and Synthesis. MIT-Press, Cambridge, Massachusetts.
- Waarts, P.H. (2000)  
Structural Reliability using Finite Element Methods. Delft University of Technology, The Netherlands, Dissertation.
- Walley, P. (1991)  
Statistical Reasoning with Imprecise Probabilities. Chapman and Hall, London.
- Wannick, P. (2007)  
“Tunnel Code of Practice” as basis for insuring tunnel projects, Tunnel, No. 8, 23-28. Available on-line: ‘www.munichre.com’.
- Williamson, R.C.; Downs, T. (1990)  
Probabilistic arithmetic I: Numerical methods for calculating convolutions and dependency bounds. International Journal of Approximate Reasoning, Vol. 4, 89-158.
- Zadeh, L.A. (1965)  
“Fuzzy sets”. Information and Control, 8, 338-353.
- Zadeh, L.A. (1978)  
Fuzzy Sets as a Basis for a Theory of Possibility. Fuzzy Sets and Systems, Vol. 1, 3-28.
- Zangeneh, N.; Azizian, A.; Lye, L.; Popescu, R. (2002)  
Application of response surface methodology in numerical geotechnical analysis. In: Proc. of the 55th Canadian geotechnical conference, Hamilton, Ontario, 321-29.
- Zhang, L.; Einstein, H.H. (2004)  
Estimating the deformation modulus of rock masses. Int. J. Rock Mech. Min. Sci., Vol. 41, 337-341.
- Zhang, L. (2005)  
Engineering Properties of Rocks. Elsevier Geo-Engineering Book Series, Vol. 4, 290.

- Zhang, J.; Zhang, L.M.; Tang, W.H. (2009)  
A Bayesian framework for characterizing geotechnical model uncertainty.  
J. Geotech. and Geoenviron. Engrg. Vol. 135, No. 7, 932-940.
- Zhang, H.; Mullen, R.L.; Muhanna, R.L. (2010a)  
Interval Monte Carlo methods for structural reliability, Structural Safety,  
Vol. 32, No. 3, 183-190.
- Zhang, H.; Mullen, R.L.; Muhanna, R.L. (2010b)  
Finite Element Structural Analysis using Imprecise Probabilities Based on  
P-Box Representation. 4<sup>th</sup> International Workshop on Reliable Engineering  
Computing (REC2010), Beer & Muhanna & Mullen (eds.), Research  
Publishing Services, Singapore, 211-225.
- Zhou, J.; Nowak, A.S. (1988)  
Integration formulas to evaluate functions of random variables. Structural  
safety, Vol. 5, No. 4, 267-284.